Novel Roles for Arginine Modifying Enzymes in Immune Regulation

Inaugural-Dissertation

zur

Erlangung des Doktorgrades

der Mathematisch-Naturwissenschaftlichen Fakultät

der Universität zu Köln

vorgelegt von

Saskia Hemmers

aus Bonn

Köln 2010

Berichterstatter: Prof. Dr. Jens Brüning

Prof. Dr. Jonathan Howard

Prof. Dr. Kerri Mowen

Tag der mündlichen Prüfung: 5.07.2010

meiner Familie

Table of Contents

Figure Index III

Table Index V

Abbreviations VI

1 Introduction 1

1.1 The Immune System 1
1.1.1 Macrophages 1
1.1.2 Neutrophils 2
1.1.3 T Helper Cells 2
1.2 Posttranslational Modifications of Arginines 3
1.3 Protein Arginine Methyltransferases (PRMTs) 5
1.3.1 The PRMT Family Members 5
1.3.2 PRMT1-Mediated Regulation of Th2 Cell Cytokine Production 9
1.3.3 Coactivator-associated Arginine Methyltransferase (CARM1) 10
1.4 Peptidylarginine Deiminases (PADs) 13
1.4.2 Peptidylarginine Deiminase 4 (PAD4) 16
1.4.3 PADs and Disease 18
1.5 Specific Aims 20

2 Materials and Methods 21

2.1 Chemicals and Reagents 21
2.1.1 Kits 21
2.1.2 Molecular Weight Markers 21
2.1.3 Antibodies 21
2.1.4 Primers 23
2.2 Technical Equipment 24
2.2.1 Computer Programs 25
2.2.2 Internet Tools 25
2.3 Tissue Culture 26
2.3.1 Cell Culture Media 26
2.3.2 Cytokines, Antibodies, and Stimuli 26
2.3.3 Cell Lines: Maintenance and Transfection 26
2.3.4 Primary Cell Culture 27
2.4 Molecular Biology 28
2.4.1 Cloning 28
2.4.2 Quantitative Real-time PCR (qPCR) 30
2.4.3 Southern Blot 31
2.4.4 Northern Blot 32
2.5 Mouse Work 34
2.5.1 Mouse Strains and Genotyping 34
2.5.2 PAD4 Conditional Knockout (cKO) Generation 34
2.5.3 Neutrophil Elicitation, Isolation, and Purification 34
2.5.4 PAD4 Monoclonal Antibody Production 35
2.6 Biochemical Methods 35
2.6.1 Recombinant Protein Expression and Purification 35
2.6.2 *In Vitro* Methylation Reactions 36
2.6.3 *In Vitro* Deimination Reactions 36
2.6.4 Western Blotting 37

2.6.5 Immunoprecipitation (IP) ... 37
2.6.6 Immunofluorescence (IF) ... 39
2.7 Cell Biology Assays ... 40
2.7.1 Arginase Activity Assay40
2.7.2 Griess Assay ... 40
2.7.3 Enzyme-Linked Immunosorbent Assay (ELISA) ... 41
2.7.4 Flow Cytometry ... 41
2.8 Mass Spectrometry ... 42
2.9 Statistical Analysis ... 42

3 Results ... 43

3.1 Deimination of NIP45 and Functional Consequences ... 43
3.1.1 Deimination of NIP45 by PAD4 ... 43
3.1.2 Deimination Can Prevent Arginine Methylation of NIP45 ... 44
3.1.3 Characterization of PAD4 Target Sites in NIP45 ... 46
3.1.4 The Role of PAD4 in NIP45-mediated IL-4 Secretion ... 50
3.1.5 PAD4 Expression Levels in Th2 Cells ... 52
3.2 Generation and Analysis of PAD4 Conditional Knockout Mice ... 54
3.2.1 Generation of PAD4 Conditional Knockout Mice ... 54
3.2.2 Immunophenotyping of PAD4 KO Mice ... 56
3.2.3 Analysis of PAD4-Deficient Th Cells ... 58
3.2.4 Analysis of Neutrophils Derived from PAD4 KO Mice ... 61
3.3 The Role of CARM1 in Bone Marrow-Derived Macrophages ... 64
3.3.1 Generation of CARM1-Deficient BMDMs ... 64
3.3.2 Classical and Alternative Activation of CARM1-Deficient Macrophages ... 66
3.3.3 Glucocorticoid-Mediated Suppression of Inflammatory Cytokine Production in CARM1-Deficient BMDMs ... 67

4 Discussion and Outlook ... 70

4.1 Regulation of NIP45-mediated IL-4 Transcription by PAD4 ... 70
4.2 Generation of PAD4-Deficient Mice ... 73
4.3 The Role of CARM1 in Bone Marrow-Derived Macrophages ... 75

5 Summary ... 78

6 Zusammenfassung ... 79

7 References ... 80

8 Acknowledgements ... 98

9 Erklärung ... 99

10 Curriculum Vitae ... 100

Figure Index

FIGURE 1: T Helper Cell Differentiation Schematic 2
FIGURE 2: Overview of Arginine PTMs 4
FIGURE 3: Overview PRMT Enzyme Family 5
FIGURE 4: Overview of PRMT Cellular Function 7
FIGURE 5: Arginines Targeted by PRMTs or PAD4 in Histone H3 and H4 8
FIGURE 6: Conversion Arginine to Citrulline 14
FIGURE 7: Effects of Arginine Deimination on Protein Structure 14
FIGURE 8: Cellular Deimination Processes 15
FIGURE 9: Histone Deimination in Transcriptional Regulation 17
FIGURE 10: *In vitro* Deimination of Recombinant NIP45 43
FIGURE 11: NIP45 Deimination *In Vivo* 44
FIGURE 12: Deimination of NIP45 Prevents Methylation 45
FIGURE 13: NIP45 Deletion Mutants 46
FIGURE 14: Deimination of NIP45 Deletion Mutants 46
FIGURE 15: Deimination Sites in Mouse NIP45 47
FIGURE 16: Fluorescence Microscopy of NIP45 Mutants in M12 Cells 48/49
FIGURE 17: Effect of NIP45 Point Mutations on IL-4 Secretion 50
FIGURE 18: PAD4 is a Negative Regulator of IL-4 Transcription in M12 Cells 51
FIGURE 19: NIP45 Interaction with PAD4 and NFAT 52
FIGURE 20: Northern Blot of PAD4 Expression 53
FIGURE 21: PAD4 Gene Targeting Overview 55
FIGURE 22: Genotyping of Mice with Targeted Insertion into the PAD4 Locus 56
FIGURE 23: T Cell Development in Thymus and Lymph Nodes of PAD4 KO Mice 57
FIGURE 24: Peripheral B Cells in Spleen of PAD4 KO Mice 58
FIGURE 25: Th Cell Cytokine Secretion in PAD4 KO Mice 59
FIGURE 26: Intracellular Cytokine Staining of Th1 and Th2 Cells 60
FIGURE 27: ChIP Analysis of Th2 Cells 61
FIGURE 28: Immunofluorescence of PAD4-deficient Neutrophils 62/63
FIGURE 29: Residual CARM1 mRNA After Cre-Mediated Deletion in BMDMs 64
FIGURE 30: BMDM Cell Numbers After Tamoxifen Treatment 65
FIGURE 31: Initial Characterization of CARM1-Deficient BMDMs 65
FIGURE 32: Classical vs Alternative Activation of CARM1-Deficient BMDMs 66
FIGURE 33: Cytokine Production by CARM1-Deficient BMDMs 67

FIGURE 34: Dexamethasone-Mediated Suppression of IL-6 and TNFα 68
FIGURE 35: qPCR Analysis of CARM1-deficient BMDMs 69
FIGURE 36: Model of PAD4-mediated Regulation of IL-4 Transcription 72

Table Index

TABLE 1:	FACS Antibody List	21/22
TABLE 2:	ELISA Antibody List	22
TABLE 3:	Antibody List (WB, IF, ChIP)	22
TABLE 4:	Genotyping Primer List	23
TABLE 5:	Cloning Primer List	23
TABLE 6:	Mutagenesis Primer List	23/24
TABLE 7:	qPCR Primer and Probe List	24
TABLE 8:	ChIP Primer List	24

Abbreviations

%	percent
3’	three prime end of a DNA sequence
4-OHT	Z-4-Hydroxytamoxifen
5’	five prime end of a DNA sequence
α	anti
A	adenosine
AA	amino acid
Ab	antibody
aDMA	asymmetric dimethylarginine
Amp	ampicillin
APC	allophycocyanin
BAC	bacterial artificial chromosome
BCA	bicinchonic acid
BMDM	bone marrow-derived macrophage
β-me	β-mercaptoethanol
bp	basepair
BSA	bovine serum albumin
C	cytosine
°C	temperature in degrees Celsius
CARM1	coactivator-associated arginine methyltransferase 1
CD	cluster of differentiation
cDNA	complementary DNA
ChIP	chromatin immunoprecipitation
CHX	cycloheximide
Ci	Curie
cit	citrulline
CO_2	carbon dioxide
Cre	site-specific recombinase (causes recombination)
d	days
dex	dexamethasone
dNTP	desoxynucleotide-triphosphate
DMEM	Dulbecco’s modified Eagle medium
DMSO	Dimethyl sulfate
DN	double negative ($CD4^-CD8^-$)
DNA	desoxyribonucleic acid
DP	double positive ($CD4^+CD8^+$)
DPBS	Dulbecco’s modified phosphate buffered saline
ds	double-stranded
DTT	dithiothritole
ECL	enhanced chemiluminescence
E. coli	*Escherichia coli*
EDTA	ethylene-diaminetetraacetic acid
EGTA	ethylene-glycol tetraacetic acid
ELISA	enzyme-linked immunosorbent assay
ER	estrogen receptor
ES	embryonic stem
EtBr	ethidium bromide
FACS	fluorescence activated cell sorting
FBS	fetal bovine serum
FITC	fluorescein-isothiocyanate

Flp	site-specific recombinase, product of yeast *FLP1*-gene
FRT	Flp recombination target
g	gramm
G	guanosine
G418	geneticin sul fate
GAR	glycine-arginine rich
h	hour
H_2O	water
H3	histone 3
H4	histone 4
HAT	histone acetyltransferase
HEPES	N-2-hydroxyethylpiperazine-N'-2-ethansulfonic acid
HRP	horseradish-peroxidase
HSV-TK	herpes simplex virus thymidine kinase
Ig	immunoglobulin
ip	intraperitoneally
IP	immunoprecipitation
kb	kilobase pairs
kD/ kDa	kilodalton
KO	knockout
l	liter
IF	immunofluorescence
IFN	interferon
IL	interleukin
LA	long arm of homology
LB	Luria-Bertani medium
loxP	locus of x-ing over of phage P1
LPS	lipopolysaccharide
M	molar
me	methyl
$(me)_2$	dimethyl
MHC	major histocompatibility locus
min	minute
ml	milliliter
mM	millimolar
MMA	monomethyl arginine
mRNA	messenger RNA
MS	multiple sclerosis
µl	microliter
µM	micromolar
NaCl	sodium chloride
NaOH	sodium hydroxide
NB	Northern blot
neo	neomycin resistance gene
NET	neutrophil extracellular trap
NFAT	nuclear factor of activated T cells
NIP45	NFAT-interacting protein 45kD
NLS	nuclear localization signal
nM	nanomolar
NO	nitric oxide
NR	nuclear hormone receptor
OD	optical density
PAD	peptidylarginine deiminase
PCR	polymerase chain reaction
PE	phycoerythrine

PE-Cy7	phycoerythrine conjugated - cyanine dye 7
PerCP-Cy5.5	peridinin chlorophyll protein - cyanine dye 5.5
PGK	3-phosphoglycerate kinase
PIPES	Piperazine-N,N'-bis(2-ethanesulfonic acid)
PRMT	protein arginine methyltransferase
PTM	post-translational modification
qPCR	quantitative PCR
RA	rheumatoid arthritis
RNA	ribonucleic acid
ROS	reactive oxygen species
rpm	rounds per minute
RT	room temperature
RU	relative units
s	second
SA	short arm of homology
SAM	S-adenosyl-L-methionine
SB	Southern blot
sDMA	symmetric dimethylarginine
SDS	sodium dodecyl sulfate
SP	single positive ($CD4^+$ or $CD8^+$)
ss	single-stranded
SSC	sodium chloride/ sodium citrate buffer
T	thymidine
TAE	Tris-acetic acid-EDTA buffer
Taq Pol	polymerase from *Thermus aquaticus*
TCR	T cell receptor
TE	Tris-EDTA buffer
TF	transcription factor
tg	conventional transgene
Th	T helper
TNF	tumor necrosis factor
Tris	2-amino-2-(hydroxymethyl-)1,3-propandiole
TWEEN	polyoxethylene-sorbitan-monolaureate
U	units
UV	ultraviolet
V	volts
v/v	volume per volume
WB	Western blot
w/v	weight per volume
WT	wildtype

1 Introduction

1.1 The Immune System

In response to an infection, cells of the innate and adaptive immune system are activated sequentially to eliminate the invading pathogen. Innate immune cells like macrophages, NK cells and neutrophils are poised to respond quickly to an invading pathogen, by phagocytosis and secretion of anti-microbial mediators. Adaptive immune cells like T and B cells, are equipped with receptors that are antigen-specific and are activated during later stages of the immune response. These cells are important effectors, since their responses are tailored to the pathogenic insult. Effector mechanisms include antibody secretion, cytotoxic killing, and cytokine secretion.

Many microbicidal mediators (e.g. cytokines, chemokines, anti-microbial peptides) are potent inflammatory agents. Excess inflammation is dangerous for the host, since it can lead to severe pathology. Therefore, it is important that the immune response is balanced to ensure clearance or containment of the pathogen, and at the same time protect the host from pathology.

This thesis focuses on the role of arginine modifying enzymes in immune regulation. More specifically, I will focus on effects of arginine posttranslational modifications on cytokine production from macrophages and T helper cells. In addition, I will evaluate histone arginine deimination in primary neutrophils.

1.1.1 Macrophages

Macrophages are monocyte-derived phagocytes. They play an essential role in both innate and adaptive immunity. As professional phagocytes, tissue-resident macrophages are important for clearance of cellular debris. This process is mediated by phagocytic receptors like Fc receptors, scavenger receptors, complement receptors, etc (for review: (Aderem and Underhill, 1999)). Macrophages also express pattern recognition receptors (PRR), e.g. TLRs. Encounter of pathogens through PRRs is followed by rapid activation and secretion of cytokines, chemokines, and other microbicidal agents (Gordon, 2002). These soluble immune mediators play an important role in clearance of the pathogen as well as the recruitment of other immune cells to the site of infection. Microbial phagocytosis activates pathogen killing and subsequent antigen processing and presentation to the cells of the adaptive immune system, placing macrophages in the group of antigen-presenting cells (APCs) (for review: (Gordon, 2003)).

Macrophage activation is influenced by external stimuli (for review: (Duffield, 2003; Ma et al., 2003; Mosser and Edwards, 2008)). Two major forms of macrophage activation can be distinguished: classical and alternative activation. Classical activation requires priming of the macrophage by IFNγ and subsequent encounter with a pathogen-derived stimulus like LPS (Dalton et al., 1993; Ehrt et al., 2001; Mackaness, 1964). Hallmarks of this type of activation are a highly proinflammatory response including IL-6, TNFα, and IP-10 secretion as well as upregulation of NOS2. NOS2 metabolizes L-arginine to nitric oxide (NO), an important bactericidal mediator. The type II cytokines IL-4 and IL-13 stimulate alternative activation (Gordon, 2003; Stein et al., 1992). This activation state is associated with resolution of an infection, since the mediators released have anti-inflammatory, fibrotic, and proliferative properties (Gordon, 2003). A hallmark of alternative activation is the upregulation of Arginase I, which metabolizes L-arginine to urea and L-ornithine (Munder et al., 1998; Munder et al., 1999). Ornithine is further metabolized into proline and polyamines, which can mediate the production of collagen and induce cell proliferation, respectively.

1.1.2 Neutrophils

Neutrophils are the most abundant immune cells in the blood. They are rapidly activated and recruited to sites of infection via a gradient of chemoattractants composed of chemokines and the bacterially derived tripeptide formylated Met-Leu-Phe (Downey, 1994). Neutrophils are equipped with potent microbicidal mediators, including anti-microbial peptides, proteases, and peroxidases, prepackaged in granules that can be released upon stimulation (for review: (Nathan, 2006; Nauseef, 2007). In addition, neutrophils produce reactive oxygen species (ROS), a highly efficient bactericidal mediator (Nathan and Shiloh, 2000). Neutrophils can release web-like extracellular traps that can bind and kill pathogens. Those neutrophil extracellular traps (NETs) are assembled from nuclear and cytoplasmic components (Brinkmann et al., 2004; Ermert et al., 2009). NETs are made of antimicrobial mediators bound to chromatin. Their release mechanism involves a novel cell death pathway that is dependent on ROS generation (Fuchs et al., 2007).

The importance of neutrophils in immunity is revealed in patients with inherited neutrophil defects that suffer from frequent and severe microbial infections (for review: (Malech and Nauseef, 1997)). Besides their direct microbicidal activities, neutrophils are also important for recruitment and activation of monocytes, macrophages, dendritic cells, and T cells (Nathan, 2006).

1.1.3 T Helper Cells

During an immune response, naïve $CD4^+$ T cells encounter their cognate antigen in the context of an antigen-presenting cell, which drives them to differentiate into a specific T helper lineage (see Figure 1). Lineage commitment is determined by environmental cues, including cytokines (O'Garra, 1998), which instruct differentiation towards the Th1, Th2, Th17, inducible T regulatory (iTreg), or T follicular cell fate (Tfh) (for review: (O'Shea and Paul, 2010; Zhou et al., 2009; Zhu and Paul, 2010)). T helper cell subsets are defined by their cytokine secretion profiles. Cytokines are not only essential during the initial steps of differentiation but also play an important role in reinforcing the cell fate decision.

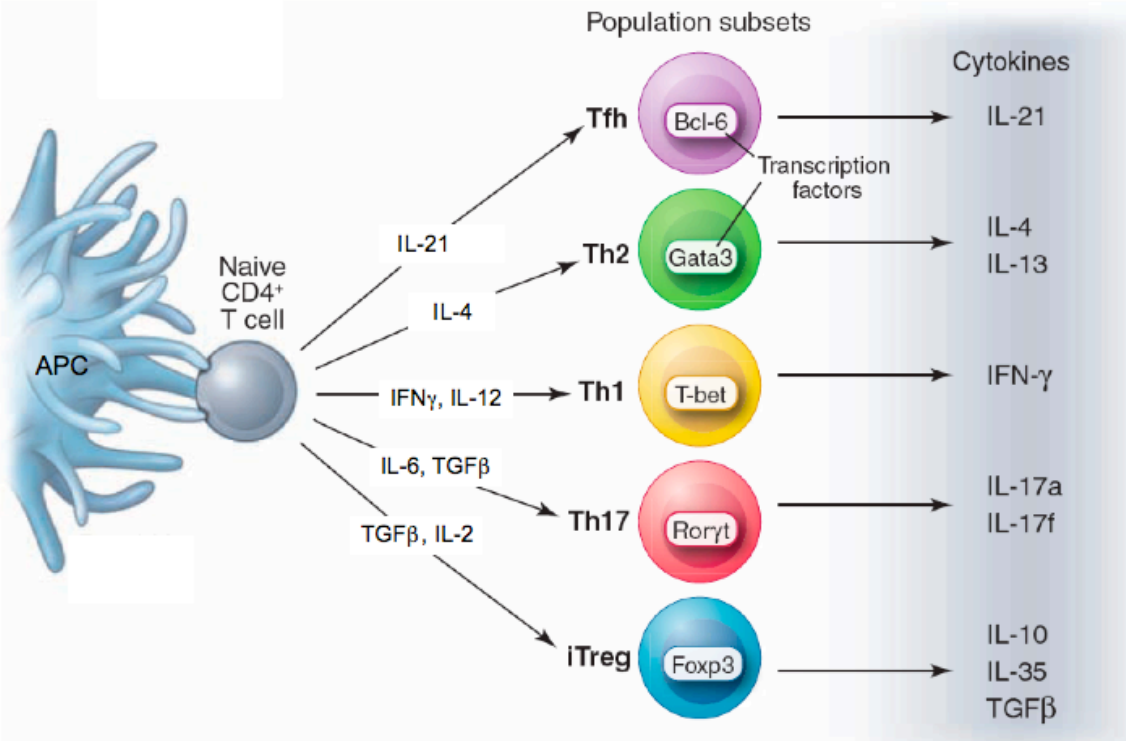

FIGURE 1: T Helper Cell Differentiation Schematic (adapted from (O'Shea and Paul, 2010)). When naïve $CD4^+$ T cells encounter their cognate antigen presented by an antigen-presenting cell (APC), they become activated and differentiate towards a Th cell lineage. This cartoon gives an overview of the cytokines involved in differentiation to a certain fate, as well as the transcription factors that are essential for lineage commitment. The effector cytokines secreted by the various Th cell subsets are listed on the right side.

1.1.3.1 Overview of T Helper Cell Differentiation

Th1 cells play an essential role in cellular immunity by aiding the clearance of intracellular bacteria and viruses through IFNγ secretion. IL-12 and IFNγ, mainly produced by activated monocytes, dendritic cells, and NK cells, drive Th1 differentiation. This process is dependent on the lineage-specifying transcription factor T-bet (Szabo et al., 2003). Th2 cells are important in defense against extracellular pathogens, like helminths. Exposure to exogenous IL-4 during the activation of the naïve $CD4^+$ T cell drives differentiation towards the Th2 lineage in a process dependent on the transcription factor GATA3. Th2 cells secrete IL-4, IL-5, and IL-13 to aid in humoral immunity against parasites as well as to reinforce their cell fate decision (Ansel et al., 2006). The more recently identified Th17 subset derived its name from its signature cytokine IL-17 and plays an important role in defense against extracellular bacterial and fungal infections. Th17 differentiation is driven by TGFβ in combination with proinflammatory cytokines, especially IL-6, and is dependent on the transcription factor RORγt (Harrington et al., 2005; Park et al., 2005). Tfh cells play an important role in regulation of B cell maturation, especially the germinal center reaction, including class switch recombination and affinity maturation. IL-21 drives Tfh differentiation, and the transcription factor Bcl-6 is required. It is not clear whether Tfh cell are truly a separate lineage, since they are very heterogeneous and can secrete IFNγ, IL-4 or IL-17 in addition to IL-21 (King et al., 2008).

The effector T cell response requires tight regulation, since all of the secreted cytokines can induce pathology if inappropriately expressed. Aberrant Th1 and Th17 responses are implicated in organ-specific autoimmunity (Damsker et al., 2010). Hyperactive Th2 cells are culprits in allergy and asthma (Passalacqua and Ciprandi, 2008). Therefore, regulatory T cells (Tregs) can suppress an immune response, and Tregs play an important role to maintaining the balance between control of infection and prevention of excessive pathology (Shevach, 2009). Tregs characteristically express Foxp3, which is required for specifying and maintaining the functional program of all regulatory T cells. There are two types of regulatory T cells, the natural Tregs (nTregs) derived from the thymus and the inducible Tregs (iTregs), which are generated in the periphery from naïve $CD4^+$ T cells. The iTreg differentiation shares similarities with the Th17 differentiation pathway since it also requires TGFβ (for review: (Vignali et al., 2008)).

1.2 Posttranslational Modifications of Arginines

Many proteins are chemically modified in a process referred to as post-translational modification (PTM). Since PTMs can change a protein's physical properties, these modifications broaden the spectrum of protein function, including activity, stability, or localization. More than 400 PTMs have been identified (Creasy and Cottrell, 2004), with the best-studied being phosphorylation, ubiquitination, acetylation, glycosylation, and methylation (Farley and Link, 2009). Many of the previously described PTMs can act as reversible on/off switches as exemplified by the antagonistic action of receptor tyrosine kinases and phosphatases in many signal transduction events (Hunter, 1998; Rogers, 1962).

Reports of the posttranslational modification of arginines go back over 50 years with the identification of the unnatural amino acid citrulline in proteins (Rogers, 1962; Rogers and Simmonds, 1958), a process referred to as deimination. Arginine methylation was first described nearly ten years later (Paik and Kim, 1967). The functional analysis of arginine methylation and deimination in cell biology is a more recent development and will be discussed in more detail later.

Arginine is a positively charged amino acid that is often involved in hydrogen bonding and amino aromatic interactions with nucleic acids. Peptidylarginines can be modified by protein arginine methyltransferases (PRMTs) through addition of monomethyl or dimethyl groups to the guanidine nitrogen atoms (Figure2) (Gary and Clarke, 1998). Three states of arginine methylation have been identified in eukaryotes, monomethylated arginine (MMA), asymmetric dimethylated arginine (aDMA), and symmetric dimethylated arginine (sDMA). These PTMs do not affect the positive charge of the arginine, but increase its bulkiness and overall hydrophobicity. Arginine deimination is catalyzed by members of the family of peptidylarginine deiminases (PADs) (Rogers et al., 1977; Takahara et al., 1986). The conversion from arginine to citrulline results in a concomitant loss of the positive charge, which transforms the former strongly basic residue into a neutral amino acid (Figure 2).

A major question in the field of arginine posttranslational modification research is whether methylation and deimination are reversible. It has been proposed that PADs and PRMTs might have antagonistic activities, since PADs, specifically PAD4, can convert histone MMA but not DMA to citrulline (Cuthbert et al., 2004; Wang et al., 2004) (Figure 2). Furthermore, arginine methylation can be blocked by preemptive deimination. However, PADs are not true demethylases, since they cannot convert the MMA back into the original arginine. In 2007 Chang *et al*., demonstrated that JMJD6, a Jumonji-domain containing enzyme, could act as an arginine-specific demethylase (Chang et al., 2007). The biological role of JMJD6 in demethylation of targets other than methylated arginines in histones still needs to be elucidated. To date, no enzyme has been identified that can catalyze the conversion of peptidyl-citrulline back into arginine.

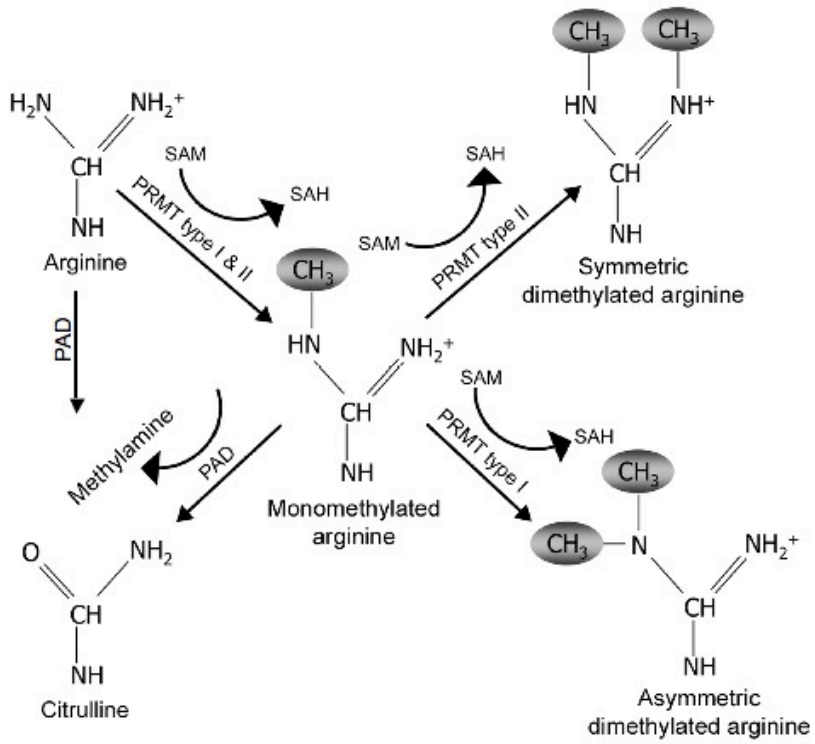

FIGURE 2: Overview of Arginine PTMs. (adapted from (Boisvert et al., 2005a)). Peptidylarginines can be monomethylated on a guanidino nitrogen atom by type I and type II arginine methyltransferases (PRMTs). Type I enzymes catalyze the addition of a second methyl group to the same nitrogen atom in a process referred to as asymmetric dimethylation. Type II PRMTs catalyze symmetric dimethylation by adding a second methyl group to the opposite nitrogen atom. Both types of PRMTs use S-adenosyl-methionine (SAM) as the methyldonor, releasing S-adenosylhomocysteine (SAH) in the process. Both arginines and monomethylated arginines can be deiminated by the peptidylarginine deiminase protein family (PAD), resulting in the formation of citrulline.

1.3 Protein Arginine Methyltransferases (PRMTs)

Arginine methylation has been linked to many cellular processes like chromatin remodeling, signal transduction, RNA processing, gene transcription, cellular transport, etc (for review: (Bedford and Clarke, 2009; Bedford and Richard, 2005; Lee and Stallcup, 2009; Wolf, 2009)). The PRMT enzyme family has been found in nearly all groups of eukaryotes. PRMT1 and PRMT5 can be traced back early in the eukaryote evolution (Krause et al., 2007). Eleven human PRMT genes have been identified so far.

PRMT enzymes catalyze the transfer of methyl groups from the universal methyl-donor S-adenosyl-L-methionine (SAM) to the terminal nitrogen atom of the guanidinium side chain of an arginine residue. The methylation reaction is a two-step process that involves a monomethylated intermediate (MMA). The PRMTs can be classified into two different groups: Type I enzymes (PRMT1, PRMT2, PRMT3, PRMT4, PRMT6, and PRMT8) catalyze the formation of MMA and aDMA; type II enzymes (PRMT5, PRMT7, and PRMT9) catalyze the formation of MMA and sDMA (Figure 2). PRMT10 and PRMT11 have not been demonstrated to exhibit enzymatic activity.

1.3.1 The PRMT Family Members

All PRMTs have a common catalytic core, which consists of the methyltransferase domain and subdomains involved in methyldonor and substrate binding (Bachand, 2007). The family members can be distinguished by their unique N-terminal domains (Figure 3).

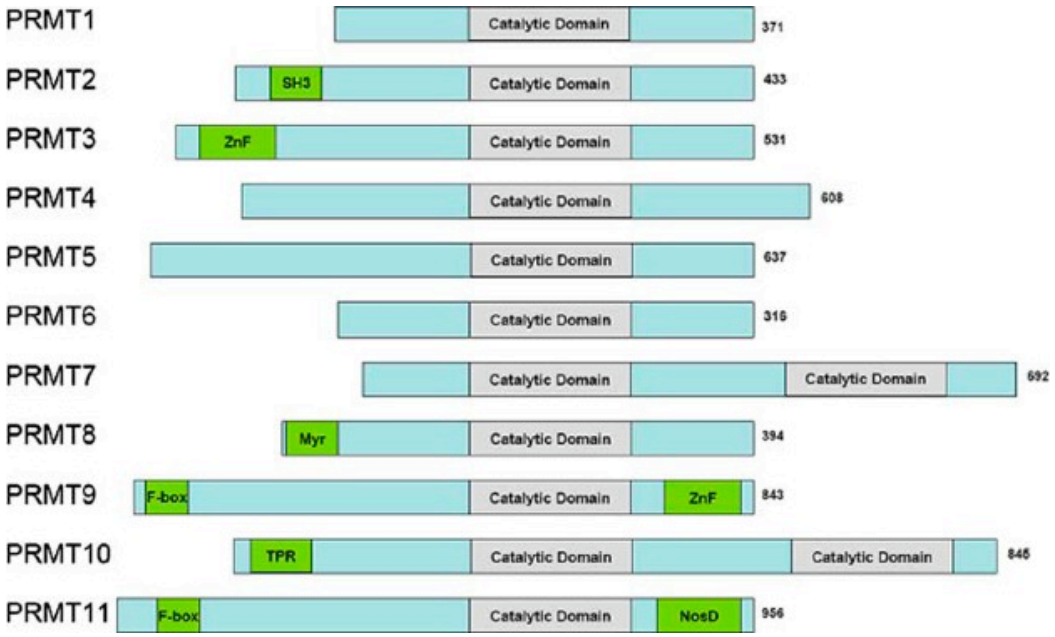

FIGURE 3: Overview PRMT Enzyme Family (adapted from (Wolf, 2009)). This cartoon depicts the schematic structure of PRMT1 through PRMT11. Features unique for each enzyme are indicated. The catalytic core domain is conserved between all family members.

Even though PRMTs share many features, they are involved in highly diverse processes. PRMT1 was the first arginine methyltransferase to be identified (Abramovich et al., 1997; Lin et al., 1996). It represents the predominant type I PRMT and has broad tissue expression (Katsanis et al., 1997; Tang et al., 2000a; Tang et al., 2000b). PRMT1 activity accounts for 85% of the observed cellular PRMT activity (Tang et al., 2000a). PRMT1 knockout mice have been generated but die during an early stage of embryogenesis (Pawlak et al., 2000). PRMT2 has an N-terminal SH3-domain, which plays an important role in protein-protein interactions (Kzhyshkowska et al., 2001). Though PRMT2 was long thought to be enzymatically inactive, in a more recent *in vitro* characterization PRMT2 demonstrates type I arginine methyltransferase activity towards histone H4R3. This finding needs to be confirmed under more physiological circumstances (Lakowski and Frankel, 2009). PRMT2 – deficient mice have been generated and are viable (Yoshimoto et al., 2006). PRMT2-deficient MEFs have a defect in E2F1-mediated cell cycle entry, positioning PRMT2 as a negative regulator of E2F1 (Yoshimoto et al., 2006). PRMT3 belongs to the type I methyltransferases and has a wide tissue distribution (Tang et al., 1998). The most distinctive feature of PRMT3 is its zinc finger domain (ZnF), which confers substrate specificity (Bachand and Silver, 2004). PRMT4 was originally described as coactivator associated arginine methyltransferase (CARM1) (Chen et al., 1999) and will be discussed in more detail below (see section 1.3.3). PRMT5, the first type II enzyme to be identified, has a wide tissue distribution (Branscombe et al., 2001). Homozygous deletion of PRMT5 in the mouse leads to immediate death of the zygote (Krause et al., 2007). PRMT6, another member of the type I family, displays predominantly nuclear cellular distribution (Frankel et al., 2002). Little is known about PRMT7, PRMT9, PRMT10, and PRMT11. PRMT8 is highly homologous to PRMT1 but has a very narrow tissue distribution and is the only PRMT with a N-terminal myristoylation sequence, which targets the enzyme to the membrane (Lee et al., 2005b; Sayegh et al., 2007).

1.3.1.1 PRMT Substrates

The list of substrates for PRMTs is continuously growing and encompasses proteins that regulate almost all cellular processes (Bedford and Richard, 2005; Lee and Stallcup, 2009; Wolf, 2009). Identification of a consensus sequence for PRMTs has remained elusive. PRMT1, 3, 6, and 8 favor glycine/arginine-rich (GAR) motifs. Substrates for PRMTs can be loosely categorized into four major cellular processes: RNA processing, transcriptional regulation, signal transduction and DNA repair (Figure 4).

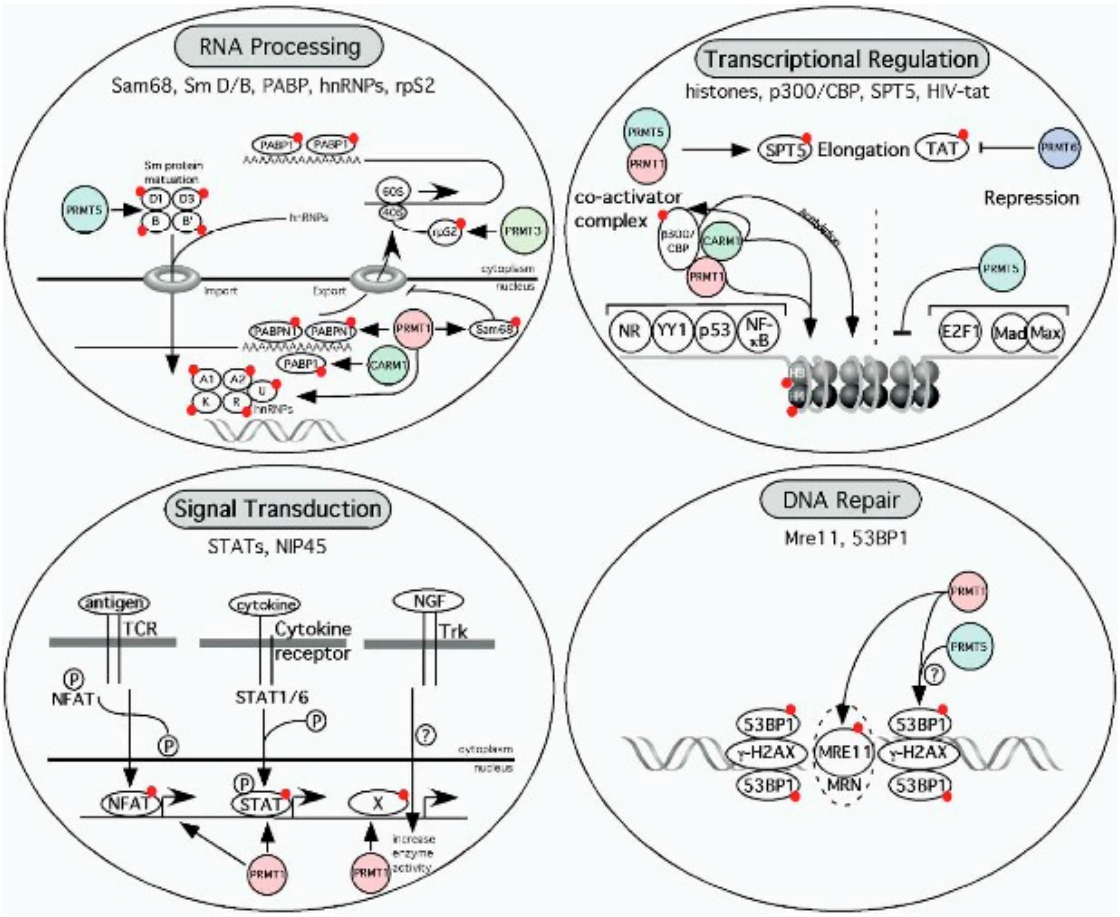

FIGURE 4: Overview of PRMT Cellular Function (adapted from (Bedford and Richard, 2005).

RNA processing:

RNA-binding proteins (RBPs) like small nuclear ribonucleoprotein particles (snRNPs) and heterogeneous ribonucleoprotein particles (hnRNPs) encompass major targets for PRMTs. Many of those RBPs harbor glycine/arginine-rich regions, which are favored by PRMT1/3/6 and PRMT5/7 (Bedford and Richard, 2005; Cote et al., 2003; Herrmann et al., 2004). Arginine methylation of RBPs bears functional consequences. For example, Sam68 hypomethylation results in mislocalization to the cytoplasm (Cote et al., 2003; Lukong and Richard, 2004). Further, arginine methylation of several Sm family members by PRMT5 is required for their proper assembly into mature snRNPs (Brahms et al., 2001; Friesen et al., 2001; Meister et al., 2001). PRMT3 methylates ribosomal protein S2, thereby, influencing ribosomal protein biosynthesis and, consequently, translation (Swiercz et al., 2005). The RBP polyA-binding protein (PABP) is methylated by CARM1 (Lee and Bedford, 2002) and PRMT1 (Smith et al., 1999), but the functional consequences of PABP methylation are unknown.

Transcriptional regulation:

The dynamic modification of chromatin during transcription illustrates the interplay of PTMs. N-terminal posttranslational modifications of the various histones serve as docking sites for chromatin-associated proteins. Different combinations of PTMs can lead to transcriptional activation or silencing. The combinatorial nature of histone PTMs has been described as the ‘histone code’ (Jenuwein and Allis, 2001; Strahl and Allis, 2000). Histone tails are targets for many PTMs, including

phosphorylation, ubiquitination, acetylation, methylation (lysine and arginine), and deimination. PRMTs, as well as PAD4, can modify histone tails. PRMT1 targets histone H4 R3; CARM1 targets histone H3 R17/R26; PRMT5 can methylate histone H3 R8 and H4 R3; and PRMT6 can modify H3 R2 and H4 R3 (Figure 5). PRMT1 and CARM1-mediated histone methylation are linked with transcriptional activation, while PRMT5 and PRMT6-mediated methylation are thought to correlate with repression (Bedford and Clarke, 2009; McBride and Silver, 2001).

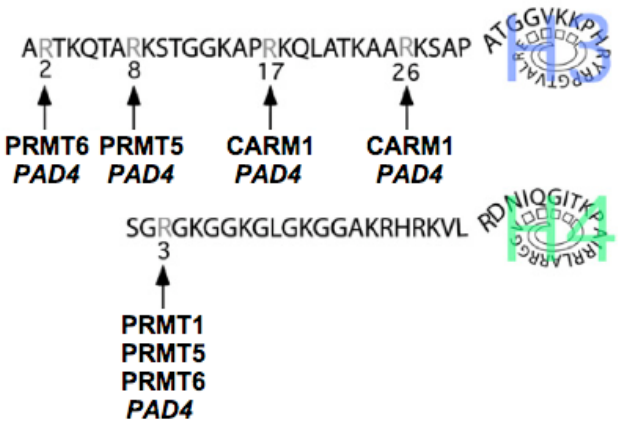

FIGURE 5: Arginines Targeted by PRMTs or PAD4 in Histone H3 and H4 (adapted from (Bedford and Clarke, 2009))

Transcriptional regulation through arginine methylation occurs on several levels (Lee and Stallcup, 2009; Pahlich et al., 2006). First, as detailed in the preceding paragraph, histones are PRMT substrates (Paik and Kim, 1967). Second, transcription is regulated during initiation and elongation. Third, several transcriptional co-activators are targets for arginine methylation. For example, the histone acetyltransferases and transcriptional coactivators CBP and p300 are both substrates for CARM1 and PRMT1 activity (Chevillard-Briet et al., 2002; Xu et al., 2001). Additionally, methylation of peroxisome proliferator-activated receptor gamma coactivator 1 alpha (PGC1α) by PRMT1 facilitates the induction of downstream targets involved in mitochondrial biogenesis (Teyssier et al., 2005). Fourth, methylation of the transcriptional elongation factor SPT5 by PRMT1 and PRMT5 modulates its interaction with RNA polymerase II (Kwak et al., 2003). Fifth, transcriptional regulation occurs on the level of the transcription factor itself. A multitude of novel transcription factor targets of PRMTs have been identified. Some of the more prominent examples include RUNX1 (Zhao et al., 2008), FOXO1 (Yamagata et al., 2008), and p53 (Durant et al., 2009; Jansson et al., 2008).

Signal transduction:

Signal transduction is a process highly regulated by PTMs, which often affect protein-protein interactions. Arginine methylation can influence those interactions. The RNA-binding protein Sam68 is methylated on arginines adjacent to proline-rich regions. Methylation prevents the association with other SH3-domain containing binding partners of Sam68 (Boisvert et al., 2005a). The Tudor domains of splicing factor SPF30 interact specifically with GAR motifs containing sDMA (Chen et al., 2001; Cote et al., 2003). The SMN protein Tudor domain facilitates the assembly of methylated Sm proteins to snRNPs (Cote et al., 2003). The methylation of histone H3R2 blocks the binding of most H3-tail binding domains, including chromo, PHD, WD40, and Tudor domains (Iberg et al., 2008).

A role for arginine methylation has been linked to several steps of type I IFN signaling (Abramovich et al., 1997; Mowen et al., 2001). PRMT1 directly interacts with the cytoplasmic tail of the type I IFN receptor alpha (Abramovich et al., 1997), and knockdown of PRMT1 in HeLa cells impairs type I IFN responses (Altschuler et

al., 1999). IFN and cytokine signaling is mediated by the JAK/STAT signaling pathway (Shuai and Liu, 2003). STAT1 is methylated by PRMT1, and this modification blocks STAT1 interaction with the inhibitor PIAS1, thereby, increasing transcriptional activation of IFN-responsive genes upon IFNα stimulation (Mowen et al., 2001).

Naïve T cell differentiation requires costimulation via the CD28 receptor together with the TCR signal. TCR engagement triggers the translocation of Nuclear Factor of Activated T cells (NFAT), a family of transcription factors that regulate multiple cytokine genes. Stimulation through CD28 increases PRMT1 activity and arginine methylation of several substrates, including Itk and Vav-1 (Blanchet et al., 2005; Blanchet et al., 2006; Lawson et al., 2007). NFAT-mediated transcription is regulated by PRMT1 mediated arginine methylation of the NFAT– interacting protein of 45 kDa (NIP45), which will be discussed in more detail below (Fathman et al., 2010; Mowen et al., 2004).

DNA repair:

DNA double strand breaks (DSBs) induced by ionizing radiation or during replication require efficient repair. MRE11, a key protein involved in the DNA double-strand break repair machinery, is a substrate for PRMT1. Its posttranslational modification has no effect on DNA binding ability but rather influences the exonuclease activity (Boisvert et al., 2005b) and recruitment to the DSB (Boisvert et al., 2005c). Additionally, arginine methylation of 53BP1 by PRMT1 modifies its ability to bind DNA (Boisvert et al., 2005d). The physiological role of 53BP1 methylation during DSB repair is not fully understood. Another important DNA damage repair enzyme, DNA polymerase β (Polβ) interacts with PRMT1 and PRMT6. These two enzymes target different arginines for methylation. PRMT6-mediated methylation enhances Polβ DNA-binding and processivity (El-Andaloussi et al., 2006). PRMT1-mediated methylation negatively regulates Polβ by blocking the interaction with the processivity factor PCNA (El-Andaloussi et al., 2007).

1.3.2 PRMT1-Mediated Regulation of Th2 Cell Cytokine Production

Upon T cell receptor (TCR) stimulation of Th2 cells, a signaling cascade is initiated that culminates with transcription factors binding to the IL-4 promoter and subsequent cytokine secretion. Nuclear-factor of activated T cells (NFAT) family members play an important role in this signal transduction pathway (for review:(Hermann-Kleiter and Baier, 2010; Rao et al., 1997)). In unstimulated Th cells, NFAT is found in the cytoplasm in a highly phosphorylated state. TCR ligation mediates Ca^{2+}-flux leading to the activation of the calmodulin-dependent phosphatase calcineurin (Clipstone and Crabtree, 1993). In turn, calcineurin dephosphorylates NFAT, which induces a conformational change, exposing a nuclear localization signal (NLS), and allowing the subsequent NFAT translocation to the nucleus. NFATs heterodimerize with various nuclear factors, like AP-1 and IRF-4, which affect their promoter binding (Macian, 2005).

NFAT-interacting protein of 45 kDa (NIP45) was identified through its interaction with the Rel-homology domain of NFAT (Hodge et al., 1996). Coexpression of NIP45 with NFAT and Th2-specific transcription factor c-Maf is sufficient to turn a non-producer B cell line into an IL-4-producing cell line. The arginine- and glycine-rich amino terminus of NIP45 is a target of arginine methylation by PRMT1 (Mowen et al., 2004). The N-terminus also mediates the interaction of NIP45 with PRMT1 and NFAT. Interestingly, PRMT1 is highly expressed in Th1 and Th2 cells and its expression is further upregulated upon TCR-stimulation. Furthermore, arginine methylation of the N-terminus of NIP45 by PRMT1 facilitates the formation of a tripartite complex of NFAT, PRMT1 and NIP45, and, thereby, promoting IL-4 transcription. *NIP45* knockout mice (Fathman et al., 2010) have a severe impairment in Th2-mediated immune responses both *ex vivo* and *in vivo*. In

the absence of NIP45, recruitment of PRMT1 to the IL-4 promoter is reduced, which is accompanied by diminished arginine methylation and acetylation of histone H4. These posttranslational H4 modifications correlate with transcriptionally active chromatin (Stallcup, 2001; Wang et al., 2001), and the diminished levels in the NIP45-deficient Th2 cells are reflected by less IL-4 transcription.

In summary, the arginine methyltransferase PRMT1 can positively influence IL-4 transcription by facilitating NIP45 methylation and therefore increasing the interaction with NFAT, which leads to strong activation of the IL-4 promoter.

1.3.3 Coactivator-Associated Arginine Methyltransferase (CARM1)

CARM1 (also referred to as PRMT4) was identified through its interaction with the C-terminal domain of the p160 coactivator GRIP1 (Chen et al., 1999), therefore the name coactivator-associated arginine methyltransferase. CARM1 methyltransferase activity preferentially targets histone H3, in contrast to the methylation of histone H4 by PRMT1 (Chen et al., 1999). The specific residues that are modified by CARM1 are located in the N-terminal tail of histone H3 at positions H3 R2, R17 and R26 (Schurter et al., 2001). CARM1 methylates glycine-arginine rich (GAR) motifs very inefficiently, thereby, setting it apart from other type I PRMTs like PRMT1 and PRMT3. The structure of the catalytic core of CARM1 has unique features compared to the other known PRMT structures of PRMT1 and PRMT3. The CARM1 dimer encompasses a substantially larger central cavity and different charge distribution, which is one possible explanation for CARM1's unique substrate specificities (Yue et al., 2007).

The biochemical control of CARM1 enzymatic activity involves several mechanisms. The enzymatically active form of CARM1 is a homodimer (Yue et al., 2007). In addition, phosphorylation inactivates CARM1 (Feng et al., 2009; Higashimoto et al., 2007). The serine 228 (S228) phosphorylation site is conserved in CARM1 among species, but not present in other PRMT family members. The kinase(s) responsible for this PTM have not been identified yet. Phosphorylation of S228 impairs cofactor binding, dimerization, and thereby catalytic activity. Moreover, coexpression of a S228E phospho-mimic mutant CARM1 with SRC-2/GRIP-1 leads to a loss of synergistic transcriptional activation of an estrogen-response element (Higashimoto et al., 2007). A second serine phosphorylation site in CARM1 at S217 is conserved among all type I PRMTs, so it potentially serves as a common PTM site. Mutation of S217 to glutamic acid leads to loss of AdoMet binding and arginine methyltransferase activity but has no effect on dimerization. Surprisingly, the S217E mutation impacts the subcellular localization of CARM1, mislocalizing it to the cytoplasm. Interestingly, during mitosis, increased levels of phosphorylated CARM1 during the G_2/M transition correlate with translocation of CARM1 from the nucleus to the cytoplasm, suggesting a potential physiological role for CARM1 phosphorylation in cell cycle regulation (Feng et al., 2009). CARM1 also automethylates, but the functional consequences of this PTM are not clear yet (Xu et al., 2001).

1.3.3.1 CARM1 and Nuclear-hormone Receptor-mediated Transcription

Nuclear hormone receptors (NRs) are a group of transcription factors that are activated by hormone binding. NR family members include the estrogen receptor (ER), androgen receptor (AR), and the glucocorticoid receptor (GR). Transcriptional activation of NR-target genes requires the presence of coactivators of the p160 coactivator family, which is comprised of steroid receptor coactivator 1 (SRC-1), SRC-2/GRIP1, and SRC3/pCIP/ACTR. These coactivators modify the local chromatin structure and help recruit RNA polymerase II to the transcription start site. The p160 family also associates with several histone acetyltransferases (HATs) like CREB-binding protein (CBP) and p300 that mediate histone acetylation, a chromatin modification associated with actively transcribed genes.

CARM1 acts as a secondary coactivator for NR-transcription in synergy with the p160 coactivator family. The coactivator function of CARM1 requires its catalytic activity (Chen et al., 1999). p160 coactivators recruit HATs, like p300 and CBP, to NR target gene promoters. A trimeric coactivator complex of SRC-3, p300 and CARM1 is required for maximal enhancement of retinoic acid-mediated transcription as well as ER, AR, and TR-induced transcription (Lee et al., 2002).

CARM1 directly interacts with p300/CBP and methylates both p300/CBP and SRC-3. Methylation of CBP/p300 in the N-terminal KIX domain selectively impairs CREB-dependent signaling pathways (Lee et al., 2002; Xu et al., 2001). Moreover, CARM1–mediated methylation of p300 in the C-terminal region affects its interaction with p160 coactivator SRC-2/GRIP1. Methylation of p300 R2142 reduces its interaction with GRIP1, whereas coexpression of active deiminase PAD4 enhances the interaction between p300 and GRIP1 (Lee et al., 2005c). Though coexpression of CARM1 with p300 and GRIP1 or other p160 coactivators enhances NR-mediated transcription, p300 methylation destabilizes the coactivator complex, thereby providing a mechanism to terminate transcription (Lee et al., 2005c). Similarly, methylation of SRC-3 by CARM1 interferes with the SRC-3/CBP interaction. Furthermore, unmethylated SRC-3 coactivates estrogen-receptor mediated pS2 transcription more potently than the methylated SRC-3. Interestingly, SRC-3 methylation also enhances its degradation (Naeem et al., 2007).

CARM1 is recruited to glucocorticoid-responsive promoters upon dexamethasone treatment and to the *pS2* estrogen-responsive promoter upon estrogen stimulation. The recruitment of CARM1 coincides with the appearance of methylated histone H3 at position R17, linking this histone mark to active transcription (Bauer et al., 2002; Ma et al., 2001). The appearance of acetylated histone H3 at K18 precedes methylation at R17 at the *pS2* promoter following estrogen stimulation, revealing functional synergy between HATs and CARM1 (Daujat et al., 2002). Further, preacetylation of H3K18 does not increase the affinity for the substrate but rather enhances the catalytic activity (Yue et al., 2007).

In summary, CARM1 is a potent secondary coactivator of NR-mediated transcription. Its coactivator function involves interaction with and methylation of primary coactivators like p300/CBP and the p160 family, as well as direct modification of histone H3, a modification associated with active gene transcription. Furthermore, CARM1-mediated methylation may serve as an off-switch to initiate the disassembly of the coactivator complex and thereby the termination of transcription.

1.3.3.2 CARM1, a Coactivator for many Transcription Factors

Besides its prominent role as a coactivator for nuclear-hormone receptor mediated transcription, CARM1 interacts with many transcription factors. CARM1 synergizes with PRMT1 and p300 to drive a subset of p53 target genes (An et al., 2004). This synergy requires a specific order of assembly: In ChIP assays of the p53 target gene promoter of *GADD45,* PRMT1-mediated H4R3 methylation appears first, followed by p300-binding and H4 acetylation, and last CARM1 binding and H3R17 methylation (An et al., 2004).

CARM1 is also a promoter-specific regulator of NFκB-dependent gene expression (Covic et al., 2005; Hassa et al., 2008; Jayne et al., 2009; Miao et al., 2006). CARM1 interacts directly with p65, a process not requiring methyltransferase activity. MIP2, MCP-1, G-CSF, ICAM-1, and IP-10 are CARM1-dependent NFκB target genes downstream of TNFα stimulation (Covic et al., 2005). The recruitment of CARM1 to several NFκB target gene promoters coincides with the appearance of H3R17 methylation and decreased H3 citrulline levels (Miao et al., 2006). p300 and p160 together with active CARM1 are required for optimal coactivation of the p65 target genes. Similar to p53 coactivation, PRMT1, CARM1, and p300 synergize to coactivate p65-driven expression of MIP2 (Hassa et al., 2008). This synergy requires

the methyltransferase activity of both PRMT1 and CARM1, as well as the p300 acetyltransferase activity. The overall requirement for CARM1 enzymatic activity is unclear because reconstitution of CARM1-deficient MEFs with either catalytically active or inactive CARM1 revealed four TNFα-induced genes that were dependent on CARM1 but independent of its catalytic activity, including Cxcl5, IL-6, Mpa2l, and MIP2. These data imply that CARM1 might function as a scaffolding protein at a subset of p65-dependent gene promoters (Jayne et al., 2009).

CARM1 coactivates many transcription factors. The mechanism of coactivation involves histone H3 methylation at the target gene promoters and/or methylation of coactivators like p300/CBP or p160 family members. IFNγ-induced MHC class II expression is mediated by coactivation through CARM1 and CBP via CIITA, the master regulator of class II expression (Zika et al., 2005). Additionally, CARM1 potentiates cAMP-induced expression of PEPCK and G6Pase, suggesting a role for CARM1 in hepatic gluconeogenesis. Furthermore, there is a stimulus-dependent interaction between CARM1 and the cAMP-responsive element-binding factor CREB (Krones-Herzig et al., 2006). Other examples of CARM1-regulated coactivation include E2F1-mediated transcription of the *Cyclin E1* gene (El Messaoudi et al., 2006), synergistic activation of LEF-1/TCF-4 together with β-catenin (Koh et al., 2002), stimulation of the activity of myogenic transcription factor MEF2C (Chen et al., 2002), positive regulation of c-Fos mediated target gene expression (Fauquier et al., 2008), and cooperative upregulation of CITED2 expression upon IL-4 stimulation in concert with STAT5 and PRMT1 (Kleinschmidt et al., 2008). All these reports describe a coactivator function of CARM1 that usually does not involve direct methylation. Recently, the pleiotropic transcription factor C/EBPβ has been identified as a target of CARM1-mediated methylation (Kowenz-Leutz et al., 2010). Interestingly, phosphorylation of the C/EBPβ regulatory domain abrogates its interaction with CARM1, which is required for transcriptional activity. Arginine methylation of C/EBPβ inhibits the interaction with the SWI/SNF and Mediator complexes, thereby negatively regulating activation of myeloid and adipogenic genes via C/EBPβ (Kowenz-Leutz et al., 2010).

1.3.3.3 CARM1 and mRNA Processing

Two members of the mRNA-stabilizing Hu protein family, HuR and HuD are methylated by CARM1 (Fujiwara et al., 2006; Li et al., 2002). LPS stimulation of the macrophage cell line RAW264.7 increases methylated HuR protein levels. Also, LPS stimulation induces HuR-mediated TNFα mRNA stabilization, suggesting a possible link between methylation of HuR and its activity (Li et al., 2002). In a study addressing the role of CARM1 in c-Fos mediated transcription, CARM1 has both a stabilizing and destabilizing effect on mRNA stability of c-Fos target genes (Fauquier et al., 2008).

Several splicing and transcription elongation factors (SmB, SAP49, U1C, and CA150) are CARM1 substrates (Cheng et al., 2007; Ohkura et al., 2005). The methylation sites map to a common protein interaction domain, the PGM motif, a proline-, glycine-, methionine-, and arginine-rich stretch (Bedford et al., 1998) found in splicing factors. Interestingly, the same splicing factors serve as substrates for the type II enzyme PRMT5 (Brahms et al., 2001; Cheng et al., 2007). Symmetric methylation of SmB mediates its interaction with spinal muscular atrophy gene product SMN Tudor domain (Brahms et al., 2001; Friesen et al., 2001). CARM1-mediated methylation of the PGM-motif of CA150 facilitates its interaction with the Tudor domain of SMN. Furthermore, catalytically active CARM1 synergizes with the splice factor CA150 to enhance splicing (Cheng et al., 2007). Overall, all studies combined suggest a role for CARM1 in the regulation of alternative splicing.

1.3.3.4 CARM1 and Development

CARM1 is important for development, since embryos with a targeted disruption of CARM1 are smaller in size and die either *in utero* or shortly after birth due to a defect in proper lung inflation (Yadav et al., 2003). CARM1-deficient MEF lines derived from E12.5 embryos are defective in estrogen-driven transcription. Transcription of estrogen-responsive genes is reduced to background levels in MEFs from CARM1 KO mice but is rescued by ectopic expression of functional CARM1 (Yadav et al., 2003).

CARM1-deficient embryos display aberrant thymocyte development. This defect includes reduced thymocyte numbers, especially pronounced in the DN and DP subsets, with an accumulation of DN1 cells. Thymocyte cyclic AMP-regulated phosphoprotein (TARPP) has been identified as a CARM1 substrate (Lee and Bedford, 2002). This defect in early thymocyte development might therefore be linked to the hypomethylation of TARPP in CARM1-deficient thymocytes (Kim et al., 2004).

A transcriptome analysis of E18.5 CARM1 WT or KO embryos stimulated with synthetic estrogen revealed a selective downregulation of genes of estrogen-regulated transcripts and lipid-associated transcripts (Yadav et al., 2008). Many of the downregulated genes in the CARM1-deficient embryos are involved in adipogenesis. Interestingly, the identified genes include peroxisome proliferator-activated receptor gamma (PPARγ) target genes, suggesting a role for CARM1 as a PPARγ coactivator. Furthermore, knockdown of CARM1 in preadipocytes reduces their differentiation capacity towards adipocytes (Yadav et al., 2008).
The small size of CARM1-deficient embryos has been linked to an endochondral ossification defect (Ito et al., 2009). CARM1 transgenic mice show enhanced endochondral bone formation. This differentiation process is tightly controlled by the transcription factor Sox9. CARM1 can both interact with and methylate Sox9. Methylation inhibits the interaction of Sox9 with β-catenin, allowing it to drive CyclinD1 expression and chondrocyte proliferation. In the absence of CARM1, Sox9 remains in complex with β-catenin, thereby, inhibiting chondrocyte proliferation (Ito et al., 2009).

Since CARM1 acts as a coactivator for many different transcription factors involved in pleiotropic cellular functions, it will be interesting to further the understanding of the physiological consequences of CARM1 deficiency with the help of celltype- or tissue-specific knockouts.

1.4 Peptidylarginine Deiminases (PADs)

The peptidylarginine deiminase (PAD) family catalyzes the conversion of peptidylarginine to a citrulline residue in a process referred to as citrullination or deimination (see Figure 6). Deimination was identified as early as 1939 (Fearon, 1939), but the first description of the PAD enzyme responsible for this modification did not come until the late 1970s (Rogers et al., 1977). Since arginine deimination changes the charge of the positively charged arginine to the neutral uncharged citrulline, this PTM can have profound effects on the modified protein (Figures 6+7).

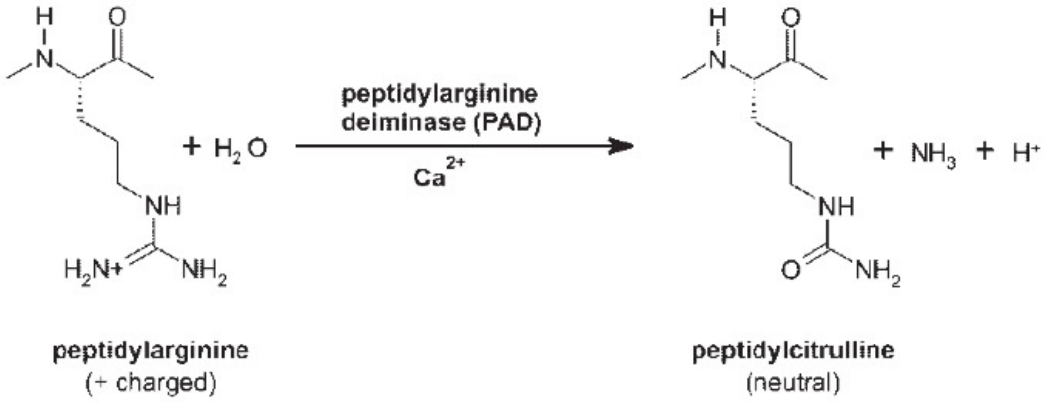

FIGURE 6: Conversion of Arginine to Citrulline (adapted from (Vossenaar et al., 2003b))

Conversion from arginine to citrulline results in an overall loss of 1 Da mass for each modified arginine. More importantly, the loss of the positive charge has an effect on the overall charge distribution, isoelectric point, as well as ionic and hydrogen bonding properties of the modified proteins, leading to altered intra- and intermolecular interactions or even protein tertiary structure (Tarcsa et al., 1996; van Venrooij and Pruijn, 2000)(Figure 7).

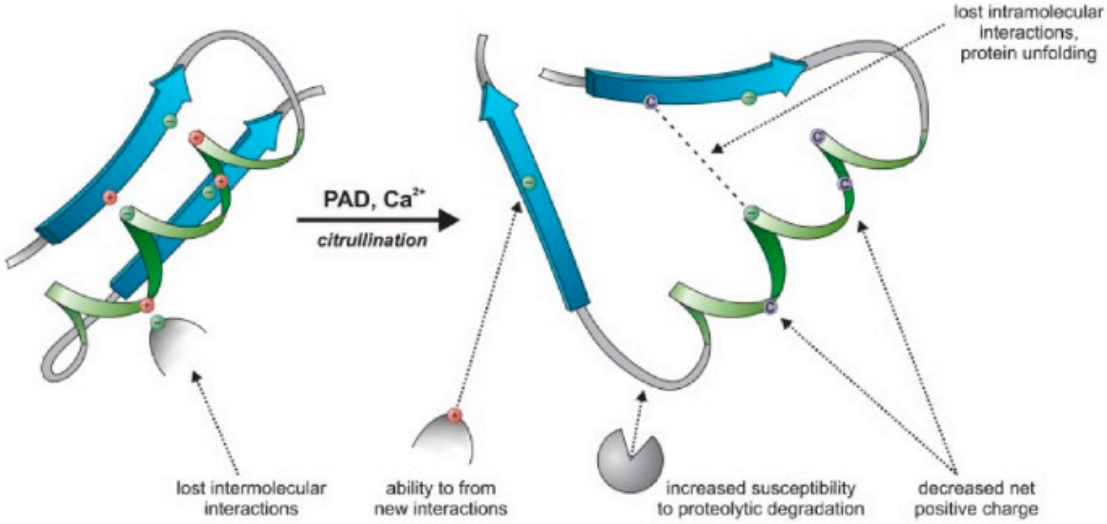

FIGURE 7: Effects of Arginine Deimination on Protein Structure (adapted from (Vossenaar et al., 2003b))

1.4.1.1 The PAD Family Members

The peptidylarginine deiminase family is comprised of five Ca^{2+}-dependent isoenzymes. All PADI genes are localized in a single gene cluster on human chromosome 1 (Chavanas et al., 2004; Vossenaar et al., 2003b). The isotypes display extensive sequence homology, but they differ by tissue distribution. PAD1 is mainly expressed in the epidermis and the uterus. PAD3 is found in hair follicles. PAD4, the only member with a putative NLS, can be detected in granulocytes, especially neutrophils. PAD6 is expressed in eggs, ovaries and the early embryo. PAD2 is the only family member with a broad tissue distribution, and it is expressed at high levels in skeletal muscle, brain, secretory glands, and spleen (for review: (Vossenaar et al., 2003b)).

1.4.1.2 Regulation of PAD Activity

Binding of calcium ions is a requirement for PAD activation (Arita et al., 2004). *In vitro* studies suggest that deimination requires very high concentrations of calcium, which are not found inside the cell under physiological conditions. There are several possibilities for the regulation of cellular PAD activity. First, PADs could be kept inactive inside the cell and be activated only under conditions that involve high intracellular Ca^{2+} concentrations, like apoptosis or terminal differentiation. Second, PADs might be released into the extracellular space (actively or passively), where they encounter activating calcium concentrations. Or third, accessory proteins might be involved that can lower or even abolish the requirement for high Ca^{2+} concentration for PAD activation. It is likely that all of the above mentioned mechanisms play a role in PAD activation.

PAD enzymes have autoregulatory capacity. Two recent studies identified a novel mechanism of PAD inactivation through autocitrullination (Andrade et al., 2010; Mechin et al., 2010).

1.4.1.3 PAD Substrates

Not much is known about the substrate specificity of PADs. *In vitro,* almost any accessible arginine can serve as a substrate, though there are considerable kinetic differences (Kubilus et al., 1980; Senshu et al., 1999). Substrate specificity *in vivo* is more likely determined by subcellular localization and accessibility of Ca^{2+} or accessory proteins. Several attempts to assign a consensus sequence around the targeted arginine have not resulted in deimination site predictability (Arita et al., 2006; Stensland et al., 2009).

A physiological role for deimination has been implicated in various cellular processes (for overview see Figure 8).

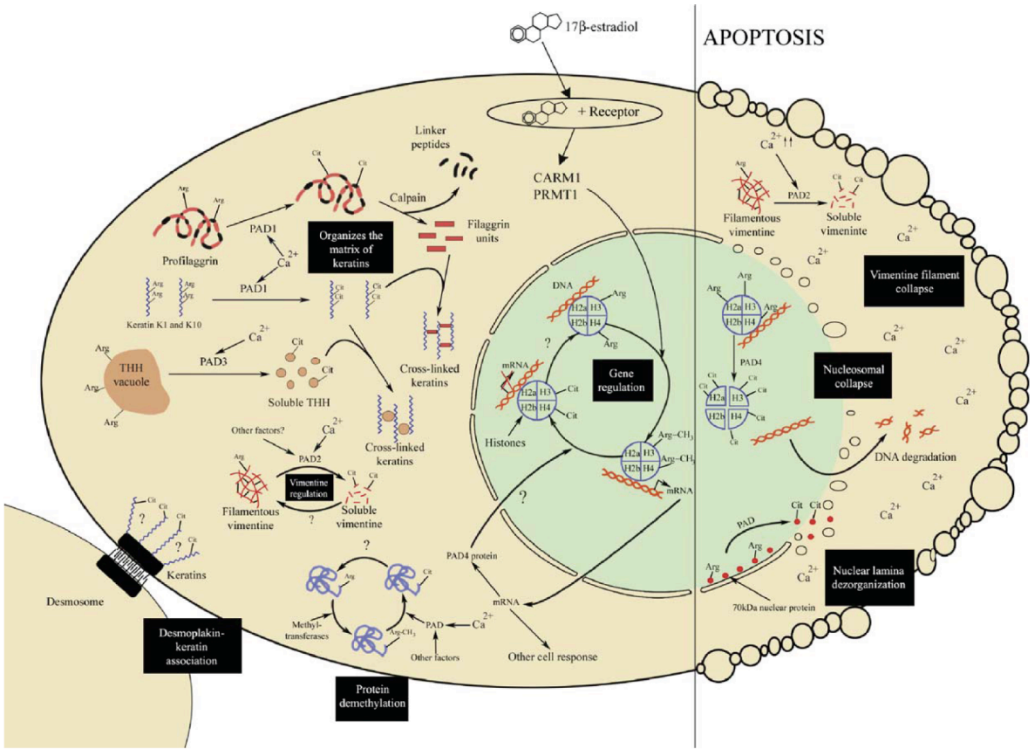

FIGURE 8: Cellular Deimination Processes (adapted from (Gyorgy et al., 2006))

PADs play an important role in the terminal differentiation of keratinocytes. During this process keratinocytes migrate from the basal epithelial layer upward culminating in the death of these cells, which involves exposure of intracellular

proteins to high Ca^{2+} concentrations. PADs, especially PAD1, deiminate keratins and the keratin-associated fillagrin (Senshu et al., 1995; Senshu et al., 1996). The deimination of profillagrin is important for its maturation that is required for its function in crosslinking keratins, an important step in the cornification of the epidermis (Ishida-Yamamoto et al., 2002).

PAD enzymes are involved in many cellular processes. PAD3 deiminates the cytoskeletal protein trichohyalin (Rogers et al., 1999; Rogers et al., 1997). PAD2 activity is directed towards more diverse substrates, likely a reflection of its wide tissue distribution. The intermediate filament protein vimentin has been shown to be a target of PAD2-mediated deimination, especially under apoptotic conditions (Asaga et al., 1998). The loss of positive charge on the headgroup of vimentin has dramatic consequences as it favors depolymerization of filaments and subsequently results in the loss of the vimentin structural network (Inagaki et al., 1989). Another important target of PAD2 activity is myelin basic protein (MBP) (Pritzker et al., 2000). More recently, a number of novel PAD targets have been identified, but it is not quite clear which PAD family member is responsible for the PTM. These novel targets include: antithrombin (Chang et al., 2005a; Ordonez et al., 2009; Pike et al., 1997), CXCL10 and CXCL11 (Loos et al., 2008), CXCL8 (Loos et al., 2009; Proost et al., 2008), CXCL12 (Struyf et al., 2009), and other targets that will be discussed in more detail in the next two sections.

1.4.2 Peptidylarginine Deiminase 4 (PAD4)

PAD4, for historic reasons also referred to as PAD5 (Asaga et al., 2001; Nakashima et al., 2002), was originally characterized and cloned from the human myeloid cell line HL-60. Differentiation of HL-60 cells either down the granulocyte or monocyte lineages, leads to an increase in PAD enzymatic activity (Nakashima et al., 1999), facilitating the cloning and characterization of PAD4. Overexpressed GFP-tagged PAD4 localizes predominantly to the nucleus, making it the only nuclear PAD enzyme (Nakashima et al., 2002). PAD4 is expressed in various cells of the hematopoietic lineage, most prominently in granulocytes and monocytes (Asaga et al., 2001; Nakashima et al., 2002; Vossenaar et al., 2004) and to a lesser extent in cells of the B, T and NK cell lineages (Vossenaar et al., 2004).

Like all other family members, PAD4 enzymatic activity is dependent on Ca^{2+}. The crystal structure of PAD4 (Arita et al., 2004) revealed two domains: an N-terminal domain containing two immunoglobulin-like subdomains (Igl1 and Igl2) and a C-terminal domain comprised of an α/β-propeller structure that is highly conserved among all family members. PAD4 contains five calcium-binding sites. Ca^{2+}-binding induces major conformational changes important for binding of the artificial substrate benzoyl-L-arginine amide (BAEE) (Arita et al., 2004).

1.4.2.1 PAD4 and Histones

PAD4 deiminates histones and nucleophosmin/B23 in granulocytes upon calcium-ionophore stimulation (Hagiwara et al., 2002; Nakashima et al., 2002). PAD4-dependent histone modifications map to the N-terminal tails of H2A (R3), H3 (R2, 8, 17, 26), and H4 (R3) (Cuthbert et al., 2004; Hagiwara et al., 2005; Wang et al., 2004). Interestingly, almost all of those deimination sites are also targets for arginine methylation by PRMT1, CARM1 and PRMT5. Indeed, PAD4 catalyzes demethylimination of histones, a process in which the monomethylated arginine (MMA) is converted into a citrulline. PAD4 exhibits no activity towards dimethylated arginines (Cuthbert et al., 2004; Wang et al., 2004). The activity of PAD4 towards MMA has been questioned in several subsequent studies (Kearney et al., 2005; Raijmakers et al., 2007), focused on *in vitro* activity towards artificial peptides. Deiminated histones can no longer be methylated by PRMTs. Therefore, PAD4 activity indirectly antagonizes arginine methylation (Figure 9).

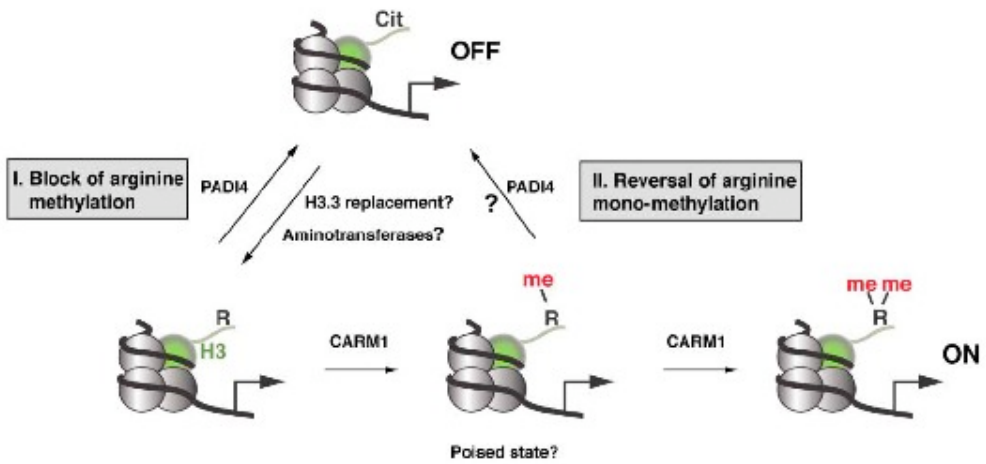

FIGURE 9: Histone Deimination in Transcriptional Regulation. Exemplified for histone H3 (adapted from (Cuthbert et al., 2004))

1.4.2.2 PAD4 as a Corepressor

PRMTs often act as transcriptional coactivators, and histone arginine methylation is associated with transcriptional activation. Conversely, PAD4-mediated deimination antagonizes methylation, thereby, mediating transcriptional repression. In the human breast-cancer cell line MCF-7, estrogen stimulation leads to PAD4 upregulation (Dong et al., 2007) dependent on estrogen-receptor α and the transcription factors AP-1, Sp1, and NF-Y. PAD4 associates with the endogenous estrogen-responsive *pS2* promoter, coinciding with increased histone deimination. Estrogen-induced PAD4 binding to the promoter leads to decreased promoter transcription. Catalytic activity is required for the transcriptional corepressor function of PAD4 (Cuthbert et al., 2004; Wang et al., 2004). PAD4 interacts with histone deacetylases (HDACs), a class of enzymes that is associated with transcriptional repression, forming a corepressor complex on the *pS2* promoter upon estrogen stimulation (Denis et al., 2009) and on p53 target gene promoters (Li et al., 2010). Overall, the collaboration between PAD4 and HDACs seems to be an emerging theme in transcriptional corepression.

1.4.2.3 PAD4 and Apoptosis

Apoptosis-mediated Ca^{2+}-influx into the cell or release of intracellular PADs has been proposed to induce PAD activation. In addition, PAD4 is implicated in the regulation of apoptosis. Overexpression of PAD4 in Jurkat T cells or HL-60 cells leads to an increase in cell cycle arrest and apoptosis (Hung et al., 2007; Liu et al., 2006). In contrast, chemical inhibition of PAD4 activity, as well as siRNA-mediated knockdown of PAD4, promotes apoptosis (Li et al., 2008; Yao et al., 2008) in a process mediated by p53. The role for PAD4 in p53-mediated transcription is still unclear, but a corepressor function for PAD4 for a subset of p53-target genes is suggested (Li et al., 2010). Interestingly, PAD4 itself is a direct transcriptional target of p53 (Tanikawa et al., 2009).

1.4.2.4 PAD4 in Neutrophils

Neutrophils, the most abundant leukocyte in mammalian blood, express high levels of PAD4 (Asaga et al., 2001). These innate effectors are part of the acute phase inflammatory response directed against bacterial infections, and they migrate out of the blood towards the site of infection. In neutrophils from peripheral human blood, PAD4 deiminates histone H3 upon a plethora of inflammatory stimuli (TNF, fMLP, LPS and H_2O_2) but not upon induction of apoptosis via chemical inducers. Moreover, neutrophils release deiminated H3 during neutrophil extracellular trap

(NET) formation (Neeli et al., 2008). Furthermore, TNFα stimulation of neutrophils leads to a strong increase of histone H4 deimination, which is localized within NETs and decondensed chromatin (Wang et al., 2009). Additionally, histone deimination influences chromosome compaction by promoting decondensation of the nucleosomes during NET formation (Wang et al., 2009).

1.4.3 PADs and Disease

Rheumatoid arthritis (RA) is a systemic autoimmune disorder that involves chronic inflammation of the synovial joint, culminating in joint erosion and bone destruction. Both genetic determinants and environmental factors increase the risk of developing RA (Wegner et al., 2010). Autoantibodies are a feature of RA, and they have been used as serological markers for diagnosis of RA patients. Rheumatoid factor (RF), an autoantibody against the Fc portion of human IgG, is present in 70-80% of patients with RA but is also observed in patients with other inflammatory diseases (Silveira et al., 2007). Anti-perinuclear factor (APF) and anti-keratin autoantibodies (AKA) are both more specific markers of disease (Silveira et al., 2007).

PAD involvement in disease was first appreciated in 1998, with the recognition of citrullinated proteins by autoantibodies associated with rheumatoid arthritis (RA) (Schellekens et al., 1998). Both APF and AKA react with mature fillagrin, more precisely with deiminated epitopes of fillagrin (Girbal-Neuhauser et al., 1999; Hoet et al., 1991; Schellekens et al., 1998; Sebbag et al., 1995; Simon et al., 1995). This discovery led to the development of enzymatic assays containing cyclic-citrullinated peptides (CCP) to screen for autoantibodies in the diagnosis of RA patients. anti-CCP assays have a diagnostic sensitivity at least equivalent to that of RF detection in serum, but a much higher specificity for RA (98%) (van Venrooij et al., 2008). Interestingly, anti-CCP reactivity can develop more than 10 years prior to clinical diagnosis of RA, and high antibody levels are closely associated with a very severe and erosive form of the disease (Nielen et al., 2004; Vencovsky et al., 2003). Moreover, the presence of anti-CCP is closely linked to the MHC class II HLA DRB1 allele that predisposes for RA (Klareskog et al., 2006; van der Helm-van Mil et al., 2007). The analysis of anti-CCP antibodies from RA patients has led to the discovery of many deiminated antigen targets: fibrinogen (Vander Cruyssen et al., 2006), vimentin (Dejaco et al., 2006), α-enolase (Kinloch et al., 2005), collagen type II (Burkhardt et al., 2005), and many more (Kinloch et al., 2008; Klareskog et al., 2008; Wegner et al., 2010).

Since PADs are the only known enzymes that catalyze the peptidylarginine to citrulline conversion, the presence of citrullinated proteins in the synovium of RA patients suggests the involvement of PAD activity in the joint (Masson-Bessiere et al., 2001). Both PAD2 and PAD4 are expressed in the joints of RA patients co-localizing with tissue inflammation and citrullinated protein deposits (Chang et al., 2005b; Foulquier et al., 2007). Moreover, there is a genetic association of functional haplotypes of the *PADI4* gene with RA (Suzuki et al., 2003). The SNPs in the disease-associated haplotype lead to stabilization of PAD4 mRNA and could, therefore, result in increased deimination activity. Replication studies in Japan and Korea confirmed this association (Ikari et al., 2005; Kang et al., 2006). In contrast, several European studies could not detect a significant association between *PADI4* and RA (Barton et al., 2004; Caponi et al., 2005; Martinez et al., 2005). Although there is a clear link between PAD activity and RA, the specific involvement of PADs in disease still needs to be elucidated. It is not clear if protein deimination represents an RA disease trigger or if it is just a consequence of high levels of joint inflammation.

Besides RA, PAD family members are associated with several other pathological conditions. Abnormal deimination of MBP is detected in the brains of

patients suffering from multiple sclerosis (MS), a progressive demyelinating disease (Moscarello et al., 2007; Wood et al., 1996). Elevated levels of both PAD2 and PAD4 are found in brain extracts from MS patients (Wood et al., 2008). MBP is an essential part of the myelin sheath surrounding neurons. The myelin sheath is dependent on ionic interactions between negatively charged lipids and basic proteins like MBP. Since deimination of MBP involves loss of positive charges, this influences the MBP lipid interaction. The ratio of citrullinated MBP to normal MBP affects the packing of the myelin sheath (Beniac et al., 2000). In children under the age of two years, almost all MBP is deiminated, which correlates with more loosely packed myelin and likely reflects the high plasticity of the brain during this developmental stage. By the age of four and throughout adulthood, the percentage of citrullinated MBP is reduced to about 18% (Moscarello et al., 1994). In addition, deimination of MBP makes it more susceptible to degradation by cathepsin D (Pritzker et al., 2000). Therefore, hypercitrullination of MBP has been implicated in the pathogenesis of diseases like multiple sclerosis and Alzheimer's disease.

Elevated PAD4 levels are detected in some malignant tumors (Chang and Fang, 2009). Increased PAD4 protein levels are also reflected in the patients' blood and correlate with elevated citrullinated antithrombin levels (Chang et al., 2009). Deimination of antithrombin is proangiogenic because it results in increased thrombin activity that, in turn, leads to elevated VEGF and integrin β3 levels (Maragoudakis et al., 2002). As described above, PAD4 is also a corepressor for p53, an important tumor suppressor (Li et al., 2008). Elevated levels of PAD4 could, therefore, promote tumorigenesis by inhibition of p53 target genes.

PAD dysregulation is a common theme in the pathological conditions described above, and more diseases that involve PAD enzymatic activity are emerging. Therefore, it is of great importance to better understand the physiological role of the PAD family members to determine if they might be suitable therapeutic targets for any of the above-mentioned diseases.

1.5 Specific Aims

Arginine modifying enzymes are important regulators of many cellular functions including signal transduction, mRNA splicing, apoptosis and transcription. PRMT and PAD family members mediate transcriptional regulation by both interaction with transcription factors to form coactivator or corepressor complexes and posttranslational modification of histones in gene regulatory regions.

Arginine methylation of NIP45 positively regulates IL-4 cytokine gene expression. Since arginine deimination can antagonize arginine methylation, I propose that NIP45-mediated IL-4 expression might be negatively regulated by arginine deimination:

Objective 1: Regulation of NIP45-mediated IL-4 expression by arginine deimination
I will test if NIP45 is a target for arginine deimination *in vitro* and *in vivo*. These studies will focus on the peptidylarginine deiminase PAD4. Further, I will evaluate the functional consequences of PAD4-mediated deimination of NIP45 on IL-4 cytokine expression.

The peptidylarginine deiminase PAD4 has been described as a corepressor for nuclear hormone receptor signaling and p53 signaling. In addition, PAD4 dysregulation is associated with several pathological conditions including RA, MS, and malignant tumors. To further the understanding of PAD4 biology, I propose to generate a PAD4 conditional KO mouse strain:

Objective 2: Generation and characterization of PAD4 conditional KO mice
I will generate PAD4 conditional KO mice by conventional gene targeting strategies. The KO will be analyzed for defects in hematopoietic development. In addition, I will analyze IL-4 expression in PAD4-deficient Th2 cells, to confirm PAD4 as a negative regulator of IL-4 transcription.

The arginine methyltransferase CARM1 is an important coactivator of nuclear hormone receptor signaling and NFκB signaling. This coactivation is mediated both by formation of a coactivator complex and methylation of histone H3R17, a posttranslational modification associated with active transcription. To date, not much is known about the role of CARM1 in immune regulation. Therefore, I propose to evaluate the role of CARM1 in proinflammatory cytokine production by macrophages:

Objective 3: Analysis of CARM1-deficient bone marrow-derived macrophages
I will generate mice with a macrophage-specific deletion of CARM1. I will differentiate BMDMs from these mice to test the proinflammatory cytokine expression in macrophages. In addition, I will test if glucocorticoid-receptor mediated suppression of proinflammatory cytokine expression is dependent on CARM1 coactivation.

2 Materials and Methods

2.1 Chemicals and Reagents

All standard lab chemicals were purchased from Sigma-Aldrich (St. Louis, MO) or Fisher Scientific (Hampton, NH). Other specific reagents used will be described in the relevant sections below.

2.1.1 Kits

Amersham RediPrime II Labelling System	GE Healthcare, Waukesha, WI
Anti-Citrulline (modified) Detection kit	Millipore, Billerica, MA
BCA Protein Assay Kit	Thermo Scientific, Rockford, IL
BD Cytofix/ Cytoperm Plus	BD Biosciences, San Jose, CA
Griess Reagent System	Promega, Madison, WI
illustra ProbeQuant G50 Microcolumns	GE Healthcare, Waukesha, WI
iScript cDNA synthesis kit	Bio-Rad, Hercules, CA
MACS $CD4^+$ T Cell Isolation Kit	Miltenyi Biotec, Bergisch Gladbach
MACS $CD4^+CD62L^+$ T Cell Isolation Kit II	Miltenyi Biotec, Bergisch Gladbach
PrepEase His Tagged Protein Purification Midi Kit – High Specificity	USB, Cleveland, OH
PureLink HiPure Plasmid MaxiPrep Kit	Invitrogen, Carlsbad, CA
QIAquick Gel Extraction Kit	Qiagen, Hilden, Germany
Qiaquick PCR Purification Kit	Qiagen, Hilden, Germany
QIAshredder	Qiagen, Hilden, Germany
QuickChange Lightning Site-Directed Mutagenesis	Agilent Technologies, La Jolla, CA
RNeasy Midi Kit	Qiagen, Hilden, Germany
RNeasy Plus Mini Kit	Qiagen, Hilden, Germany
TOPO XL PCR Cloning Kit	Invitrogen, Carlsbad, CA
Zero Blunt TOPO PCR Cloning Kit	Invitrogen, Carlsbad, CA

2.1.2 Molecular Weight Markers

Precision Plus Prestained Protein Standard	Bio-Rad (Hercules, CA)
100 bp DNA ladder	Invitrogen, Carlsbad, CA
1 kb DNA ladder	Invitrogen, Carlsbad, CA

2.1.3 Antibodies

Antibody	Clone	Conjugate	μg/stain	Vendor
Anti-mouse F4/80	BM8	PE	0.125	eBioscience
Anti-mouse CD11b	M1/70	FITC	0.25	eBioscience
Anti-mouse B220	RA3-6B2	APC	0.125	eBioscience
Anti-mouse B220	RA3-6B2	PE	0.25	eBioscience
Anti-mouse TCRβ	H57-597	APC	0.06	eBioscience
Anti-mouse CD4	RM4-5	PE	0.1	Caltag Lab.
Anti-mouse CD4	RM4-5	PE-Cy7	0.25	eBioscience
Anti-mouse CD8α	53-6.7	FITC	0.25	eBioscience
Anti-mouse CD3	17A2	PE	0.25	BioLegend
Anti-mouse IgM	II/41	PerCP-eFluor710	0.25	eBioscience
Anti-mouse IgD	11-26c	FITC	0.5	eBioscience

Anti-mouse CD16/32	2.4G2	unconjugated	1.0	Bio Express
Anti-mouse IFNγ	XMG1.2	FITC	0.5	eBioscience
Anti-mouse IL-4	11B11	APC	0.25	BD Bioscience

TABLE 1: FACS Antibody List

Antibody	Clone	Dilution	Vendor
Anti-mouse IFNγ	AN-18	1:250	eBioscience
Biotin anti-mouse IFNγ	R4-6A2	1:500	eBioscience
Anti-mouse IL-4	11B11	1:250	eBioscience
Biotin anti-mouse IL-4	BVD6-24G2	1:500	eBioscience
Anti-mouse IL-6	MP5-20F3	1:250	eBioscience
Biotin anti-mouse IL-6	MP5-32C11	1:500	eBioscience
Anti-mouse IL-10	JES5-2A5	1:250	BD Pharmingen
Biotin anti-mouse IL-10	JES5-16E3	1:500	BD Pharmingen
Anti-mouse IL-17A	eBio17CK15A5	1:250	eBioscience
Biotin anti-mouse IL-17A	eBio17B7	1:500	eBioscience
Anti-mouse TNFα	Goat IgG	1:250	R&D Systems
Biotin anti-mouse TNFα	Goat IgG	1:500	R&D Systems

TABLE 2: ELISA Antibody List

Antibody	Species	Dilution	Vendor
Gata 3 (HG3-31)	mouse	1:1000 (WB)	Santa Cruz Biotechnologies
H4 cit 3 (07-596)	rabbit	1:500 (IF) 2 μl/ IP (ChIP)	Millipore
H4R3(me)$_2$ (39275)	rabbit	3 μl/ IP (ChIP)	Active Motif
H4 acetyl (17-229)	rabbit	1 μl/ IP (ChIP)	Millipore
CARM1 (ab51742)	rabbit	1:1000 (WB)	abcam
tubulin (ab6046)	rabbit	1:3000 (WB)	abcam
citrulline (17-347)	rabbit	1:1000 (WB)	Millipore
H3cit (ab5103)	rabbit	1:100 (IF)	abcam
H3R17(me)$_2$ (07-214)	rabbit	1:1000 (WB)	Millipore
huPAD4	rabbit	1:3000 (WB) 1:100 (IF)	gift from
2206 A	rabbit	1:2000 (WB)	generated in collaboration with Imgenex
MPO (A 0398)	rabbit	1:300 (IF)	DAKO
NIP45 mix	mouse	1:1000 (WB)	gift from Laurie Glimcher
T-bet (4B10)	mouse	1:1000 (WB)	gift from Laurie Glimcher
FLAG M2 HRP (F1804)	mouse	1:3000 (WB)	Sigma
FLAG M2 agarose	mouse	5 μl/ IP	Sigma
myc tag (71D10)	rabbit	1:1000 (WB)	Cell Signaling Technologies
HA agarose (A2095)	mouse	5 μl/ IP	Sigma
HA HRP (3F10)	mouse	1:2000 (WB)	Roche
GFP (A6455)	rabbit	1:5000 (WB)	Invitrogen
normal rabbit IgG	rabbit	1:200 (IF) 1 μl/ IP (ChIP)	Millipore
rabbit HRP (G21234)	goat	1:10000 (WB)	Invitrogen
mouse HRP (81-6720)	rabbit	1:10000 (WB)	Invitrogen
rabbit Oregon Green 488	goat	1:1000 (IF)	Invitrogen

TABLE 3: Antibody List (WB, IF, ChIP)

2.1.4 Primers

Name	Sequence (5' to 3')	Annealing (°C)
PAD4 mice		
Padi4 5' lox F	CAGGAGGTGTACGTGTGCA	59°C
Padi4 3' lox F	CTAAGAGTGTTCTTGCCACAAG	
Padi4 3' lox R	AGTCCAGCTGACCCTGAAC	
Padi4 3' FRT R	AGGAAGTCTTCATTGTCAGAAAC	
Cre ERt mice		
IMR 1084	GCGGTCTGGCAGTAAAAACTATC	65°C
IMR 1085	GTGAAACAGCATTGCTTGTCACTT	
IMR 3621	CGTGATCTGCAACTCCAGTC	
IMR 3622	GGAGCGGGAGAAATGGATATG	
Flp deleter mice		
IMR 1348 (Flp F)	CACTGATCTTGTAAGTAGTTTGC	56°C
IMR 1349 (Flp R)	CTAGTGCGAAGTAGTTGATCAGG	
CARM1fl/fl mice		
CARM1 FOR	CCCACTTCTGTTACCTCCTTTG	53°C
CARM1 REV	TAACTAAAAGAAAATGGAATGG	
CMV-Cre, Lck-Cre, lysM-Cre		
CRE FOR	GACGGAAATCCATCGCTCGACCAG	60°C
CRE REV	GACATGTTCAGGGATCGCCAGGCG	

TABLE 4: Genotyping Primer List

Name	Sequence (5' to 3')	Annealing (°C)
Exon 9-10 SalI FOR	TA**GTCGAC**TAACTCCTGCCCTCAGCCTCT	62°C
Exon 9-10 SalI REV	TA**GTCGAC**ATGATGCCCAAGAGATGGAACTCT	
5' ARM BamHI FOR	TA**GGATCC**TCTGTGTAGCCTTGCCTGTC	62°C
5' ARM BamHI REV	TA**GGATCC**TATTTTGCCATTCCCAGAAAATGC	
3' ARM FseI FOR	TA**GGCCGGCC**TGTCCTTTGGGGGCTACACTG	68°C
3' ARM FseI REV	TA**GGCCGGCC**TCACGGCTGGCTGCCTCTG	
5' probe 9-10 FOR	TGCCTAACATGTCTGATGTCATA	62°C
5' probe 9-10 REV	TGACTTTGGTAGGTCACTTGC	
3' probe 9-10 FOR	TGAATCAAGTCCATGGATGATGG	62°C
3' probe 9-10 REV	TGTGCCTGGTGCCCGAGGA	
rat PAD4 F2	GTGGATGCAGGATGAAATGGAGA	61°C
rat PAD4 T7P R	GAATTAATACGACTCACTATAGGGAGAGCACGTTGGTG CCACAGTGA	
mu GAPDH F	ATGGTAAAGGTCGATGTGAAC	58.5°C
mu GAPDH T7P R	GAATTAATACGACTCACTATAGGGAGACATGTAGGTCC ACCACCCT	

TABLE 5: Cloning Primer List

Name	Sequence (5' to 3')
NIP45 R32Q	TCCTCGCGCCCAGCAGTCTCCGG
NIP45 R32Q AS	CCGGAGACTGCTGGGCGCGAGGA
NIP45 R32K	GTGTCCTCGCGCCAAGCAGTCTCCGGCT
NIP45 R32K AS	AGCCGGAGACTGCTTGGCGCGAGGACAC
NIP45 R37Q	CCGGCAGTCTCCGGCTCAGCTCATTCCAGACA
NIP45 R37Q AS	TGTCTGGAATGAGCTGAGCCGGAGACTGCCGG
NIP45 R37K	GGCAGTCTCCGGCTAAGCTCATTCCAGAC
NIP45 R37K AS	GTCTGGAATGAGCTTAGCCGGAGACTGCC
NIP45 R37F	CCGGCAGTCTCCGGCTCAGCTCATTCCAGACA
NIP45 R37F AS	TGTCTGGAATGAGCTGAGCCGGAGACTGCCGG
NIP45 R103Q	CGGCGGCGGCAGCGGCTGCTG
NIP45 R103Q AS	CAGCAGCCGCTGCCGCCGCCG
NIP45 R103K	CGAAGTCTCCGGCTAAGCTCATTCCAGAC
NIP45 R103K AS	TCCAGCAGCCGCTTCCGCCGCCGTCG

NIP45 R103F	GCGACGGCGGCGGTTCCGGCTGCTGGATC
NIP45 R103F AS	GATCCAGCAGCCGGAACCGCCGCCGTCGC
NIP45 R104Q	GCGGCGGCGGCAGCTGCTGGATC
NIP45 R104Q AS	GATCCAGCAGCTGCCGCCGCCGC
NIP45 R104K	CGGCGGCGGCGGAAGCTGCTGGATCC
NIP45 R104K AS	GGCTCCAGCAGCTTCCGCCGCCGCCG
NIP45 R104F	ACGGCGGCGGCGGTTCCTGCTGGATCCCG
NIP45 R104F AS	CGGGATCCAGCAGGAACCGCCGCCGCCGT

TABLE 6: Mutagenesis Primer List

Name	Sequence (5' to 3')	Reference
mTNFα FOR	AGCCGATGGGTTGTACCT	(Nomiyama et al., 2007)
mTNFα REV	TGAGTTGGTCCCCCTTCT	
IL-6 F	GGACCAAGACCATCCAATTC	(Kim et al., 2007)
IL-6 R	ACCACGTGAGGAATGTCCA	
HPRT FOR	GCCCTTGACTATAATGAGTACTTCAGG	
HPRT Rev	GAGTACTTCCGCTCATCTTAGG	(Sandler et al., 2003)
CARM1 FOR	TGGCTCAGCATGCAGAGG	(in house)
CARM1 REV	TGCCAGGGATGACCACG	
IP10 FOR	CCTGCCCACGTGTTGAGAT	(Doyle et al., 2002)
IP10 REV	TGATGGTCTTAGATTCCGGATTC	

Name	assay number	supplier
mouse IL-4 AOD	Mm 00445259_m1	Applied Biosystems
mouse ACTB	4353933E	Applied Biosystems

TABLE 7: qPCR Primer and Probe List

Name	Sequence (5' to 3')	Reference
IL-4 pr FOR	GGCCCAGAATAACTGACAATCT	(Ansel et al., 2004)
IL-4 pr REV	GCAATGCTGGCAGAGGTC	
IFNγ pr FOR	GCTTTCAGAGAATCCCACAAGAAT	(Ansel et al., 2004)
IFNγ pr REV	GCTATGGTTTTGTGGCATGTTAGA	
HS IV FOR	TGCCCACATGAAATACCAGC	(Doyle et al., 2002)
HS IV REV	GCATACCTTCCCTGATTGGC	
CNS I Th2 FOR	CACACACTGGTCCACTGTGATG	(Hayashida et al., 2006)
CNS I Th2 REV	GACGCAGGCACCAAAATTAAA	

TABLE 8: ChIP Primer List

2.2 Technical Equipment

5415D Eppendorf Table-top Centrifuge	Eppendorf, Hauppauge, NY
5415R Eppendorf Table-top Centrifuge	Eppendorf, Hauppauge, NY
5810R Eppendorf Centrifuge	Eppendorf, Hauppauge, NY
7900HT Fast Sytem Real-Time PCR machine	Applied Biosystems, Foster City, CA
Accumet Basic AB15 pH Meter	Fisher Scientific, Pittsburgh, PA
Autoclave Amsco Scientific Series	Steris Corporation, Mentor, OH
Axiovert 100 Microscope	Zeiss, Goettingen, Germany
Bioruptor	Diagenode Sparta, NJ
CO_2 Incubator Forma Series II water-jacketed	Thermo Scientific, Waltham, MA
Forma -86C ULT Freezer	Thermo Scientific, Waltham, MA
Owl Gel Separation System	Thermo Scientific, Waltham, MA
Gene Amp PCR System 2700	Applied Biosystems
Gene Pulser XCell	Bio-Rad, Hercules, CA
Isotemp 125D Heating Blocks	Fisher Scientific, Pittsburgh, PA

Isotemp Freezer	Fisher Scientific, Pittsburgh, PA
Isotemp Hybridization Incubator	Fisher Scientific, Pittsburgh, PA
Isotemp Incubator	Fisher Scientific, Pittsburgh, PA
Labline Lab Rotator Platform	Barnstead, Dubuque, IA
Legend T centrifuge	Thermo Scientific, Waltham, MA
MACS Multi Stand	Miltenyi Biotec, Bergisch Gladbach
Micromaster Inverted Microscope	Fisher Scientific, Pittsburgh, PA
Mini Protean 3 Cell	Bio-Rad, Hercules, CA
Model 583 Gel Dryer	Bio-Rad, Hercules, CA
Power Pac 3000	Bio-Rad, Hercules, CA
Power Pac Basic	Bio-Rad, Hercules, CA
PTC-100 Peltier Thermal Cycler	MJ Research, Waltham, MA
RC5C Sorvall Centrifuge	Thermo Scientific, Waltham, MA
Refrigerator Isotemp	Fisher Scientific, Pittsburgh, PA
Scale Adventurer AR5120	Ohaus Corp, Pine Brook, NJ
Series 25 Incubator Shaker	New Brunswick Scientific Co., Inc
Smart Spec Plus Spectrophotometer	Bio-Rad, Hercules, CA
Spectrolinker XL-1000 UV Crosslinker	Spectromics Corp., New York, NY
SRX-101A Medical Film Processor	Konica Minolta, Wayne, NJ
Sterilgard Hood class II	Baker Company, Sanford, ME
Stirrer/ Hot Plate	Corning Inc., Corning, NY
Thermolyne Labquake Shaker	Barnstead, Dubuque, IA
Thermolyne Labquake Shaker/Rotisserie	Barnstead, Dubuque, IA
Transfer Blot Semi Dry Transfer Cell	Bio-Rad, Hercules, CA
Vmax kinetic microplate reader	Molecular Devices, Sunnyvale, CA
Vortex Genie 2	Scientific Industries, Bohemia, NY
Water Bath Isotemp 3016	Fisher Scientific, Pittsburgh, PA
Water Purification System	Millipore, Billerica, MA

2.2.1 Computer Programs

AxioVision AC 4.2	Zeiss, Goettingen, Germany
Endnote X	Endnote, Carlsbad, CA
FACS DIVA 6.0	BD Biosciences, San Jose, CA
FlowJo 8.8.4	Tree Star, Ashland, OR
Prism 5 (for MAC OS X)	GraphPad Software, La Jolla, CA
SerialCloner 1.3	Serial Basics
SoftMax Pro 4.7.1	Molecular Devices, Sunnyvale, CA

2.2.2 Internet Tools

http://biogps.gnf.org
http://uswest.ensembl.org/index.html
http://www.ncbi.nlm.nih.gov/sites/entrez?db=pubmed
http://www.stratagene.com/sdmdesigner/default.aspx

2.3 Tissue Culture

2.3.1 Cell Culture Media

RPMI 1640	(HyClone)
DMEM/ High Glucose	(HyClone)
IMDM Modified	(HyClone)
HEPES 1M Solution (100x)	(Cellgro)
Sodium Pyruvate 100mM Solution (100x)	(HyClone)
MEM Non-Essential Amino Acids (NEAA) (100x)	(HyClone)
L-Glutamine 200mM Solution (100x)	(HyClone)
Penicillin-Streptomycin Solution (P/S) (10000 units/ml) (200x)	(HyClone)
β-Mercaptoethanol (βME)	(Sigma-Aldrich)
Trypsin 0.25% (1x)	(HyClone)
DPBS/ Modified	(HyClone)
Fetal Bovine Serum (FBS)(Advantage)	(Atlanta Biologicals)
OptiMEM I	(Gibco)

2.3.2 Cytokines, Antibodies, and Stimuli

IFNγ	(10μg/ml)	(R&D Systems)
IL-4	(10μg/ml)	(PeproTech Inc.)
IL-12	(10μg/ml)	(eBioscience)
IL-2	(100U/μl)	(NCI)
IL-6	(10μg/ml)	(R&D Systems)
IL-23	(10μg/ml)	(eBioscience)
hTGFβ	(10μg/ml)	(R&D Systems)
α CD3 (2C11)	(4.33mg/ml)	(BioExpress)
α CD28 (37.51)	(1.2mg/ml)	(BioExpress)
α IL-4 (11B11)	(4.2mg/ml)	(BioExpress)
α IFNγ (R4-6A2)	(5mg/ml)	(BioExpress)
LPS *(E.coli* 0111:B4 strain)	(5mg/ml stock)	(Invivogen)
dexamethasone	(10mM stock in EtOH)	(Sigma-Aldrich)
cycloheximide	(10mg/ml stock in H_2O)	(Sigma-Aldrich)
ionomycin	(10mM stock in DMSO)	(EMD)
phorbol-12-myristate-13-acetate	(1mg/ml in DMSO)	(EMD)
Z-(4)-Hydroxytamoxifen	(1mM stock in EtOH)	Alexis Biochemicals

2.3.3 Cell Lines: Maintenance and Transfection

All cell lines were maintained in humidified tissue culture incubators at 37°C under 5% CO_2. Cell numbers were determined by counting in a Neubauer counting chamber. Dead cells were excluded by trypan blue staining (HyClone).

2.3.3.1 M12 Cells

The murine B cell lymphoma cell line M12 was grown in RPMI 1640 supplemented with 10% FBS, HEPES, P/S, L-glutamine, NEAA, sodium pyruvate, and 50 μM βME (RPMI complete). The cells grow semi-adherently and were passaged by scraping.

24h prior to transfection, the cells were plated with fresh media to ensure optimal growth conditions. M12 cells were transfected by electroporation. 20 μg total plasmid DNA was mixed with $5x10^6$ cells resuspended in 400 μl OptiMEM I. The mixture was transferred to 4mm electroporation cuvettes (Genesee Scientific) and

pulsed at 280V, 975 μF in a Gene Pulser XCell (Bio-Rad). After electroporation, the cells were allowed to rest for 5min at RT prior to addition of 800 μl RPMI complete. The transfected cells were transferred into 5ml prewarmed media and split into two wells of a 6-well tissue culture plate (Costar). Half of the wells were analyzed by IF the next day or for IL-4 transcript 30h post-transfection, and the other half was harvested 72h post-transfection. Overexpression of the transfected constructs was analyzed by WB, and the supernatants were screened for IL-4 secretion by ELISA.

2.3.3.2 293T Cells

The human kidney cell line HEK293T was maintained in DMEM supplemented with 10% FBS, HEPES, P/S, and L-glutamine. The cells grow in an adherent monolayer and were passaged by trypsinization.

293T cells were utilized for overexpression studies. 3.0×10^6 cells were plated per 6-well tissue culture plate the day prior to transfection in 2ml media/well. 293T cells were transfected using the LTX reagent (Invitrogen). 2.5μg total plasmid DNA was resuspended in 500μl OptiMEM I for each transfection. 6.25 μl LTX reagent was added to the solution. The tube was vortexed briefly and incubated at RT for 30min. The mixture was added dropwise to the cells. Transfections were analyzed 24h later. Cells were rinsed once with ice-cold PBS and stored at -80C prior to lysis.

2.3.3.3 L929 Cells

The L929 murine fibroblast cell line was maintained in DMEM supplemented with 10% FBS, HEPES, and P/S. The cells were passaged by trypsinization.

L929 cells were used as a source for colony-stimulating factor (CSF), which is an important growth factor for bone- marrow derived macrophage culture. To produce L929 conditioned media, 1×10^6 cells were plated in 150ml DMEM complete per $162cm^2$ tissue culture flask. The supernatant was harvested twice ten days apart, yielding 300ml of conditioned media from each flask. The supernatants were combined and stored at -20C in 15ml aliquots.

2.3.3.4 HL60 Cells

The human promyelocytic leukemia cell line HL60 was cultured in RPMI complete (see M12 cell culture section). HL60 cells can be differentiated towards a granulocyte-like cell by addition of 1.25% DMSO to the culture medium. Cells were seeded at a density of 4.0×10^5 cells/ml and were grown in 30ml media in 15cm tissue culture plates. DMSO was added at a final concentration of 1.25%, or cells were left untreated. After 72h in culture, the cells were harvested by pipetting. Pellets were rinsed in ice-cold DPBS and frozen at -80C until lysates were prepared.

2.3.4 Primary Cell Culture

2.3.4.1 T Helper Cell Isolation and Differentiation

Murine CD4+ T cells were isolated from pooled spleen and lymph nodes of four to six week old mice. A single-cell suspension was obtained by passing the organs through 70μm sterile cell strainers (Fisher Scientific). The cells were lysed in red blood cell lysis buffer (RBC) and resuspended in MACS buffer. The cell mixture was purified either with the MACS $CD4^+$ T Cell Isolation Kit (Miltenyi Biotec) for ChIP assays and RNA prep or with the MACS $CD4^+CD62L^+$ T Cell Isolation Kit II (Miltenyi Biotec) for all other applications following the manufacturer's suggestions.

MACS-purified cells were differentiated *in vitro* on αCD3 (1μg/ml)/ αCD28 (2μg/ml)- coated 24 well tissue culture plates. Cells were grown in RPMI complete for Th1 and Th2 differentiation and in IMDM complete for Th17 differentiation. IMDM complete contained the same supplements as RPMI complete.

To differentiate the cells towards the various lineages, a cytokine cocktail was added for each condition: Th1 cells were differentiated by addition of 100U/ml IL-2, 5ng/ml IL-12, and 10μg/ml αIL-4. For Th2 cells, 100U/ml Il-2 were added together with 10ng/ml IL-4, and 10μg/ml αIFNγ. On day 3, the cells were taken off the coated plates and plated into 6 well plates containing fresh RPMI complete supplemented with IL-2 (100U/ml) and grown until they were ready for harvest or restimulation. Th17 differentiation required the addition of 10ng/ml IL-23, 20ng/ml IL-6, 0.3ng/ml hTGFβ, 10ug/ml αIL-4, and 10ug/ml αIFNγ. The cells were cultured continuously on αCD3/ αCD28-coated plates and harvested on day 4.

RBC lysis	MACS buffer
10mM KHCO3	DPBS
150mM NH4Cl	0.5% BSA
1mM EDTA	2mM EDTA
filter sterilized	filter sterilized and degassed

2.3.4.2 Bone-Marrow Derived Macrophage (BMDM) Culture

Bone marrow was harvested from front and hind legs of mice. Femur and tibia of the legs were prepped and placed in ice-cold sterile DPBS. Excess muscle and tendon were removed. The bone marrow was flushed with sterile DPBS and collected by centrifugation. Red blood cells were lysed by addition of RBC lysis buffer. The cells were resuspended in 10ml DMEM containing 10% FBS, HEPES, and P/S (DMEM complete) and passed through a sterile cell strainer to obtain a single cell suspension. Bone marrow was plated on one 10cm plastic dish per mouse (untreated plastic) and placed in the tissue culture incubator for 3-4h to allow fibroblasts to adhere. The non-adherent cells were harvested and resuspended in 100ml conditioned DMEM (10%FBS, HEPES, P/S, 30% L929 sup) and distributed among ten 10cm plates (untreated plastic). The media was replaced on d3 of culture and the cells were harvested on d6.

For CreERt-mediated deletion during BMDM differentiation, 10 nM 4-hydroxytamoxifen (4-OHT) was added to the supplemented media at the start of the culture and at d3 during refeeding of the cells. After cell harvest on d6, the cells were maintained in DMEM complete without 4-OHT.

To detach the BMDMs from plastic, the culture media was removed and replaced with 5ml detachment solution per plate. After incubation at 37C for 15min, the cells were detached with a cell lifter and pooled by centrifugation. The cells were resuspended in DMEM complete. For stimulations, cells were replated at the following densities: $1.25x10^5$ cells/ well for 48 well plates, $2.5x10^5$ cells/well for 24 well plates, and $1.0x10^6$ cells/well for 6 well plates.

BMDM maturation was assayed by FACS analysis of CD11b and F4/80 expression levels. After six days of culture, more than 95% were double-positive for those markers.

Detachment solution:

1:1 mixture of	RPMI with 20% FBS
and	DPBS with 2mM EDTA

2.4 Molecular Biology

2.4.1 Cloning

All cloning primers and annealing temperatures are listed in Table 5. In general, DNA was amplified by polymerase chain reaction (PCR) using the KOD Hot Start Polymerase (Novagen) with the following cycling conditions:

5µl 10x KOD buffer	95°C	2:00min
3µl 25nM $MgSO_4$	95°C	0:20min
5µl dNTPs (2mM each)	variable	0:10min
1µl KOD Pol	70°C	0:20min/ kb
1µl template DNA	go to step 2 for 34 cycles	
1.5µl 10µM FOR primer	70°C	5:00min
1.5µl 10µM REV primer	4°C	hold
32µl H_2O		

All PCR products were gel purified using the Qiagen Gel Extraction kit following the manufacturer's instructions. The purified DNA was subcloned using the TOPO blunt cloning kit (Invitrogen).

The only exception was the amplification of the 3'ARM for the targeting vector cloning, which was amplified using the TaKaRa LA Taq polymerase (Takara) with the following cycling conditions:

5µl 10x buffer	94°C	1:00min
8µl dNTP mix	98°C	0:05min
1µl template DNA	68°C	4:00min
1µl 10µM FOR primer	go to step 2 for 34 cycles	
1µl 10µM REV primer	72°C	10:00min
0.5µl LA Taq DNA pol	4°C	hold
33.5µl H_2O		

The 3'ARM PCR product was subcloned using the TOPO XL kit (Invitrogen).

All subcloned PCR fragments were verified by analytical restriction digest and sequencing of mini prep DNA using the Fast Mini prep kit (5Prime). Verified clones were further expanded by maxi prep using the HiPure maxi kit (Invitrogen) for further cloning steps.

All restriction digests were performed using NEB enzymes with conditions recommended by the manufacturer. Linearized plasmids and inserts were ligated using the T4 DNA ligase (high concentration) from Invitrogen, allowing the ligations to proceed overnight at 4°C.

2.4.1.1 PAD4 targeting vector cloning

The PAD4 targeting vector was generated by use of the pRAPIDflirt vector (gift from A. Waisman). This vector comprises a FRT-flanked PGKneoR cassette and the HSV thymidine kinase gene for positive and negative selection, respectively. All cloning fragments were amplified from BAC DNA that contained the whole PAD4 genomic locus (RP23-48K5). The 5' and 3' homology arms (1.9kb and 5.3kb) were amplified using the following primers: 5' ARM BamHI FOR, 5' ARM BamHI REV, 3' ARM FseI FOR, and 3' ARM FseI REV. The 5' ARM was cloned into pRAPIDflirt via the *Bam*HI site, and the 3' ARM was cloned via the *Fse*I site. The conditional region, including exons 9 and 10 (1.7kb), was amplified with Exon 9-10 SalI FOR and Exon 9-10 SalI REV. It was cloned into the targeting vector via the *Sal*I restriction site between the two loxP sites.

All cloning steps were verified by analytical restriction digests and sequencing of the targeting vector. 150µg of a maxiprep of the targeting vector DNA was linearized with *Not*I prior to electroporation into Bruce4 ES cells in the Gene Targeting Core at the Scripps Research Institute.

2.4.1.2 Northern and Southern Probe Cloning

Similar to the targeting vector cloning, the Southern blot probes were amplified using BAC DNA as a template. The primers for the 5' probe were 5' probe 9-10 FOR and REV and for the 3' probe were 3' probe 9-10 FOR and REV. Both primer pairs yielded PCR products of 606bp.

Northern blot probes were amplified using the primers rat PAD4 F2, rat PAD4 T7P R, mu GAPDH F, and mu GAPDH T7P R. The reverse primers contained the T7 polymerase promoter sequence required for synthesis of the probe. The PAD4 specific probe (700bp) was amplified from an expression vector containing ratPAD4 cDNA. The GAPDH probe (1kb) was amplified from C57BL/6 macrophage cDNA.

2.4.1.3 Mutagenesis

All mutagenesis primers were designed using the QuickChange primer design program and are listed in Table 6. Mutagenesis was performed using the QuickChange Lightning Mutagensis kit (Stratagene). The template was a pEGFPc2-NIP45 expression plasmid, and the extension time was 3:30min. All mutants were confirmed by sequencing.

2.4.2 Quantitative Real-time PCR (qPCR)

qPCR was used to determine transcript levels of stimulated BMDMs or transfected M12 cells. Both TaqMan and SYBR green technology was utilized. Primers and probes are listed in Table 7. All reactions were analyzed on the 7900HT Fast Real-Time PCR System (Applied Biosytems). Data was analyzed in Excel using the ΔCt method. In summary, the mRNA amounts of the gene of interest (GOI) were standardized against the mRNA levels of a housekeeping gene (HPRT or β-actin) and expressed as ΔCt (= $Ct_{housekeeping}$-Ct_{GOI}). The mRNA copy ratio of GOI to housekeeping gene was calculated as $2^{\Delta Ct}$ and normalized to a reference sample.

2.4.2.1 RNA Extraction and Purification

RNA from BMDMs or M12 cells was prepped using the RNeasyPlus Mini Prep kit (Qiagen) following the manufacturer's instructions. The homogenization step was performed using QIAshredder columns (Qiagen). RNA was eluted in 40μl RNase-free water supplied with the kit. RNA concentration and quality was determined via spectrophotometry.

2.4.2.2 cDNA Synthesis

Depending on the yield of the RNA prep, 200ng- 2μg of RNA were used for cDNA synthesis. The RNA was treated with DNaseI (Invitrogen) to remove genomic DNA contamination from the samples. RNA was incubated with 1μl of 10xDNaseI buffer and 1μl DNaseI for 30min at 37°C. 1μl of 25mM EDTA was added to inactivate the enzyme, and the reaction was incubated for 15min at 65°C. 5μl of the DNase-treated RNA was used to synthesize cDNA with the iScript cDNA synthesis kit (Bio-Rad) following the manufacturer's protocol.

2.4.2.3 qPCR

cDNA samples were run in duplicates for each primer pair or probe. RNA minus reverse transcriptase and water were included as negative controls. Usually, 1μl of cDNA was used for each reaction.

TaqMan assays-on-demand (20x) probes were used to analyze IL-4 transcript levels in M12 cells upon overexpression of various proteins. The reactions were run in 20μl total volume using the TaqMan Universal PCR MasterMix (2x) (Applied Biosystems) reagent with standard settings on the 7900HT cycler.

BMDMs were analyzed for IL-6, TNFα, and IP-10 transcript levels relative to HPRT. The reactions were run in 20μl final volume using the 2xPowerSYBR green reagent (Applied Biosystems) using standard settings on the 7900HT cycler. The primers were used at 187.5nM final concentration. To assess the quality of the amplified product, a dissociation stage was added to each run to monitor the product peaks.

2.4.3 Southern Blot

Southern blotting refers to the transfer of DNA fragments from an electrophoresis gel to a membrane. The transfer immobilizes the DNA fragments, so the membrane carries a reproduction of the banding pattern of the gel. The membrane can be hybridized with radioactively labeled probes and visualized by autoradiography (Southern, 1975).

Southern blotting was used to screen for homologous recombination in ES cells for the generation of PAD4 ko mice, as well as confirmation of germline transmission of the targeted allele in mice.

2.4.3.1 Genomic ES Cell DNA Preparation

The ES cells were electroporated and selected at the Gene Targeting Core Facility at the Scripps Research Institute. Cells from confluent 24 well plates were lysed by adding 200μl ES cell lysis buffer per well. The plates were incubated overnight in a water bath at 55°C. Lysates were transferred to 1.5ml tubes. After addition of 400μl EtOH, the tubes were inverted 20x to precipitate the DNA. The DNA was pelleted by centrifugation at 13000rpm for 10min. The pellets were rinsed once with 70% EtOH and allowed to air-dry at RT. The pellets were resuspended in 150μl sterile TE and dissolved or 4h at 55°C.

<u>ES cell lysis buffer</u>
100mM Tris-HCl, pH 8.5
5mM EDTA
0.2% SDS
200mM NaCl
100mg/ml proteinase K

2.4.3.2 Genomic DNA Digest

Genomic DNA was digested with *Hind*III or *Bam*HI (NEB) to generate fragments that would yield an altered pattern in gene-targeted ES cells or mice with germline-transmission. 15-30μl of genomic DNA were digested with 50-100U of the restriction enzyme of choice with the corresponding buffer in a total volume of 50μl. To allow efficient digest in the presence of proteins and RNA, spermidine (1mM), BSA (100μg/ml), DTT (1mM), and RNaseA (50μg/ml) were added to the restriction mix. Digests proceeded overnight at 37°C. The digested DNA was mixed with 5xDNA loading dye (50% glycerol with bromophenol blue and xylene cyanol).

2.4.3.3 DNA Gel and Transfer

Large DNA fragments were separated in low percentage agarose gels. 0.7% (w/v) agarose gels were prepared in 1xTAE buffer. Digested DNA was separated by electrophoresis at 40V in 1xTAE running buffer. A 1kb DNA ladder was run in parallel to provide a marker for fragment sizes. The gel was incubated in denaturation buffer for 1h at RT to obtain single-stranded DNA. Afterwards, the gel was rinsed with H2O and incubated in neutralization buffer for 1h at RT. The gel was transferred onto a membrane (Zeta Probe blotting membrane, Bio-Rad) using downward capillary

transfer in 10xSSC transfer buffer. The following day, the membrane was rinsed in water and crosslinked once (autocrosslink settings, Spectralinker XL-1000).

50xTAE	denaturation buffer	neutralization buffer
2M Tris base	1.5M NaCl	1.5M NaCl
1M glacial acetic acid	0.5N NaOH	500mM Tris HCl pH 7.5
500mM EDTA		

2.4.3.4 Probe Labeling and Hybridization

DNA probes were labeled using the Amersham RediPrime II Labelling System following the manufacturer's instructions. The labeled probes were purified using illustra ProbeQuant G50 Microcolumns (GE Healthcare). While the probes were labeling, the membrane was prehybridized in UltraHyb (Ambion) at 42°C. The purified probes were boiled for 5min and added to the prehybridization solution. The membranes were incubated overnight at 42°C. The next day, membranes were washed twice with 2xSSC, 0.1% SDS for 15min at 42°C and once with 0.1xSSC, 0.1% SDS for 20min at 42°C. The membranes were exposed to film at -80°C for various timepoints.

2.4.4 Northern Blot

Northern blotting is used to analyze gene expression in RNA samples isolated from tissue or cells (Alwine et al., 1977). It involves separation of RNA on an agarose gel, transfer of the RNA to a membrane and hybridization of the membrane with a radioactively labeled probe specific for you gene of interest.

2.4.4.1 RNA Sample Preparation

RNA was isolated from whole tissue or differentiated Th cell subsets using the RNeasy midi prep kit (Qiagen) following the manufacturer's instructions. RNA sample concentration and purity was determined by spectrophotometry, measuring OD_{260} versus OD_{280}. 10μg of RNA were precipitated by addition of 1/10 vol. 1M NaOAc pH 4.8 and 2.5 vol. ice-cold 100% EtOH. Precipitating samples were incubated at -20°C for at least 3h. The precipitate was collected by centrifugation (13000rpm, 25min, 4°C), washed with 80% EtOH, and air-dried. The pellet was resuspended in 10μl formamide loading dye and incubated overnight at 4°C.

Formamide loading dye (store at -20C)
5mM EDTA
in deionized formamide
0.1% (w/v) bromophenol blue
0.1% (w/v) xylene cyanol

2.4.4.2 RNA Gel and Transfer

Samples were separated on a 1.2% agarose/ formaldehyde gel. 2.0g agarose were dissolved in 120ml H_2O by boiling. The solution was allowed to cool down to 65°C, and 16.6ml 10xMOPS and 28.8ml formaldehyde were added. While the gel was solidifying, the RNA samples were incubated at 55°C for 15min. The tubes were vortexed briefly, and 10μl of 2xMOPS/ formaldehyde LB was added. The samples were boiled for 5min and loaded on the gel. The gel was run at 120V on ice in RNA running buffer for 4-6h. Afterwards, the gel was washed for 30-60min in 10xSSC with slow agitation. The RNA was transferred onto a membrane (Zeta probe blotting membrane, Bio-Rad) by downward capillary transfer overnight at RT using 10xSSC as transfer buffer. The next day, the moist membrane was crosslinked twice

(autocrosslink settings on the Spectrolinker XL-1000) and was ready for hybridization.

10xMOPS buffer	2xMOPS/ formaldehyde LB	RNA running
200mM MOPS pH 7.0	2xMOPS	800ml 1xMOPS
80mM sodium acetate	30% formaldehyde	20ml formaldehyde
10mM EDTA, pH 8.0	5mM EDTA	precool at 4C

20xSSC
3M NaCl
0.3M sodium citrate
pH to 7.0 with HCl

2.4.4.3 Labeling and Hybridization

The crosslinked membrane was placed in a hybridization bottle, and prewarmed hybridization solution was added. The bottles were incubated in the hybridization oven at 65°C at least 2h prior to addition of the labeled probe.

The labeling procedure described here requires that the probe template contains the T7 promoter sequence. Labeling reactions were incubated at 37°C for 5h:

4µl	5x T7 Pol buffer
1µl	100mM DTT
1µl each	10mM ATP, 10mM GTP, 10mM CTP
2µl	0.1mM UTP
2µl	template (500ng total)
3µl	α^{32}P-UTP (10mCi/ml)
1µl	RNase inhibitor
1.5µl	T7 polymerase
2.5µl	H_2O
20µl	

After labeling, 30µl H_2O were added to the reaction, and the labeled probe was purified with illustra ProbeQuant G50 Microcolumns. The purified probe was mixed with 800µl hybridization buffer and boiled for 5min. Then the mixture was added to the prehybridized membrane and incubated at 65°C overnight. The next day, the membrane was washed with 0.5xSSC, 0.1% SDS for 15min at 65°C and exposed to x-ray film at -80°C for various timepoints.

50x Denhardt's reagent
1% (w/v) Ficoll (Type400)
1% (w/v) polyvinylpyrrolidone 40
1% (w/v) BSA (fraction V)
store at -20C

hybridization solution
10ml deionized formamide
4ml 10x SSC
1ml 10% SDS
0.5ml 1M Na-phosphate pH 6.5
0.5ml 10mg/ml yeast RNA (boiled, 2min)
2ml 50x Denhardt's reagent
2ml H_2O

2.5 Mouse Work

Scripps Research Institutional guidelines were followed for all procedures involving mice.

2.5.1 Mouse Strains and Genotyping

C57BL/6 and Balb/c inbred strains were obtained from the Scripps Custom Breeding Facility. C57BL/6 albino (C57BL/6J-Tyrc-2J/J) females were purchased from the Scripps Gene Targeting Core Facility and used to screen PAD4 chimeras for germline transmission. Mice expressing Flp enzyme (B6.Cg-Tg(ACTFLPe)9205Dym/J) were purchased from the Gene Targeting Core Facility and were used to delete the FRT-flanked neomycin resistance cassette from PAD4 gene-targeted mice. Cre-deleter mice (B6.C-Tg(CMV-cre)1Cgn/J) were purchased from Jackson laboratories. This strain was intercrossed with PAD4fl/+ mice to obtain deletion of the loxP targeted region in the gene locus. Other Cre strains, all obtained either in house or through Jackson, include the CreERt strain (B6;129-Gt(ROSA)26Sor<tm1(cre/ERT)Nat>/J), the Lck Cre strain (B6.Cg-Tg(Lck-cre)548Jxm/J), and lysM Cre mice (B6.129P2-Lyz2tm1(cre)Ifo/J).

Strains with conditional alleles included CARM1fl/fl (Yadav et al., 2003) obtained from Prof. Bruening and PAD4fl/fl mice that were generated in this thesis. The CARM1fl/fl mice were backcrossed for 12 generations onto the C57BL/6 background.

Mice were genotyped using genomic DNA extracted from tail clips of mice. All primers and annealing temperatures can be found in Table 4.

2.5.2 PAD4 Conditional Knockout (cKO) Generation

Bruce 4 ES cells were electroporated with the linearized PAD4 targeting vector (for cloning see 2.4.1.1) in the Scripps Gene Targeting Core. Cells were subjected to positive and negative selection with G418 and ganciclovir, respectively. 300 clones were picked and screened for homologous recombination by Southern blot with the 5'probe. ES cells that carried the targeted insertion in the PAD4 locus were injected into C57BL/6 albino blastocysts. Chimeric males were mated with C57BL/6 albino females, and black offspring was genotyped by PCR and Southern blot for presence of the targeted allele. PAD4fl/+ mice were intercrossed with CMV-Cre and Flp-deleter strains to yield PAD4flΔneo/+ and PAD4+/- offspring.

2.5.3 Neutrophil Elicitation, Isolation, and Purification

Neutrophils were isolated from mouse peritoneal fluid following a protocol published in Current Protocols in Immunology (Luo and Dorf, 2001). This method is based on the recruitment of neutrophils into the peritoneal cavity after injection of a sterile inflammatory reagent.

Seven week old female PAD4-sufficient or –deficient mice were injected intra-peritoneally (ip) with 1ml sterile casein solution. The mice were injected a second time 14h after the first injection. Three hours later, the mice were euthanized by CO2 asphyxiation. The peritoneal cavity (PC) was flushed with 10ml harvest solution using a 10ml syringe and a 23G needle. The cells were pelleted by centrifugation (200xg, 7min, RT) and rinsed three times with 10ml DPBS. The cells were resuspended in 1ml DPBS and layered on top of 9ml Percoll gradient solution. The cell mixture was purified by ultracentrifugation (Beckman Ultima XL-100; SW41 rotor; 22200rpm, 20min, 4°C). The band containing polymorphonuclear cells was harvested. Cells were resuspended in 1ml DPBS, and total cell numbers were obtained by counting in a Neubauer chamber with trypan blue exclusion. This method yielded 1-5x10^6 neutrophils per mouse. These cells were adjusted to the appropriate cell density and used for immunofluorescence microscopy.

casein solution	harvest solution	Percoll gradient solution
9g casein	DPBS	10ml 10xPBS, pH7.2
into PBS	0.01% EDTA	90ml sterile Percoll
with 0.9mM CaCl2	sterile	
and 0.5mM MgCl2		
boil and autoclave		

2.5.4 PAD4 Monoclonal Antibody Production

Six eight-week old female Balb/c mice were injected (ip) each with 500µl antigen solution containing 22.5µg GST-PAD4 in complete Freund's adjuvant (CFA; Sigma-Aldrich). On day 14 and 35, the injections were repeated, but GST-PAD4 was emulsified in incomplete Freund's adjuvant (IFA). Eye bleeds were collected on day 24 and 45 and screened by ELISA against untagged recombinant PAD4. On day 56, the four best responders were injected with 25µg GST-PAD4 in PBS (ip). On day 59, all mice were euthanized by CO_2 asphyxiation. The spleen from the best responder was harvested. The splenocytes were fused to the Sp2/0 myeloma cell line following the instructions from Current Protocols in immunology "Production of Mouse monoclonal antibodies" (Yokoyama et al., 2006). Briefly, after fusion of splenocytes and myeloma cells, the cells were selected for successful hybridoma generation in a 96 well format. Surviving clones were expanded, and supernatants from these cells were screened for PAD4 reactivity. The best 20 responders were expanded. To ensure clonality, the most promising clones were recloned by serial dilution cloning, usually for two rounds, and then used for large scale monoclonal antibody production. The limiting dilution cloning and final expansion for antibody production steps were performed by the Antibody Production Core Facility of the Scripps Research Institute.

2.6 Biochemical Methods

2.6.1 Recombinant Protein Expression and Purification

Recombinant proteins were used in a variety of *in vitro* methylation and deimination assays, as well as for immunization of mice to generate a PAD4 monoclonal antibody. Protein quality was checked by SDS page and protein staining using the Biosafe Coomassie from Bio-Rad.

2.6.1.1 GST-PAD4 and GST-NIP45

Both GST-PAD4 and GST-NIP45 were recombinantly expressed using the pGEX4T vector system (GE Healthcare). Briefly, BL21(DE3)CodonPlus RIL cells (Stratagene) were transformed with the respective expression plasmids. Bacteria were cultured in 2xYT media with 100µg/ml ampicillin in a shaking incubator at 37°C until they reached OD_{600} of 0.6. The cultures were induced with 0.1mM IPTG and allowed to grow for an additional 18hrs at RT. The cultures were pelleted (4000rpm, 10min, 4°C), and the pellets were resuspended in DPBS containing 1% triton X-100 and protease inhibitors. Cells were lysed by sonication in the Bioruptor. The soluble fraction was purified using GST bind resin (Novagen) and eluted with 20mM glutathione pH 7.4. The eluted fractions were pooled, dialyzed against PBS for 48h, and concentrated to about 0.5mg/ml. In some preps, the GST-NIP45 was kept on the GST bind resin.

2xYT
16g bacto tryptone.
10g bacto yeast extract.
5g NaCl.

adjust pH to 7.0 with 5N NaOH.
adjust to 1L with distilled H_2O
autoclave to sterilize

2.6.1.2 His-NIP45

His-tagged NIP45 was expressed using the pET29a-vector. BL21(DE3)CodonPlus RIL cells were transformed with the expression plasmid. Cultures were grown in 2xYT with 30μg/ml kanamycin at 37°C until they reached an OD_{600} of 0.7, induced with 0.4mM IPTG, and grown for an additional 18h at RT. The cells were harvested by centrifugation. Cells were lysed, and His-NIP45 was purified using the PrepEase His Tagged Protein Purification Midi Kit (USB). Recombinant His-NIP45 was dialyzed against PBS for 48h and concentrated to about 0.5mg/ml.

2.6.2 *In Vitro* Methylation Reactions

Methylation reactions were performed on GST-NIP45 bound to GST bind resin. Beads equivalent to 2μg of protein were incubated with 1μg recombinant PRMT1 (gift from J. Hevel) and 2μl of ^{3}H-S-adenosyl-L-methionine (SAM) (1mCi/ml, Amersham), a tritiated methyl-donor, in methylation buffer (final volume 20μl). Reactions were allowed to proceed for 1h30min at RT and were stopped by addition of 5μl of 5xSDS LB. If followed by a deimination reaction, the beads were washed three times with high volume of methylation buffer and then resuspended in deimination buffer instead.

methylation buffer	5xSDS LB
20mM Tris HCl pH6.8	312.5mM Tris HCl pH 6.8
200mM NaCl	50% glycerol
	10% SDS
	bromophenol blue
	5% β-mercaptoethanol

Methylation was analyzed by autoradiography. To this end, 15μl of the reaction sample was run on a 7.5% 10 well SDS gel. The gel was stained with Biosafe Coomassie (Bio-Rad) for 1h at RT. After rinsing in several changes of water, the gel was fixed for 30min (10% MeOH, 10% acetic acid) and then soaked in Amplify reagent (GE Healthcare) for an additional 30min to enhance the radioactive signal. The gel was washed in five changes of water and dried onto Whatman paper. The dried gel was placed into an intensifying screen (Kodak BioMax, Transcreen LE) and exposed to film (Hyperfilm MP, GE Healthcare) for 48h at -80C.

2.6.3 *In Vitro* Deimination Reactions

In vitro deimination reactions were performed using various sources of PAD4 enzyme: recombinant PAD4 (gift from P. Thompson), GST-PAD4, or immunoprecipitated HA-tagged PAD4. In all cases, reactions were performed in deimination buffer in a final volume of 20μl and allowed to proceed for 1h30min at 50°C. 1μg of recombinant PAD4 were used to deiminate 2μg of GST-NIP45 or His-NIP45. 2μl 0.5M EGTA were added to reactions to inhibit PAD4 activity. If PAD4 was immunoprecipitated from 293T cell lysates, the bead-bound enzyme was resuspended in reaction buffer, and recombinant substrate was added. Reactions were stopped by addition of EGTA or 5xSDS LB.

deimination buffer
40mM Tris HCl pH7.5
4mM CaCl2

4mM DTT (added fresh)

Deimination of NIP45 was analyzed by Western blotting using the Anti-Citrulline (modified) Detection kit (Millipore).

2.6.4 Western Blotting

Proteins were separated by SDS gel electrophoresis and transferred onto either PVDF or nitrocellulose membranes. The systems used were the Mini-Protean 3 Cell (Bio-Rad) gel electrophoresis system and the Semi-Dry blotting apparatus. 4-20% gradient gels (10 well or 15 well) or 7.5% SDS gels (10 well or 15 well) were purchased from Bio-Rad (Tris-HCl Ready Gels).

Protein lysates were prepared in either RIPA or 1% triton lysis buffer. Briefly, cells were rinsed in ice-cold DPBS and lysed in lysis buffer containing 1mM PMSF and 1mM sodium vanadate for at least 10min on ice. Cell debris was pelleted by centrifugation at 13000rpm, 10min, 4°C. Protein concentration was determined with the BCA assay kit (Pierce). Equal amounts of protein were mixed with either 2xLaemmli buffer or 5xSDS LB and boiled for 5min to denature the sample. Samples were loaded on SDS gels together with a prestained protein marker (Bio-Rad) and run at 120V for 1h10min in 1xSDS running buffer. After separation, proteins were transferred onto PVDF or nitrocellulose membranes (Bio-Rad) in 1xTransfer buffer using a semi-dry transfer apparatus (Bio-Rad)(15V, 45min). After transfer, membranes were blocked in either 5% milk/ TBST or 1% ovalbumin/TBST, depending on the antibodies used. Primary antibodies, which can be found in Table 3, were diluted in 5% BSA/ TBST or 1% OVA/TBST and incubated with the membrane for 1h at RT or overnight at 4°C. Membranes were rinsed three times for seven minutes and incubated for 1h in secondary species-specific HRP-conjugated antibody in 5% milk/ TBST. Membranes were washed as before, and signal was developed using Western Lightning Plus reagent (Perkin-Elmer). The membranes were exposed to Denville HyBlot CL film.

RIPA buffer	1% triton lysis	2xLaemmli buffer
50mM Tris HCl pH7.4	20mM HEPES pH7.4	125mM Tris HCl pH6.8
150mM NaCl	100mM NaCl	20% glycerol
1mM EDTA	50mM NaF	5% SDS
1% triton X-100	10mM β-glycerophosphate	bromophenolblue
1% sodium deoxycholate	1% triton X-100	5% β-mercaptoethanol
0.1% SDS		

5xSDS running buffer	1xTransfer buffer	TBST
5g SDS	2.9g glycine	50mM Tris HCl pH7.5
15.2g Tris base	5.8g Tris base	150mM NaCl
72.1g glycine	in 800ml H_2O	0.1% Tween-20
in 1l H_2O	add 200ml methanol	

2.6.5 Immunoprecipitation (IP)

Immunoprecipitations were carried out to either separate overexpressed proteins from 293T lysates for various downstream applications or to check for interaction with other coexpressed proteins (CoIP). Both IPs and CoIPs were carried out with lysates prepared from transfected 293T cells. Whole cell lysates (WCL) were generated with 1% triton lysis buffer. 10% of the lysates were kept aside as an input control. The rest of the lysate was precleared for 1h at 4°C by incubation with proteinG sepharose (Bio-Rad). The supernatants were incubated with HA- or FLAG-agarose (5μl/IP) together with 20μl proteinG sepharose and incubated overnight at

4°C. The next day, the beads were washed five times with vortexing and resuspended in 50µl 2xLaemmli buffer. After boiling the samples for 5min, the proteins were separated by SDS page and were analyzed by Western blotting as described above.

2.6.5.1 Endogenous IP of PAD4

Endogenous PAD4 was immunoprecipitated from HL-60 lysates to test the IP capacity of the PAD4 hybridomas. Those lysates were generated using RIPA buffer. Protein content was determined by BCA assay, and 500µg of protein were incubated with 200µl of the hybridoma sups in a final volume of 500µl. The IP was allowed to proceed overnight at 4°C. The next day, 50µl of proteinG sepharose were added to each sample and, after 1h at 4°C, the beads were collected and washed five times as described earlier. The beads were resuspended in 50µl 2xLaemmli buffer and boiled for 5min. Samples were analyzed by Western blotting.

2.6.5.2 Chromatin Immunoprecipitation (ChIP)

Chromatin immunoprecipitation (ChIP) was used to study the chromatin modifications at several genomic regulatory regions in Th2 cells. Briefly, cells were crosslinked, the genomic DNA was fragmented by sonication, and antibodies to a specific chromatin posttranslational modification were used to precipitate fragments that contain those modifications. The DNA pulled down by the antibodies was purified and used in a qPCR reaction. This qPCR reaction amplifies regulatory regions of interest. The signal can be compared to the input DNA signal, and percent enrichment for this modification can be measured for a particular regulatory region.

$CD4^+$ T cells were isolated from wt and PAD4 ko mice and differentiated to Th2 cells. On day 7, $4.5x10^7$ cells were either stimulated with PMA and ionomycin or left untreated. After 2h at 37°C, the cells were fixed with 1% formaldehyde for 10min at RT, and quenched by adding 0.125M glycine. The crosslinked cells were rinsed with DPBS containing 0.125M glycine and lysed in 400µl SDS lysis buffer by incubation on ice for 10min. 600µl ChIP dilution buffer was added to the samples that were sonicated in a Bioruptor 3x7min on high (30sec on, 30sec off). Cell debris was pelleted, and the supernatants were transferred into 15ml conical tubes containing 3ml ChIP dilution buffer. The samples were precleared for 1h at 4°C by addition of 100µl blocked protein A sepharose (Millipore) and 1µl of normal rabbit IgG (Millipore). The supernatants were distributed into four Eppendorf tubes and antibodies for IP were added (see Table 3). 40µl of the supernatants were set aside for the input samples. The IPs were allowed to proceed overnight at 4°C while rotating. The next day 30µl proteinA/ sepharose were added to each sample and incubated for an additional 45min. The beads were washed sequentially with ChIP wash 1, 2, and 3 for 10min each and then washed twice with TE pH8.0, 5min each. To elute the DNA, the beads were resuspended in 50µl ChIP elution buffer twice and eluted for 15min at RT. The input samples were mixed with 60µl of elution buffer, and all samples were incubated at 65°C overnight after addition of 6.6µl 5M NaCl to reverse the crosslinks. On d3, the supernatants were treated with proteinase K (2µl 0.5M EDTA, 2.66µl 1M Tris HCl pH6.5, 1.33µl 10mg/ml proteinase K) for 1h30min at 37°C. 550µl buffer PB were added to the supernatants and the DNA was purified using the QIAquick PCR purification kit. The DNA was eluted with 50µl EB and 100µl H_2O were added.

SDS lysis buffer	ChIP dilution buffer	ChIP wash 1
50mM Tris HCl pH8.0	16.7mM Tris HCl pH6.8	20mM Tris HCl pH8.0
1% SDS	67mM NaCl	150mM NaCl
10mM EDTA	1.2mM EDTA	2mM EDTA

	1.1% trition X-100	1% triton X-100 0.1% SDS
ChIP wash 2	ChIP wash 3	ChIP elution buffer
20mM Tris HCl pH 8.0	10mM Tris HCl pH 8.0	1% SDS
500mM NaCl	0.25M LiCl	0.1M $NaHCO_3$
2mM EDTA	1mM EDTA	
1% triton X-100	1% NP-40	
0.1% SDS	1% sodium deoxycholate	

The amount of precipitated DNA was analyzed by qPCR with primers described in Table 8. For each primer pair, a standard curve was generated using genomic DNA ranging from 40ng to 0.064ng. Data was expressed as % input after subtraction of the background IgG samples. All samples were run in duplicates.

2.6.6 Immunofluorescence (IF)

All immunofluorescent pictures were taken on an Axiovert 100 microscope and recorded using Axiovision AC.

2.6.6.1 GFP-NIP45 Localization

After identifying potential PTM sites in NIP45, mutants for those residues were generated. To ensure that the mutation would not affect subcellular localization, M12 cells that overexpressed those GFP-tagged mutants were analyzed by fluorescence microscopy.

24h after transfection, 2.0×10^5 M12 cells were seeded onto poly-L-lysine (Sigma) coated coverslips (0.01% poly-L-lysine in H_2O). The cells were resuspended in RPMI containing 0.1% BSA and were allowed to settle for 30min at 37°C. The media was removed and replaced with 1% paraformaldehyde (PFA) in PBS and fixed for 15min at RT. The cells were rinsed twice with DPBS, and nuclei were stained with DAPI (1mg/ml, Sigma) 1:2500 in DPBS for 10min at RT. Cells were rinsed with DPBS again and mounted onto microscopy slides with Dako fluorescence mounting medium.

2.6.6.2 Primary Neutrophil IF

Elicited mouse neutrophils were plated onto poly-L-lysine coated coverslips (0.001% in H_2O) in 6 well plates at a density of 1.2×10^5 cells in RPMI containing 0.1% BSA. Cells were allowed to adhere for 30min at 37°C. The media was changed to RPMI containing 0.1% BSA with 2mM $CaCl_2$ and 100ng/ml LPS. After 4h of stimulation at 37°C, cells were fixed and permeabilized in IF Fix for 15min at RT. Coverslips were rinsed three times with PBST and blocked for 1h30min in IF Block at RT. Primary antibodies (see Table 3) were added in 100µl IF Block per coverslip and incubated in a humidified chamber overnight at 4°C. The next day, coverslips were washed three times for 5min with PBST, and anti-rabbit Oregon Green 488 was added 1:1000 in IF Block and incubated for 2h at RT. Cells were washed twice 10min each with PBST and nuclei were stained with DAPI (1mg/ml; Sigma) 1:2000 in PBST for 15min at RT. Coverslips were washed twice for 5min in PBST and mounted onto microscopy slides with Dako fluorescence mounting medium.

IF Fix	IF Block	PBST
3.8% PFA	PBST	DPBS
2% NP-40	2% BSA	0.1% Tween 20
1% triton X-100	5% goat serum	

2.7 Cell Biology Assays

2.7.1 Arginase Activity Assay

The upregulation of Arginase I expression and activity is a hallmark of alternatively activated macrophages. Stimulation of BMDMs *in vitro* with type 2 cytokines like IL-4 or IL-13 can recapitulate this alternative activation pathway. Arginase I is involved in the metabolism of L-arginine. It degrades arginine into urea and ornithine.

To measure Arginase activity in BMDMs, I used a colorimetric assay modeled after Corraliza *et al*. (Corraliza et al., 1994). Cells were grown in 24 well plates and stimulated in triplicate with 10ng/ml IL-4 or left untreated. After 48h, the cells were rinsed twice with ice-cold DPBS and lysed with 100 μl 0.1% trition lysis buffer for 30min while shaking. Afterwards, 100μl $MnCl_2$ solution were added to the wells, and the plate was incubated for 10min in a waterbath at 55°C. 50μl of the lysates were transferred to 1.5ml Eppendorf tubes, mixed with 50μl arginine solution, and incubated at 37°C for 30min. After addition of 800μl stop solution and 50μl ISPF solution, the tubes were boiled for 45min. A standard curve ranging from 1.5-30μg/ml urea was treated using the same conditions (100μl standard + 800μl stop sol. + 50μl ISPF sol.). The colorimetric change was monitored by reading the samples in a plate reader at OD_{540}. A standard curve was generated with GraphPad software by linear regression, which allowed to calculate the amount of urea produced by the Arginase enzyme in the BMDM lysates.

0.1% triton lysis buffer	$MnCl_2$ solution	arginine solution
0.1% (v/v) triton X-100 in H_2O	10mM $MnCl_2$	0.5M arginine in H_2O
1mM PMSF	50mM Tris pH 7.5	
1mM sodium vanadate	(make fresh!)	

stop solution	ISPF solution
1 part H_2SO_4	9% (w/v) α isonitroso-propiophenone (MP Biomedicals) in ethanol
3 parts H_3PO_4	
7 parts H_2O	

2.7.2 Griess Assay

In an inflammatory environment, macrophages are exposed to various stimuli, like IFNγ and LPS, that lead to classical activation. One hallmark of a classically activated macrophage is upregulation of nitric oxide synthase 2 (NOS2). This enzyme converts L-arginine into OH-arginine and then into nitric oxide (NO). One way to calculate NO formation is by measuring nitrite (NO_2-), a primary and stable breakdown product of NO. The Griess Reagent System (Promega) can be used to measure nitrite production in the supernatants of stimulated BMDMs. This colorimetric assay is based on a diazotization reaction that was originally described by Griess in 1879.

BMDMs were grown in 24 well plates and stimulated in triplicates for 24h. The cells were treated with 10ng/ml IFNγ with 5ng/ml LPS or left untreated. After 24h, the supernatants were collected and analyzed with the Griess Reagent System following the manufacturer's instructions. Color development was analyzed in a plate reader at OD_{540} and the standards were used to generate a standard curve (linear regression) using the GraphPad software.

2.7.3 Enzyme-Linked Immunosorbent Assay (ELISA)

ELISAs were used to detect cytokine levels in supernatants of αCD3 stimulated Th cells or of stimulated BMDMs. The general protocol is the same for all cell types and is based on standard sandwich ELISA protocols.

96 well ELISA plates were coated with 2μg/ml capture antibody diluted in carbonate binding buffer (50μl/well). An exception is the TNFα capture antibody, which requires dilution in DPBS. The plates were incubated overnight at 4°C. The next day, the plates were washed four times with ELISA wash buffer and blocked with blocking buffer (200μl/well) for at least 2h to reduce nonspecific binding. Supernatants and standards of the cytokine of interest were diluted with dilution buffer in a separate low-protein binding plate. 50μl of the dilutions were transferred to the blocked 96 well plate and incubated overnight at 4°C. On the final day, the plates were washed four times, and 1μg/ml biotinylated detection antibody was added to the wells (50μl/well). The plates were incubated at RT for 1h and washed again. Alkaline phosphatase conjugated to avidin was used to detect the signal. Avidin-AP (Sigma) was diluted 1:1000 in dilution buffer and added to the wells (50μ/well) for 30min at RT. 5ml of detection buffer was mixed with 10μl of 1M $MgCl_2$ and one tablet of phosphatase substrate (Sigma-Aldrich). The plates were washed six times, and 50μl detection solution was added to the well. Color development was monitored, and the reaction was stopped by adding 50μl 2N NaOH. The plates were read at OD_{405} subtracting the background at OD_{450}. A standard curve was generated with SoftMaxPro, and only absorbances within the range were used to generate data.

carbonate binding buffer	blocking buffer	dilution buffer
6.15 parts 0.2M Na_2CO_3	1% BSA (fraction V)	blocking buffer
1 part 0.2M $NaHCO_3$	in DPBS	with 0.05% Tween
pH 9.4	(filtered)	

detection buffer	wash buffer
0.65ml 0.5M Na_2CO_3	DPBS
1.85ml 0.5M Na_2HCO_3	0.1% Tween
47.5ml H_2O	

2.7.4 Flow Cytometry

Flow cytometry is a technique that allows the analysis of protein expression in live cells on the single-cell level. In a flow cytometer, single cells labeled with fluorescent dyes pass through a laser beam. The fluorochromes are excited, the emitted light is detected by photomultipliers, and the intensity of the signal can be visualized. The forward and the sideward scatter of the laser beam gives an indication for the size and granularity of the cells.

Cells are usually stained with a cocktail of fluorescently- labeled antibodies, which can be used to distinguish cell populations in a mixture of cells. Unstained cells and single-stained cells were included in every experiment to allow compensation of the signal. All experiments were performed with a FACS Canto (BD Bioscience), and the data was analyzed with FloJo software (TreeStar).

2.7.4.1 Staining of Cell Surface Markers

Flow cytometry was used to analyze cell surface expression of *in vitro* generated BMDMs to check for proper maturation and for immune phenotyping of PAD4-deficient mice. For both purposes, the basic staining procedures were similar.

Cells were kept on ice during the whole procedure and protected from light once the antibodies were added. In general, $1x10^6$ cells (single-cell suspension) were used for each stain. The cells were washed with 1ml FACS buffer and collected by centrifugation (1200rpm, 4min, RT). The pellets were resuspended in 100μl FACS

buffer and 0.25μl Fc block antibody (anti-mouse CD16/32) was added to each tube. This is important since Fc receptors can unspecifically bind to the constant region of antibodies used in subsequent staining steps. The cells were incubated on ice for 15min. Afterwards, the cells were washed three times with 1ml FACS buffer, resuspended in 100 μl FACS buffer, and stained with the desired antibody-cocktails. Staining proceeded for 20-30min at 4°C. The cells were washed twice and resuspended in 1ml FACS buffer prior to analysis.

FACS buffer
DPBS
1% FBS

2.7.4.2 Intracellular Cytokine Stain (ICCS)

Flow cytometry cannot only be used for analysis of molecules on the cell surface but also for intracellular stains. This method requires permeabilization of the cell.

Th1 and Th2 cells were differentiated *in vitro* from naïve $CD4^+CD62L^+$ T cells as described in section 2.3.4. At day 7 of the culture, $5x10^6$ cells were resuspended at $1x10^6$ cells/ml in culture media and plated into one well of a 6 well plate. T cells were stimulated with 50ng/ml PMA and 1μM ionomycin in the presence of 1μg/ml brefeldin A for 5h at 37°C. Brefeldin A inhibits transport of proteins from the ER to the Golgi, thereby, preventing the secretion of cytokines by the Th cells. After stimulation, the cells were rinsed with FACS buffer and fixed in 1ml fixing buffer for 10min at RT. The cells were washed twice with FACS buffer and resuspended in permeabilization buffer at a concentration of $1x10^6$ cells/ 100μl. $1x10^6$ cells were used for each stain. Antibodies were added and cells were stained in the dark at 4°C for 30min. Cells were rinsed twice with permeabilization buffer and resuspended in 1ml FACS buffer prior to analysis on the FACS Canto.

Fixation buffer	permeabilization buffer
4% (w/v) paraformaldehyde in DPBS	0.1% (w/v) saponin (Sigma-Aldrich) 1% FBS in DPBS

2.8 Mass Spectrometry

GST-NIP45 was deiminated *in vitro* with recombinant PAD4. To determine the sites of deimination, the proteins were subjected to mass spectrometry. The mass analysis was performed in collaboration with the Ali Sarkeshik at the Yeast Resource Center (YRC). Briefly, 15μg of GST-NIP45 were deiminated with 15μg PAD4 using standard deimination reaction conditions. The deiminated proteins were precipitated with TCA, washed with acetone three times, and air-dried. The dried samples were submitted for mass spectrometric analysis where they were subjected to trypsin digestion.

2.9 Statistical Analysis

Data are presented as mean +/- SEM and were graphed with either GraphPad Prism or Excel. Statistical significance was determined using the Student's *t*-test. $P<0.05$ was considered as statistically significant. Significance levels were *, $P<0.05$; **, $P<0.01$; ***, $P<0.001$.

3 Results

3.1 Deimination of NIP45 and Functional Consequences

NIP45, an NFAT-interacting protein, can potentiate IL-4 production in a murine B cell line (Hodge et al., 1996). The arginine methyltransferase PRMT1 is a positive regulator of this process. Methylation of the arginine-rich N-terminus of NIP45 facilitates the interaction of NIP45 with NFAT, thereby, driving IL-4 transcription (Mowen et al., 2004). Furthermore, NIP45-deficient mice display severe defects in type 2 immunity, specifically, a strongly reduced IL-4 secretion by Th2 cells (Fathman et al., 2010).

Since the PAD family can also modify targets of PRMT-mediated methylation, NIP45 might serve as a target for deimination, providing a possible mechanism for negative regulation of NIP45 function in IL-4 transcription. Since NIP45 is predominantly expressed in the nucleus, PAD4, the only nuclear PAD, is the primary candidate for NIP45 deimination.

3.1.1 Deimination of NIP45 by PAD4

In order to test if NIP45 can be deiminated by the arginine deiminase PAD4, recombinant GST or GST-NIP45 were subjected to *in vitro* deimination assays with recombinant PAD4. Since PAD4 activity is Ca^{2+}-dependent, addition of EGTA was included to inhibit enzymatic activity. Deimination reactions were analyzed by Western blotting with an antibody recognizing chemically modified citrulline. GST-NIP45 could be deiminated by PAD4 *in vitro* in a Ca^{2+}-dependent manner (Figure 10A). To rule out the possibility that the GST-tag, which contains arginines, compromised the results, the deimination reactions were repeated with His-tagged NIP45, confirming the calcium-dependent deimination of NIP45 by PAD4 (Figure 10B).

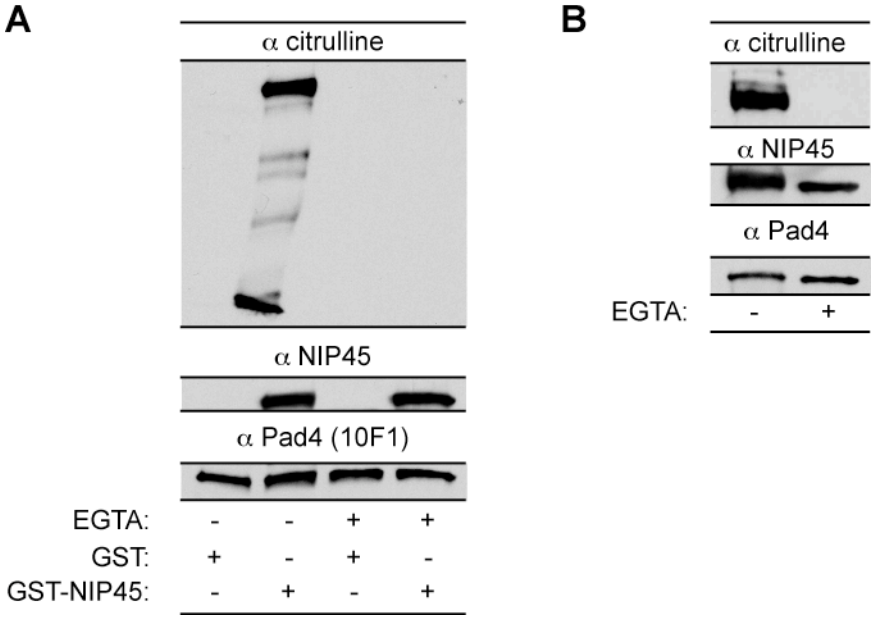

FIGURE 10: *In vitro* Deimination of Recombinant NIP45. (A) Recombinant GST or GST-NIP45 was incubated with PAD4 in the presence or absence of EGTA (50mM). The reactions were analyzed by Western blot to detect citrullinated protein. Equal amounts of protein were confirmed by probing for NIP45 and PAD4. (B) His-NIP45 was incubated with PAD4 with or

without EGTA. Citrullination was detected by α citrulline WB. Loading was confirmed with α NIP45 and α PAD4.

Additionally, I immunoprecipitated HA-tagged PAD4 and demonstrated that, like recombinant PAD4, HA-PAD4 was able to deiminate GST-NIP45 *in vitro* (Figure 11A). As expected, a catalytically inactive PAD4 mutant (HA-PAD4 C645S) failed to deiminate NIP45.

To address if endogenous NIP45 can be deiminated by PAD4, FLAG-NIP45 and myc-PAD4 were coexpressed in HEK293T cells. FLAG-NIP45 was immunoprecipitated and analyzed by probing with an antibody recognizing citrullinated proteins. Indeed, deiminated FLAG-NIP45 could be detected but only when myc-PAD4 was coexpressed (Figure 11B). Interestingly, myc-PAD4 co-immunoprecipitated with NIP45, demonstrating interaction between these two proteins. Furthermore, a signal corresponding to the size of myc-PAD4 was also visible in the α citrulline blot, confirming studies of auto-deimination by PAD enzymes (Andrade et al., 2010; Mechin et al., 2010)(Figure 11B).

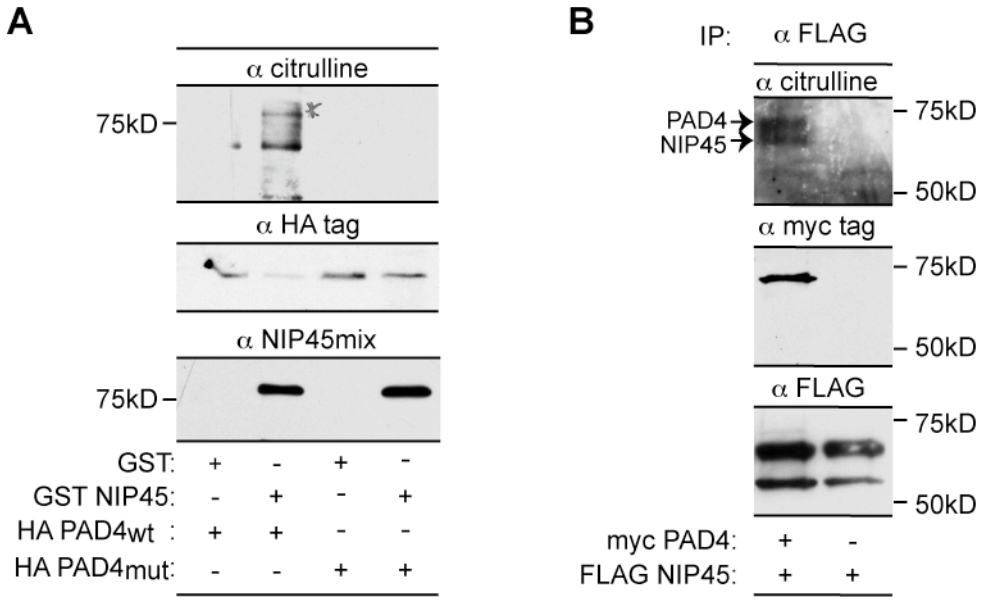

FIGURE 11: NIP45 Deimination *In Vivo.* (A) 293T cells were transfected with HA-PAD4 constructs (wt vs mut). Overexpressed PAD4 was immunoprecipitated with HA-agarose beads and mixed with recombinant GST or GST-NIP45 in a deimination reaction. Citrullination was detected by α citrulline blot. IP efficiency was tested with α HA probe, equal amounts of GST-NIP45 were confirmed by α NIP45 blot. (B) FLAG-NIP45 and myc-PAD4 were coexpressed in 293T cells. Lysates were immunoprecipitated with FLAG-agarose beads, and IPs were analyzed by immunoblotting with α citrulline, α myc tag, and α FLAG, respectively.

In conclusion, PAD4 and NIP45 can interact when coexpressed in HEK293T cells and NIP45 is deiminated by PAD4 *in vitro* and *in vivo*.

3.1.2 Deimination Can Prevent Arginine Methylation of NIP45

PAD and PRMT enzymes target peptidylarginines for posttranslational modification. These two enzyme families often compete for the same substrate. In many cases, the targeted residues overlap, which is best exemplified in the modification of histone H3 and H4 tails (see Figure 5). Several studies have shown that monomethylated but not dimethylated arginines can be deiminated by PAD4

(Cuthbert et al., 2004; Wang et al., 2004). Conversely, PRMTs have no activity towards peptidyl-citrullines.

Since PRMT1-mediated methylation regulates NIP45 function, I tested if PRMT1 and PAD4 target the same arginine residues in NIP45, by sequential methylation and deimination reactions. Figure 12A shows NIP45 methylation. When GST-NIP45 was deiminated by PAD4 prior to methylation by PRMT1 using a tritiated methyl-donor, the signal for methylated GST-NIP45 was reduced to background levels (Figure 12A, lanes 1 and 2). When NIP45 was methylated by PRMT1 prior to deimination by PAD4, the overall methylation level did not change (Figure 12A, right half). These results suggest that most of the arginines methylated by PRMT1 can also be deiminated by PAD4. Interestingly, PAD4 itself was methylated by PRMT1, a novel observation (Figure 12A, lanes 3 and 4). Methylation and deimination reactions were also analyzed for deimination of GST-NIP45 (Figure 12B). Surprisingly, methylation of NIP45 prior to deimination by PAD4 did not interfere with NIP45 deimination (Figure 12B, lanes 2 and 3), suggesting that PAD4 targets arginines not modified by PRMT1.

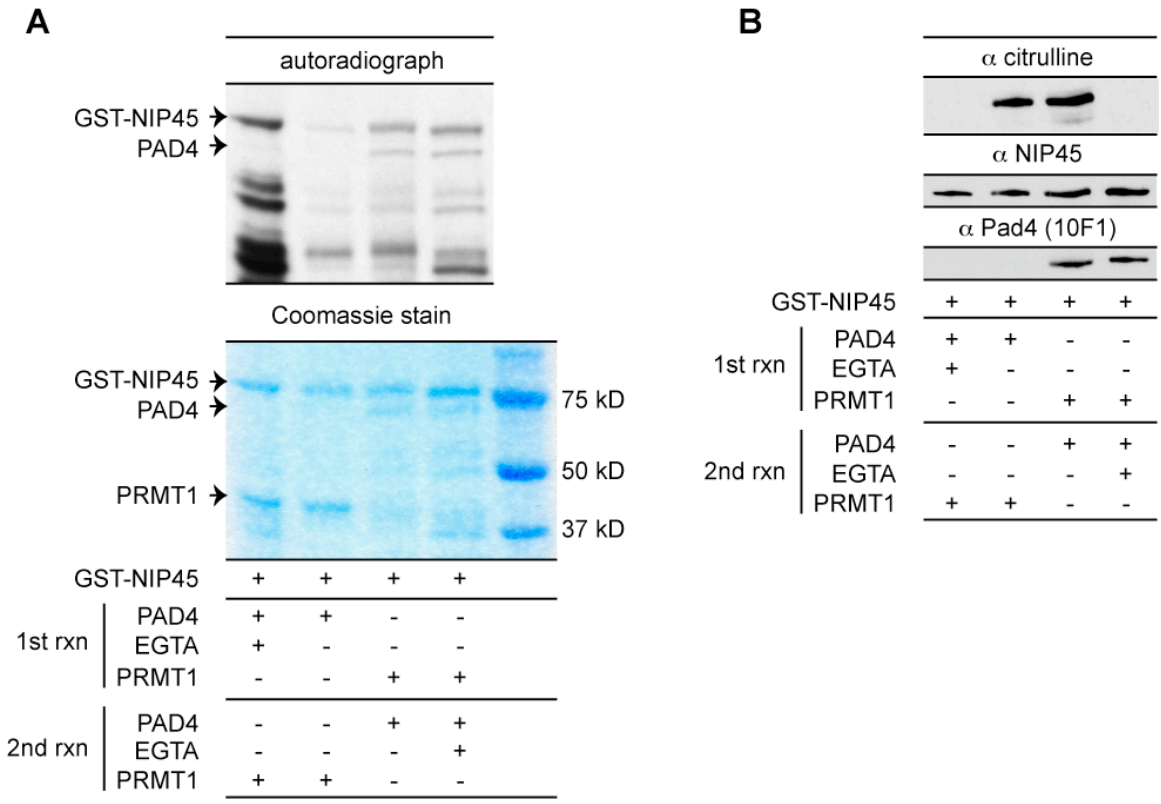

FIGURE 12: Deimination of NIP45 Prevents Methylation. Recombinant GST-NIP45 was sequentially deiminated with PAD4 (+/- EGTA, 50mM) and then methylated with PRMT1 in the presence of ^{3}H-SAM as the radioactively labeled methyl-donor, or methylated first and then deiminated by PAD4 (+/- EGTA, 50mM). (A) 15μl of the reactions were run on a 7.5% SDS page and stained with Coomassie to confirm equal amounts of protein loading. The dried gels were exposed to film to reveal methylation by autoradiography. (B) 4μl of the reactions were analyzed by immunoblotting for α citrulline to detect deiminated GST-NIP45, and with α NIP45 and α Pad4 to detect equal protein input.

In conclusion, deimination of NIP45 can prevent subsequent methylation by PRMT1, but PRMT1 methylation does not affect subsequent deimination of NIP45 by PAD4, suggesting different arginine preferences for PAD4 and PRMT1.

3.1.3 Characterization of PAD4 Target Sites in NIP45

Methylation of NIP45 is concentrated within the first 32 amino acids, as a deletion mutant lacking residues 1-32 (FLAG-NIP45ΔN) cannot be methylated by PRMT1 *in vitro* (Mowen et al., 2004). The results in Figure 12 suggest that PAD4 deiminates additional residues outside of this arginine-and glycine-rich region. Therefore, PAD4 enzymatic activity was tested against a panel of deletion mutants (Figure 13). (Note that the mutant lacking the first 32 AA is referred to as NIP45ΔRGG from now on, and NIP45ΔN describes a deletion of the first 188 AA).

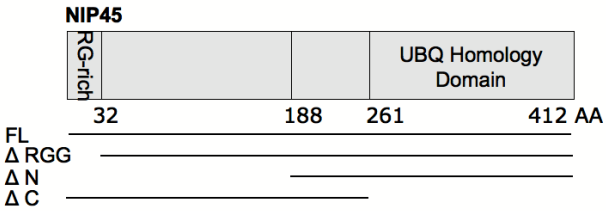

FIGURE 13: NIP45 Deletion Mutants. The schematic overview shows the functional domains of NIP45. Deletion mutants are indicated below (FL= full length). An additional mutant ΔNC is comprised of AA 188-261.

Myc-PAD4 and FLAG-tagged NIP45 mutants (Figure 13) were coexpressed in 293T cells. After immunoprecipitation for the FLAG-tagged constructs, the precipitated proteins were analyzed for deimination by immunoblot. Since FLAG-PRMT4/CARM1 is not a target for deimination *in vitro* (data not shown), it was included as a negative control. The strongest signal for deiminated protein was obtained with the full-length NIP45 construct, but all other deletion mutants except NIP45ΔNC were also detected (Figure 14, top panel). The NIP45ΔNC mutant could not be resolved in the citrulline blot due to unspecific background signal in this size range. Of note, the NIP45ΔC mutant was detected in the citrulline blot, though it expressed very poorly and was not detectable in the α FLAG reprobe blot (Figure 14, bottom panel).

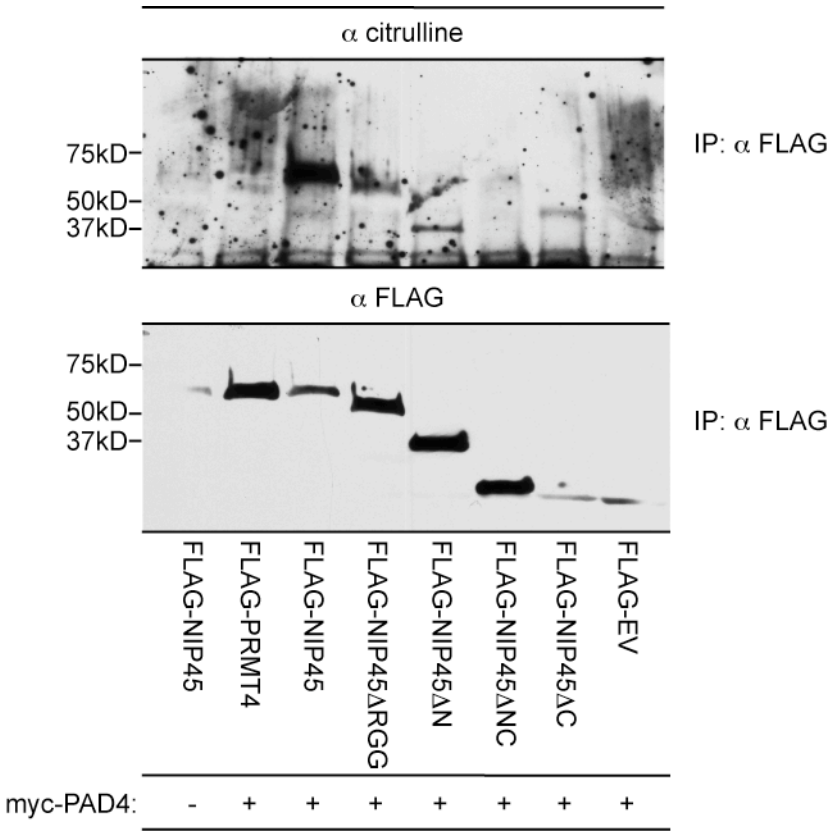

FIGURE 14: Deimination of NIP45 Deletion Mutants. FLAG-tagged expression constructs were coexpressed with myc-PAD4 in 293T cells. Cells were lysed and proteins were immunoprecipitated with FLAG-agarose beads. The immunoprecipitates were analyzed for citrulline modification and IP efficiency by immunoblotting.

To summarize, NIP45 deimination sites were broadly distributed throughout the whole protein. All of the NIP45 deletion mutants could be deiminated by PAD4. The ΔNC mutant could not be resolved properly; therefore it is unclear if it contains PAD4 deimination targets.

3.1.3.1 Mass Spectrometry of Deiminated GST-NIP45

To identify specific PAD4 deimination sites in NIP45, *in vitro* deiminated GST-NIP45 was subjected to mass spectrometric analysis. This work was performed in collaboration with Ali Sarkeshik and John Yates at Scripps through the Yeast Resource Center. Although the mass difference between arginine and citrulline is only 1Da, we could identify several deiminated arginines in GST-NIP45. Unfortunately, the sequence coverage, especially of the glycine- and arginine-rich N-terminus was very poor. Deiminated arginines are highlighted in red in Figure 15 and are at positions R32, R37, R103, and R104. Interestingly, R103 and R104 are part of the nuclear localization signal (NLS) sequence (underlined in Figure 15).

```
1     maeplrgrgp rsrggrgarr argargrcpr aRqspaRlip dtvlvdlvsd sdeevlevad
61    pvevpvarlp apakpeqdsd sdsegaaegp agaprtlvrr rrRRlldpge apvvpvysgk
121   vqsslnlipd nssllklcps epedeadltn sgsspsedda lpsgspwrkk lrkkcekeek
181   kmeefpdqdi splpqpssrn ksrkhtealq klrevnkrlq dlrsclspkq hqspalqstd
241   devvlvegpv lpqssrlftl kircradlvr lpvrmseplq nvvdhmanhl gvspnrilll
301   fgeselspta tpstlklgva diidcvvlas sseatetsqe lrlrvqgkek hqmleislsp
361   dsplkvlmsh yeeamglsgh klsfffdgtk lsgkelpadl glesgdliev wg
```

FIGURE 15: Deimination Sites in Mouse NIP45. The amino acid sequence of murine NIP45 is depicted above. Highlighted in red are the deimination sites that were identified by mass spectrometry. The NLS sequence is underlined.

3.1.3.2 Characterization of NIP45 Point Mutants

Ectopic expression of NFAT, c-Maf and NIP45 in a murine B cell line leads to detectable IL-4 secretion (Hodge et al., 1996). To understand the potential role of NIP45 deimination in the regulation of IL-4 transcription, I generated three different point mutants for each identified site: an arginine to lysine substitution (R->K) to conserve the positive charge, an arginine to phenylalanine substitution to mimic dimethylation (R->F), and an arginine to glutamine substitution to mimic deimination (R->Q) (Bates et al., 2002).

The mutants were generated by site-directed mutagenesis using pEGFP-NIP45 as the template. Since R103 and R104 are part of the NLS, it was important to check if the mutants retained nuclear localization. M12 cells, a murine B cell line, were cotransfected with HA-NFAT, c-Maf, and the GFP-NIP45 point mutants. The deletion mutants NIP45ΔRGG and NIP45ΔN (see Figure 13) were included for reference. The transfected cells were analyzed by fluorescence microscopy in four independent experiments. With the exception of GFP-NIP45ΔN, all mutants were expressed primarily in the nucleus (Figure 16). GFP-NIP45ΔN and GFP (EV) displayed cytoplasmic localization. The mislocalization of NIP45ΔN was expected since this mutant lacks the NLS.

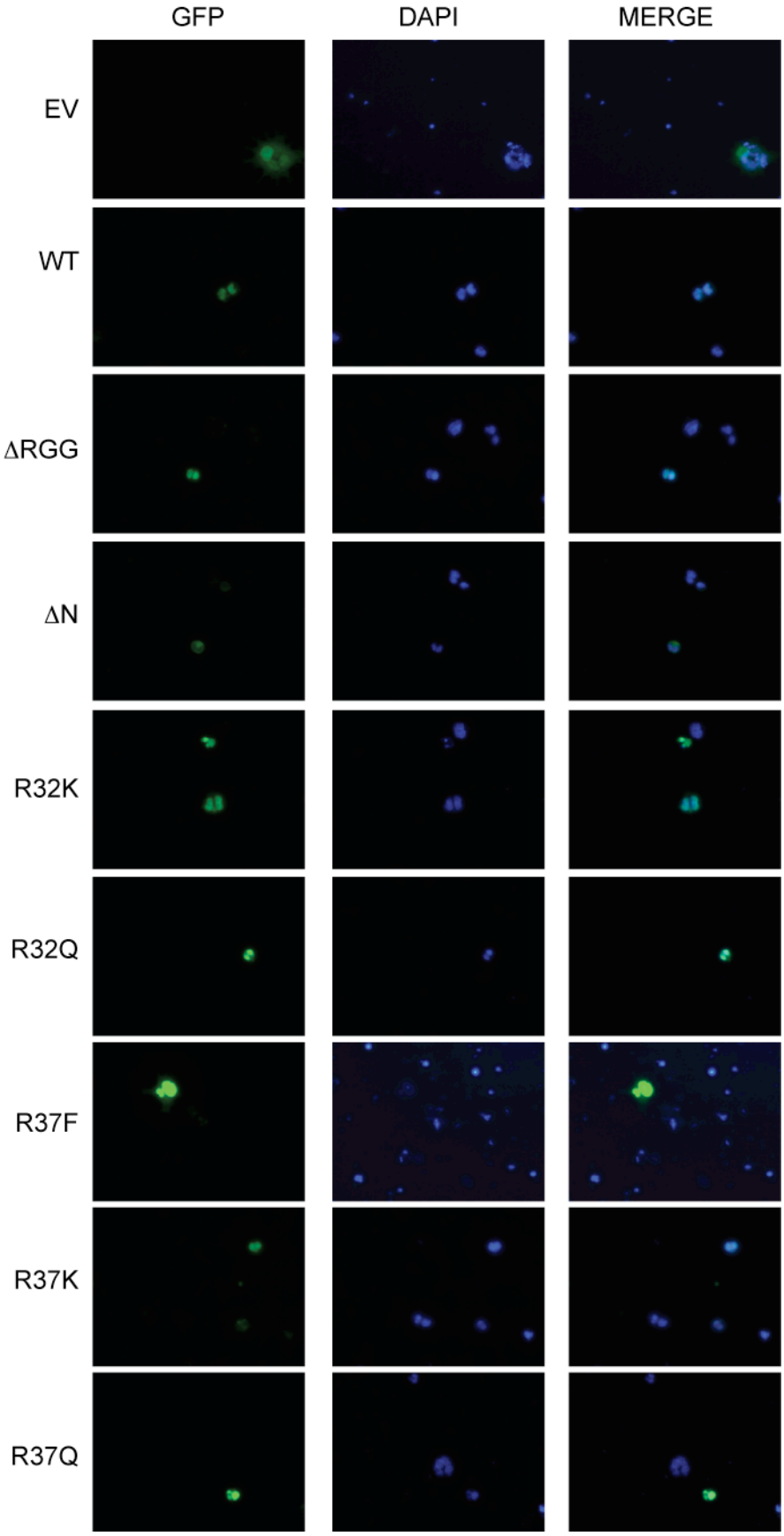
GFP
DAPI
MERGE
EV
WT
ΔRGG
ΔN
R32K
R32Q
R37F
R37K
R37Q

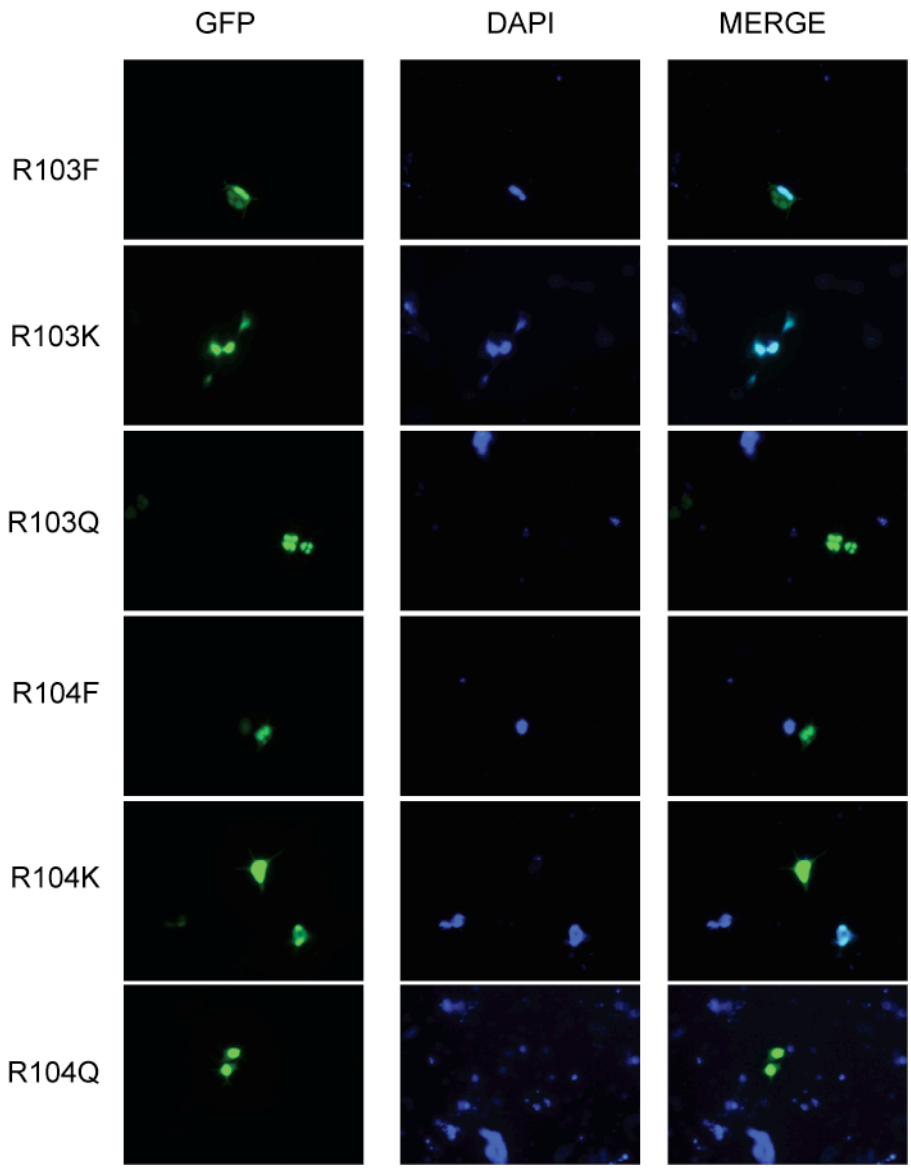

FIGURE 16: Fluorescence Microscopy of NIP45 Mutants in M12 Cells. M12 cells were co-transfected with HA-NFAT, c-Maf and various pEGFP-NIP45 constructs. The particular mutants are indicated on the left. 24h post transfection, the cells were plated onto poly-L-lysine coverslips, fixed, and stained with DAPI. Pictures were taken with 40x objective. Representative pictures from four independent experiments are shown.

To test the transcriptional potential of all NIP45 mutants, supernatants of the cells that were used in the IF studies were analyzed for IL-4 secretion. As expected, overexpression of GFP-NIP45 together with HA-NFAT and c-Maf induced spontaneous IL-4 secretion in M12 cells (Figure 17A and B). R37F substitution had no effect on cytokine secretion, while R37K or R37Q substitutions significantly reduced IL-4 secretion by 40-50%. The R103 mutants showed a reverse phenotype with R103F and R103K significantly reducing the secretion by 50-60%, but R103Q had no effect on IL-4 production. The R104 mutants had little or no effect on IL-4 secretion (Figure 17A).

The R32 mutants were analyzed in a separate experiment and compared to NIP45ΔRGG and NIP45ΔN. Both deletion mutants severely impacted IL-4 secretion with ΔN reducing it to background levels (compare to EV). The R32K substitution had an intermediate effect on IL-4 secretion, and the effect of R32Q was negligible (Figure 17B).

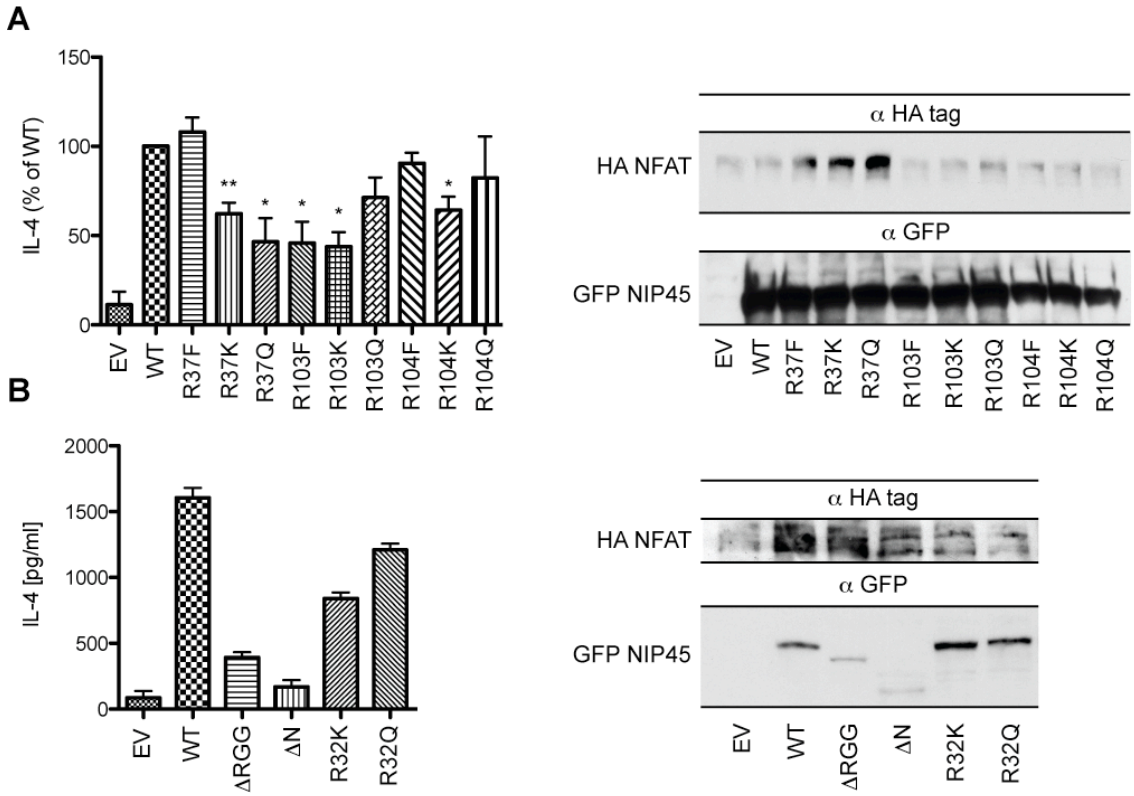

FIGURE 17: Effect of NIP45 Point Mutations on IL-4 Secretion. M12 cells were cotransfected with HA-NFAT and c-Maf in combination with pEGFP-NIP45 expression vectors as indicated above. IL-4 secretion was analyzed 72h after transfection. Transfection efficiencies were analyzed by immunoblotting of whole cell lysates. (A) Data from four independent experiments were combined. ELISA data is represented as % of NIP45 WT transfected cells. Statistically significant differences relative to NIP45 WT are indicated for the respective constructs. Transfection efficiency of a representative experiment is shown on the right. (B) IL-4 ELISA data of respective transfections is shown on the left. Expression levels of the relevant constructs are displayed on the right.

In summary, NIP45 is deiminated by PAD4 inside the glycine- and arginine-rich N-terminus, both overlapping with PRMT1 methylation sites and throughout other parts of the protein. Four specific deimination sites were identified by mass spectrometry. Generation of NIP45 point mutants mimicking deimination at those sites revealed a potential role for deimination of R37 in negative regulation of IL-4 secretion. None of the mutants tested enhanced NIP45's ability to potentiate IL-4 secretion in M12 cells.

3.1.4 The Role of PAD4 in NIP45-mediated IL-4 Secretion

PRMT1-mediated methylation of the N-terminus of NIP45 facilitates the formation of a trimeric NFAT/NIP45/PRMT1 complex that can fully activate IL-4 transcription. If PRMT1 is inactivated, IL-4 transcription is reduced, making PRMT1 a positive regulator of IL-4 transcription (Mowen et al., 2004). Deimination of NIP45 can prevent arginine methylation (Figure 12), and the NIP45 R37Q deimination mimic impairs IL-4 secretion from M12 cells (Figure 17). Together, these data suggest a role for PAD4 as a negative regulator of IL-4 transcription. To test this notion, M12 cells were transfected with expression constructs for HA-NFAT and c-Maf in combination with myc-NIP45 and HA-PAD4. Both wildtype (wt) and an enzymatically inactive mutant (mut) of PAD4 were used. IL-4 expression was

analyzed on the transcript level by qPCR (Figure 18A) and on the protein level by IL-4-specific ELISA of the supernatants (Figure 18 B). As expected, coexpression of NIP45 with NFAT and c-Maf potentiated IL-4 expression and secretion of M12 cells (Figure 18A and B, lanes 1&2). Coexpression of PAD4 reduced IL-4 levels to basal levels (Figure 18A and B, lanes 3&4). Surprisingly, this effect was independent of PAD4's enzymatic activity. To ensure comparable expression levels of the various constructs, whole cell lysates were analyzed by Western blotting (Figure 18C).

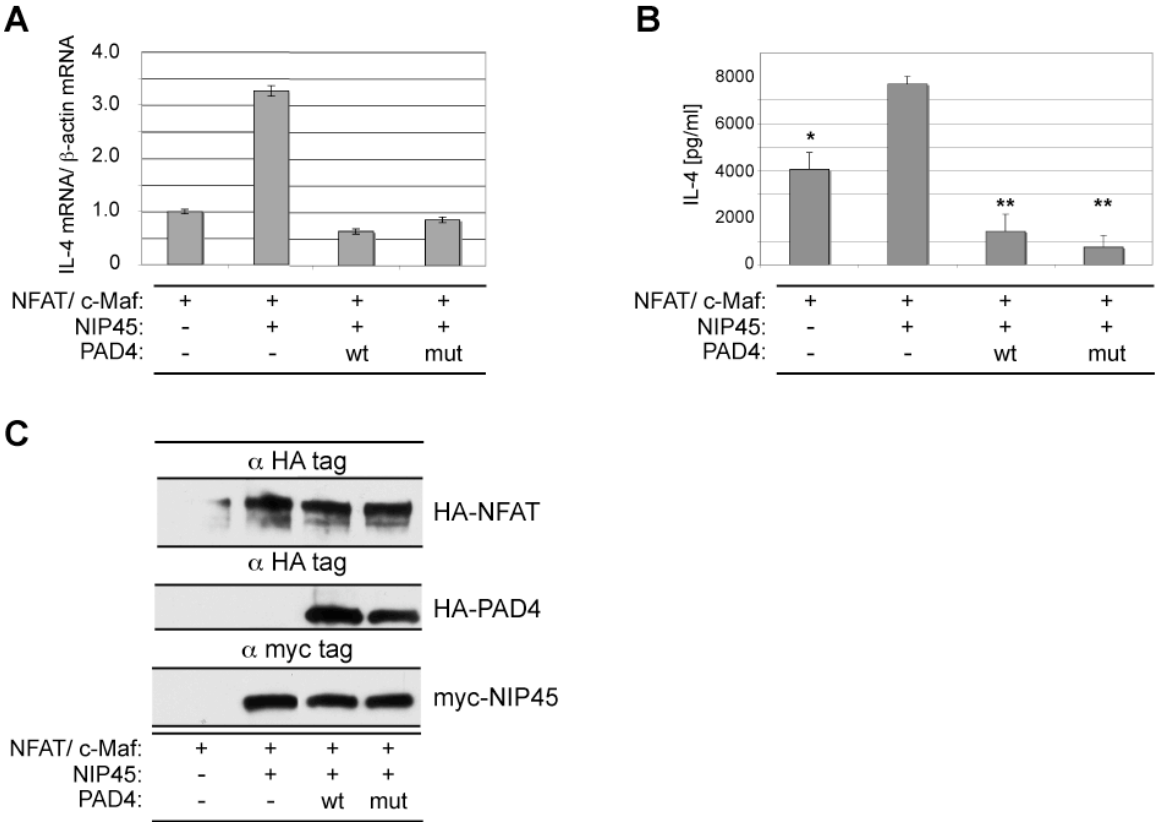

FIGURE 18: PAD4 is a Negative Regulator of IL-4 Transcription in M12 Cells. HA-NFAT, c-Maf, myc-NIP45 and HA-PAD4 (wt or mut) were co-expressed in M12 cells as indicated. IL-4 expression was analyzed 30h post transfection by qPCR (A) and 72h after transfection by ELISA (B). Transfection efficiency was analyzed by immunoblotting (C).

NIP45 can form a trimeric complex with NFAT and PRMT1 (Mowen et al., 2004). Since PAD4 can deiminate NIP45 and inhibit NIP45-mediated potentiation of IL-4 expression, I tested whether NIP45 could form a trimeric complex with PAD4 and NFAT. Epitope-tagged expression constructs of NIP45, PAD4, and NFAT were coexpressed in 293T cells. NIP45 was immunoprecipitated, and the reactions were analyzed for interaction with NFAT and PAD4 by Western blotting (Figure 19). Indeed, NIP45 interacted with NFAT and PAD4 both alone and in combination. Comparable expression was confirmed by immunoblotting of the total lysates (WCL) (Figure 19).

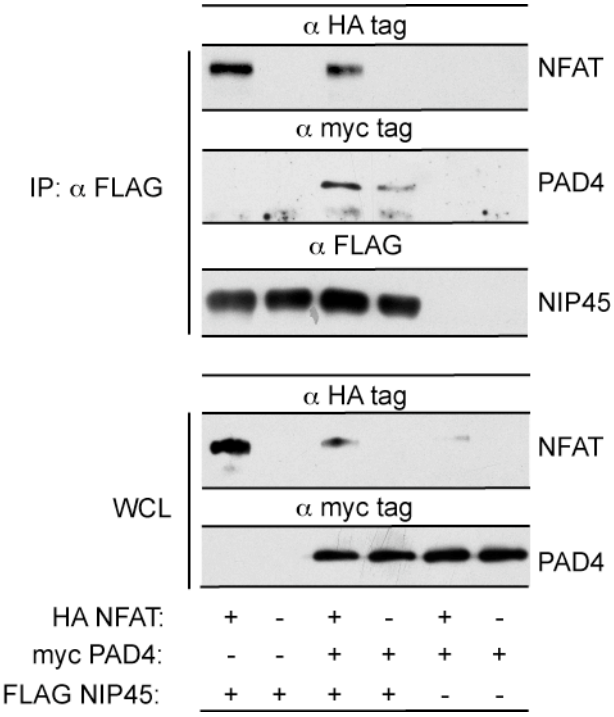

FIGURE 19: NIP45 Interaction with PAD4 and NFAT. 293T cells were co-transfected with HA-NFAT, myc-PAD4, and FLAG-NIP45. Lysates were immunoprecipitated with FLAG agarose. IPs were analyzed by immunoblotting with α HA tag, α myc tag, and α FLAG. To ensure comparable protein input, whole cell lysates (WCL) were probed with α HA tag and α myc tag.

In conclusion, NIP45-driven IL-4 expression in M12 cells can be abrogated by ectopic expression of PAD4. Interestingly, PAD4's catalytic activity is not required for this process. Furthermore, NIP45 can form a trimeric complex with NFAT and PAD4 *in vivo*.

3.1.5 PAD4 Expression Levels in Th2 Cells

The primary IL-4 producers are Th2 cells. The importance of NIP45 for IL-4 secretion by Th2 cells is signified by the severe reduction of IL-4 production in NIP45-deficient Th2 cells (Fathman et al., 2010). PAD4 can negatively regulate NIP45-mediated IL-4 expression in M12 cells. Expression analysis has revealed that PAD4 is not only expressed in myeloid cells, but also to a lesser extent in $CD3^+$ cells, which encompass all T cells (Vossenaar et al., 2004). Therefore, it was important to check if PAD4 is expressed in Th2 cells.

RNA from total bone marrow (BM), naïve CD4+ T cells (Thp) and differentiated Th1 and Th2 cells was prepared and analyzed on a Northern blot. PAD4 was detected with a PAD4-specific RNA probe (Figure 20). A strong signal for PAD4 was detected in BM after several hours of exposure. The signal for PAD4 in Th2 cells could only be detected after 7d exposure at -80C. No signal could be detected in either Thp or Th1 cells. To confirm equal loading of RNA, the membrane was reprobed with an RNA probe specific for the housekeeping gene GAPDH (Figure 20).

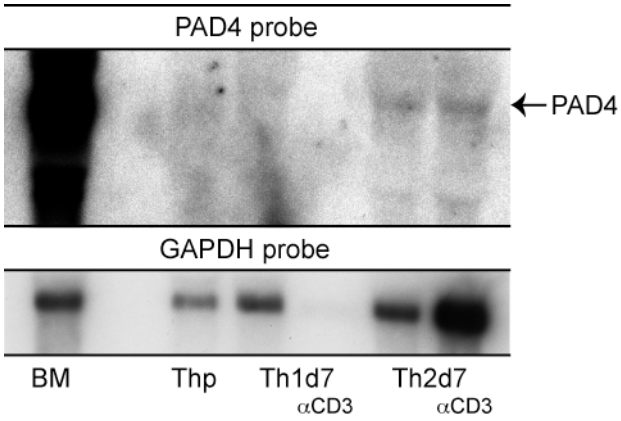

FIGURE 20: Northern Blot of PAD4 Expression. RNA (10μg/sample) was separated by electrophoresis and transferred onto a positively charged nylon membrane. Membranes were probed with a radioactively labeled PAD4 RNA probe. The membrane was exposed to film for one week. To ensure equal loading, the membrane was reprobed with a labeled GAPDH-specific probe.

In summary, NIP45 is deiminated by PAD4 both *in vitro* and *in vivo*. Unlike arginine methylation of NIP45, deimination is not limited to the glycine- and arginine-rich N-terminus of the protein, but the sites are dispersed across the whole protein. Several novel deimination sites could be identified by mass spectrometry, and at least one is implicated in the negative regulation of IL-4 secretion. Moreover, ectopic expression of PAD4 reduces NIP45-mediated IL-4 expression to background levels. This effect is independent of the enzymatic activity of PAD4. Finally, IL-4-producing Th2 cells express low levels of the PAD4 transcript.

3.2 Generation and Analysis of PAD4 Conditional Knockout Mice

The peptidylarginine deiminase PAD4 is the only PAD family member that predominantly localizes to the nucleus via its NLS (Nakashima et al., 2002) and, thereby, can directly influence transcription by deimination of histone tails (Cuthbert et al., 2004; Hagiwara et al., 2005; Wang et al., 2004). Histone deimination is associated with negative regulation of transcription (Cuthbert et al., 2004; Denis et al., 2009; Wang et al., 2004). In addition, PAD4 is a corepressor of nuclear-hormone receptor signaling and p53-mediated signaling (Denis et al., 2009; Li et al., 2010). The expression of PAD4 is highly restricted to the hematopoietic lineage, especially granulocytes and monocytes (Nakashima et al., 2002; Vossenaar et al., 2004). Interestingly, deiminated histones are associated with NETs released by neutrophils, linking PAD4 activity to an innate defense mechanism (Neeli et al., 2008; Wang et al., 2009). Furthermore, PAD4 has been implicated in the pathogenesis of several diseases, including rheumatoid arthritis (Suzuki et al., 2003), multiple sclerosis (Wood et al., 2008), and malignant tumors (Chang and Fang, 2009).

Since PAD4 is an important regulator of diverse cellular processes and dysregulation of its activity has been associated with various pathological conditions, I generated a mouse model with targeted disruption of the *PADI4* gene. This model will be useful in studying many aspects of PAD4 biology and addressing its role in various disease models.

3.2.1 Generation of PAD4 Conditional Knockout Mice

PAD4 conditional knockout mice (cKO) were generated by flanking exons 9 and 10 of the endogenous *PADI4* gene with loxP sites. Exons 9 and 10 contain aspartate 352, which is part of the active site, as well as four additional residues that are essential for Ca^{2+} binding (Q351, E353, E355, D371). Furthermore, deletion of these two exons results in a frameshift. The targeting vector was cloned and linearized as described in section 2.4.1.1. C57BL/6-derived Bruce 4 ES cells were electroporated with the linearized construct and underwent G418 and ganciclovir selection (Figure 21A). Surviving clones were analyzed by Southern blotting. *Hind*III and *Bam*HI digests of genomic ES cell DNA were probed with a radioactively labeled 5' probe (Figure 21A). Two successfully targeted clones, 116 and 261, were identified (Figure 21B and C). Both clones were expanded and injected into C57BL/6 albino blastocycts to derive chimeric mice. Chimeric males were bred to C57BL/6 albino females. Black pups were screened for germline transmission of the targeted allele by PCR, and the results were confirmed by Southern blot of *Hind*III-digested tail DNA (Figure 21D).

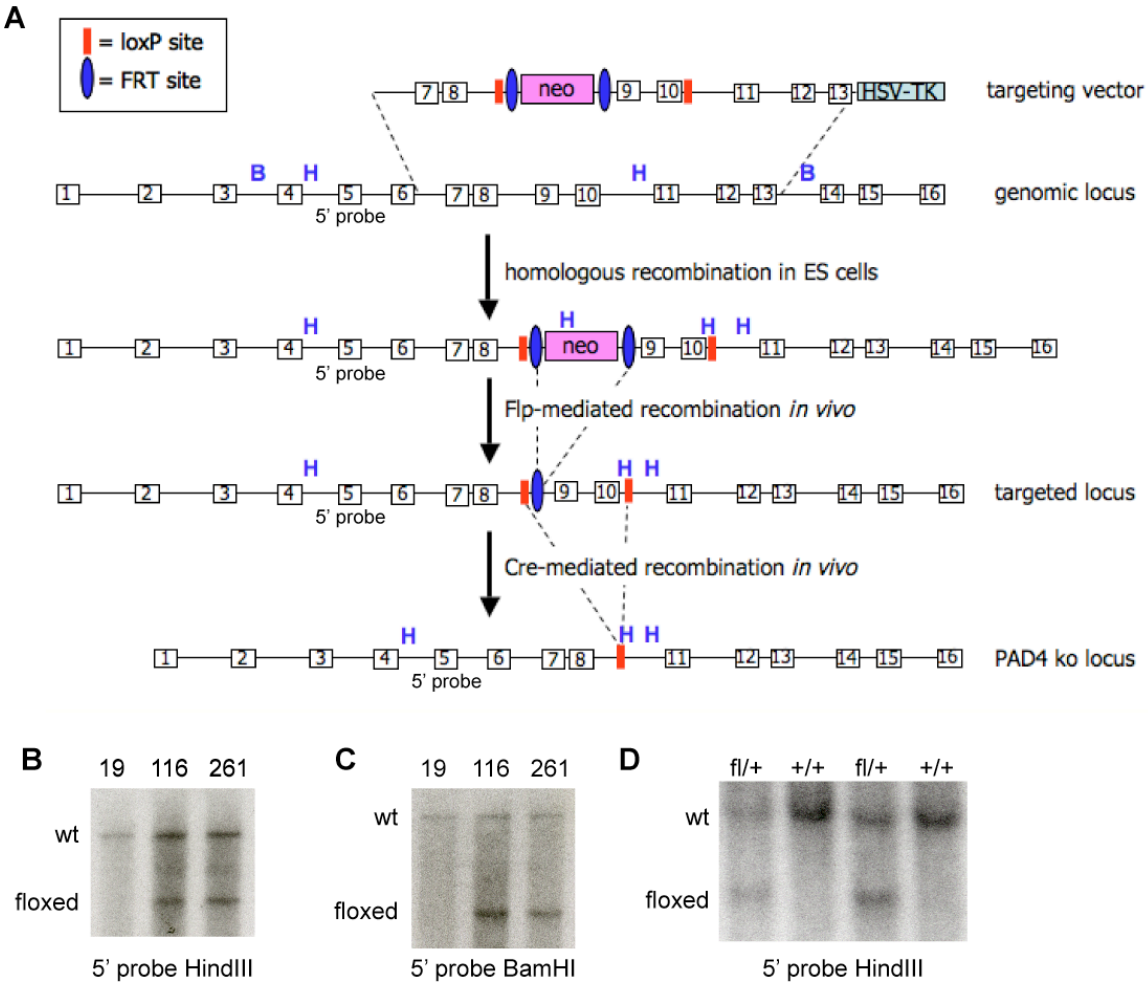

FIGURE 21: PAD4 Gene Targeting Overview. (A) Schematic overview of the PAD4 targeting strategy. Exons are represented as numbered boxes; *Hind*III and *Bam*HI restriction sites are labeled with B and H, respectively (blue); the placement of the external 5'probe is depicted; FRT sites (blue ovals) and loxP sites (red rectangles) are indicated; the selectable markers neo (neomycin resistance) and HSV-TK are shown as boxes. The dashed lines indicate integration or recombination sites. (B) Genomic DNA from three ES cell clones was digested with *Hind*III and analyzed by Southern blotting with a labeled 5'probe. The wt band (9.5 kb) and the floxed band (5.9 kb) sizes are indicated. (C) BamHI digested ES cell DNA was screened with the labeled 5'probe. The wt band (15.5 kb) and the targeted band (floxed) (6.6 kb) are indicated. (D) Mouse genomic tail DNA was screened for integration of the targeting vector. Genotypes as identified by PCR are indicated on top.

Mice carrying the targeted allele (fl/+) were bred to Flp-deleter or CMV-Cre deleter mice to generate PAD4flΔneo/+ and PAD4+/- mice, respectively (Figure 21A and Figure 22). PAD4-deficient mice were obtained by intercross of the latter. Deletion of the neomycin cassette upon breeding to the Flp-deleter mice was confirmed by PCR on genomic tail DNA (Figure 22A and B). CMV-Cre mediated deletion of the loxP-flanked exons 9 and 10 was confirmed as well (Figure 22A and C). To confirm the absence of PAD4 on the protein level, lysates of peritoneal cavity-derived cells (mainly granulocytes and monocytes) were probed with all available PAD4 antibodies. None of the antibodies could detect protein in the lysates from the KO (-/-) mice. A representative immunoblot is shown in Figure 22D.

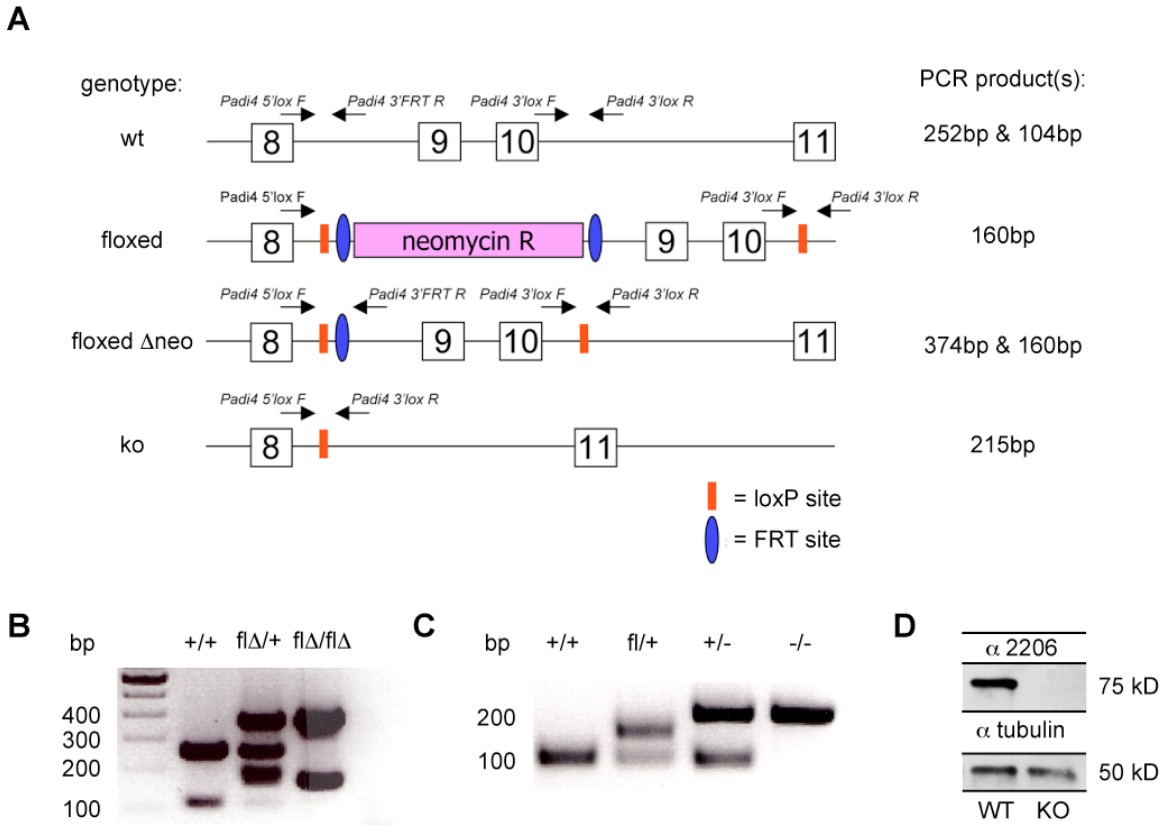

FIGURE 22: Genotyping of Mice with Targeted Insertion into the PAD4 Locus. (A) PCR primers used for genotyping of PAD4 gene-targeted mice are indicated. Expected PCR product sizes are shown on the right, the corresponding genotype is shown on the left. (B+C) Representative pictures of genotyping results are depicted. Sizes (in bp) are indicated on the left, genotypes on top. (D) Peritoneal cavity cells were isolated from a PAD4 WT and KO mouse. Protein lysates were analyzed by immunoblotting using α 2206, an antibody specific for mouse PAD4. The lysates were reprobed with α tubulin to ensure equal loading between the samples.

In conclusion, PAD4 conditional knockout mice have been generated successfully. Mice with a complete deletion of PAD4 (PAD4-/-) are viable, with no overt developmental defects. PAD4 flΔ/+ mice are currently bred to several Cre-lines (Lck-Cre, lysM-Cre, Cre-ERt) to generate cell-type specific or inducible KO strains.

3.2.2 Immunophenotyping of PAD4 KO Mice

PAD4 expression is restricted to the hematopoietic lineage (Vossenaar et al., 2004). Therefore, PAD4 WT and KO mice were analyzed by flow cytometry to check for potential defects in the development of the hematopoietic system. Bone marrow, spleen, lymph nodes, thymus, and cells from the peritoneal cavity were isolated and stained with a variety of B cell- and T cell-lineage specific surface markers (examples are shown in Figures 23 and 24). Overall, there were no obvious differences in numbers or percentages of all developmetal stages analyzed. Both B- and T cell development progressed normally in PAD4-deficient mice.

Thymocytes were analyzed by staining for CD4 and CD8α (Figure 23A) and several other maturation markers (data not shown), but no perturbations in thymocyte development were found in PAD4-deficient mice. Not surprisingly, normal frequencies of $CD4^+$ and $CD8^+$ T cells were detected in the periphery (Figure 23B).

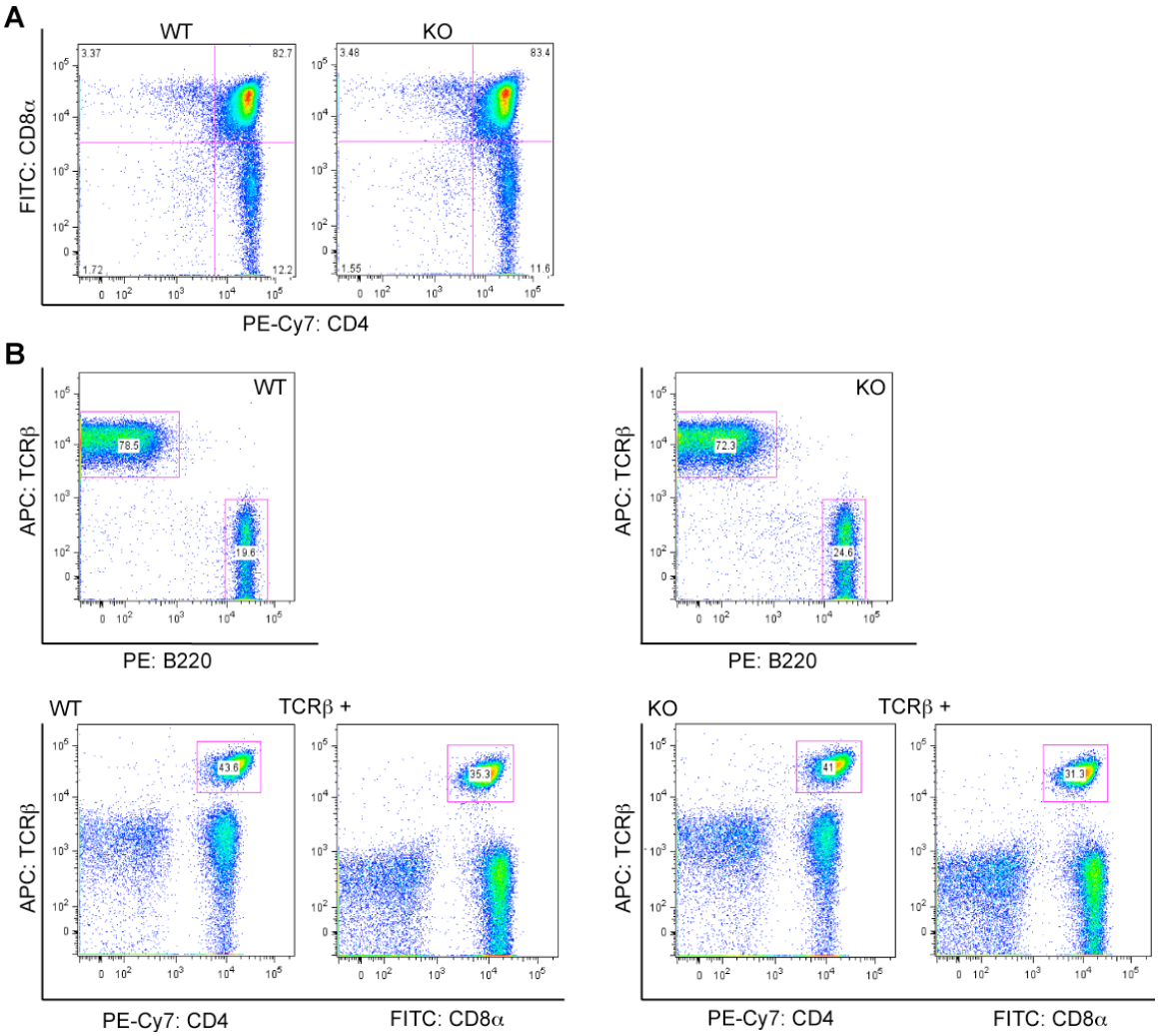

FIGURE 23: T Cell Development in Thymus and Lymph Nodes of PAD4 KO Mice. Single cell suspensions from thymus and lymph nodes of PAD4 WT or KO mice were stained with the indicated fluorescently labeled antibodies. Cells were analyzed by flow cytometry. (A) Thymocytes were stained with CD4- and CD8α-specific antibodies to check thymocyte development progression. (B) Lymph node cells were stained with B220 and TCRβ to discriminate between B and T cells. The TCRβ positive cells were analyzed for CD4 and CD8α expressing cells, respectively. Percentages of gated cells are indicated.

B cell development in PAD4-deficient mice was analyzed in bone marrow, lymph nodes, spleen, and peritoneal cavity. All developmental stages analyzed showed no perturbations in PAD4 KO mice. As an example, a representative stain of splenic B cells is shown in Figure 24. The co-stain for IgM and IgD revealed proper development from immature (IgM^+, IgD^-) to mature peripheral B cells (IgM^+IgD^+).

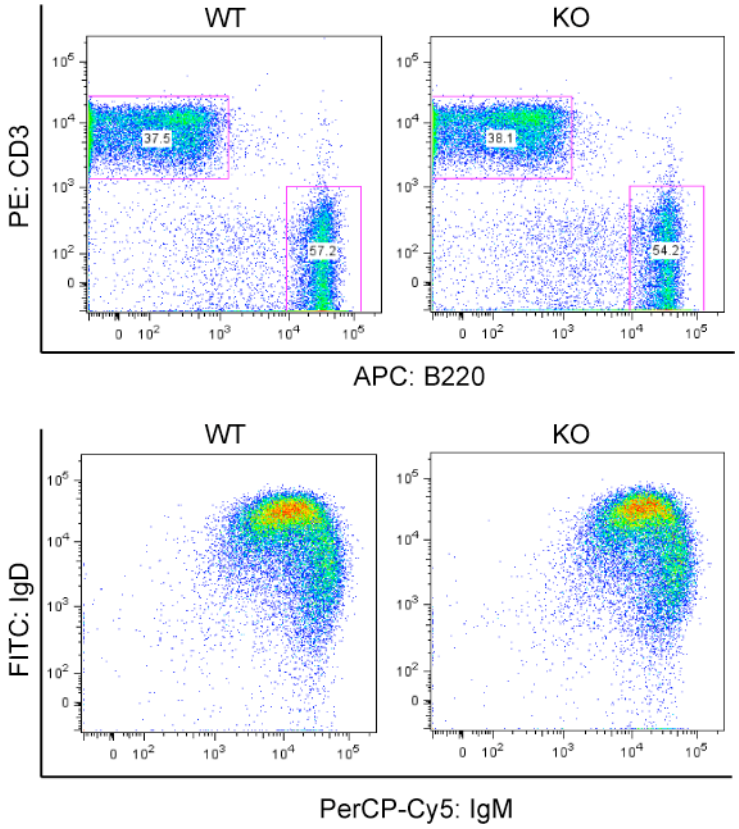

FIGURE 24: Peripheral B Cells in Spleen of PAD4 KO Mice. Splenic cells from PAD4 WT and KO mice were stained with α CD3 and α B220 to discriminate between T and B cells (upper panel). $B220^+$ cells were costained with IgM and IgD to monitor B cell maturation (lower panel).

Overall, both B and T cell development was not perturbed in PAD4-deficient mice. Future studies are needed in order to address the functional capacities of both B and T cells in this mouse strain.

3.2.3 Analysis of PAD4-Deficient Th Cells

Since PAD4 can negatively regulate NIP45-mediated IL-4 expression in M12 cells, Th2 cells, the main source of IL-4 in the mouse, were analyzed for their IL-4 secretion capacity. I hypothesized that PAD4-deficiency should release inhibition and lead to elevated IL-4 levels.

$CD4^+CD62L^+$ naïve T cells were isolated from spleen and lymph nodes of PAD4 WT or KO mice. The cells were differentiated *in vitro* towards the Th1, Th2, and Th17 lineages. The differentiated Th cells were restimulated with αCD3 for 24h, and cytokine secretion was analyzed by ELISA. Upon TCR stimulation, Th1 cells from PAD4 KO mice produced slightly less IFNγ (Figure 25A). This was not due to a change in the level of T-bet, the master regulator of Th1 differentiation (Figure 25D). IL-17A production by Th17 cells was not affected in the absence of PAD4 (Figure 25B). In Th2 cells however, PAD4 deficiency led to increased IL-4 secretion, supporting a role for PAD4 as a negative regulator of IL-4 expression (Figure 25C). Gata 3 is the master regulator of Th2 differentiation. Furthermore, slightly elevated Gata 3 levels in Th2 cells accompanied the increase in IL-4 secretion from PAD4 KO mice.

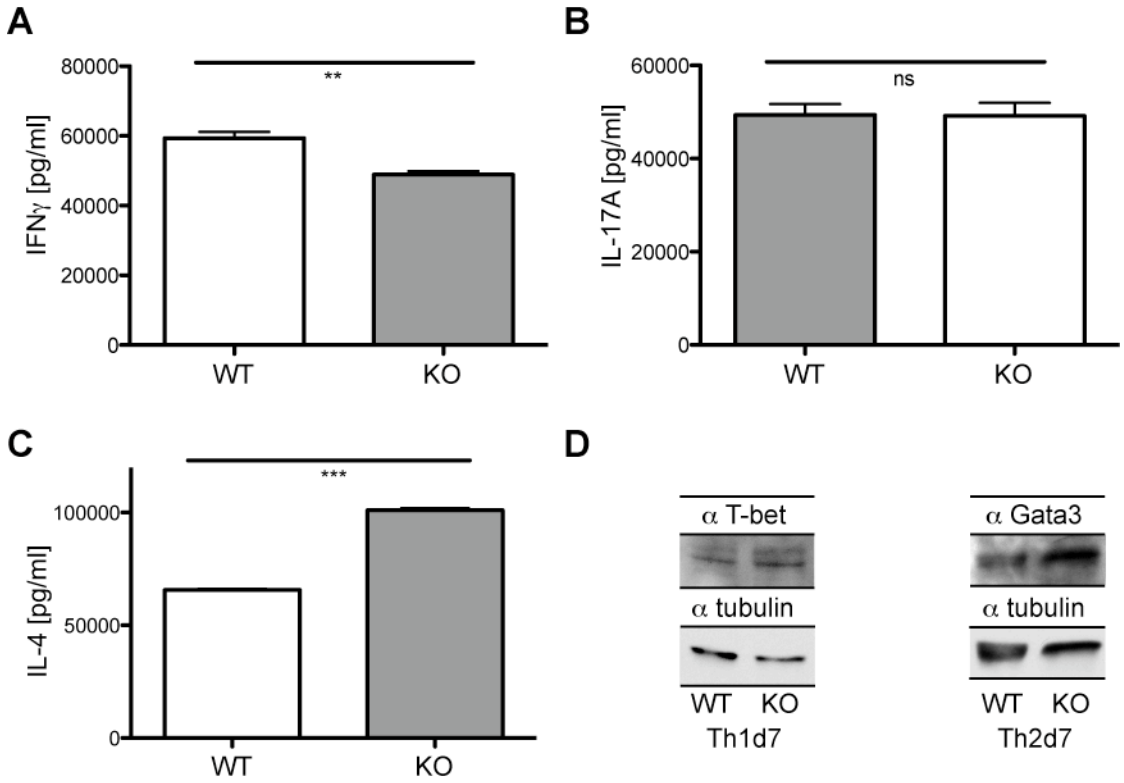

FIGURE 25: Th Cell Cytokine Secretion in PAD4 KO Mice. $CD4^+CD62L^+$ T cells were isolated from WT (white bars) and KO PAD4 (grey bars) mice. The cells were differentiated *in vitro* to become Th1, Th2, or Th17 cells. Cytokine secretion was assessed by restimulation of those cells with α CD3 for 24h. Th1 (A) and Th2 cells (C) were restimulated after 7d in culture, Th17 cells (B) were restimulated after 4d. (D) Protein lysates from restimulated Th1 and Th2 cells were analyzed by immunoblotting with α T-bet or α Gata 3, respectively. Equal loading was confirmed with an α tubulin blot.

Additionally, *in vitro* differentiated Th1 and Th2 cells were analyzed by intracellular cytokine staining for IFNγ and IL-4. Th1 cells derived from PAD4 WT or KO mice displayed no difference in percentage of IFNγ-producers (39.5% vs 40.6%). The amount of IFNγ-production per Th1 cell, which can be analyzed by comparing the mean fluorescence intensities (MFI), was indistinguishable (MFI WT: 2388; MFI KO: 2406)(Figure 26A). Th2 cells from PAD4-deficient mice contained a higher percentage of IL-4 producing cells (WT: 13.5%; KO: 20.0%), and they also expressed more IL-4 on a per cell basis (MFI WT: 1842; MFI KO: 1988)(Figure 26B).

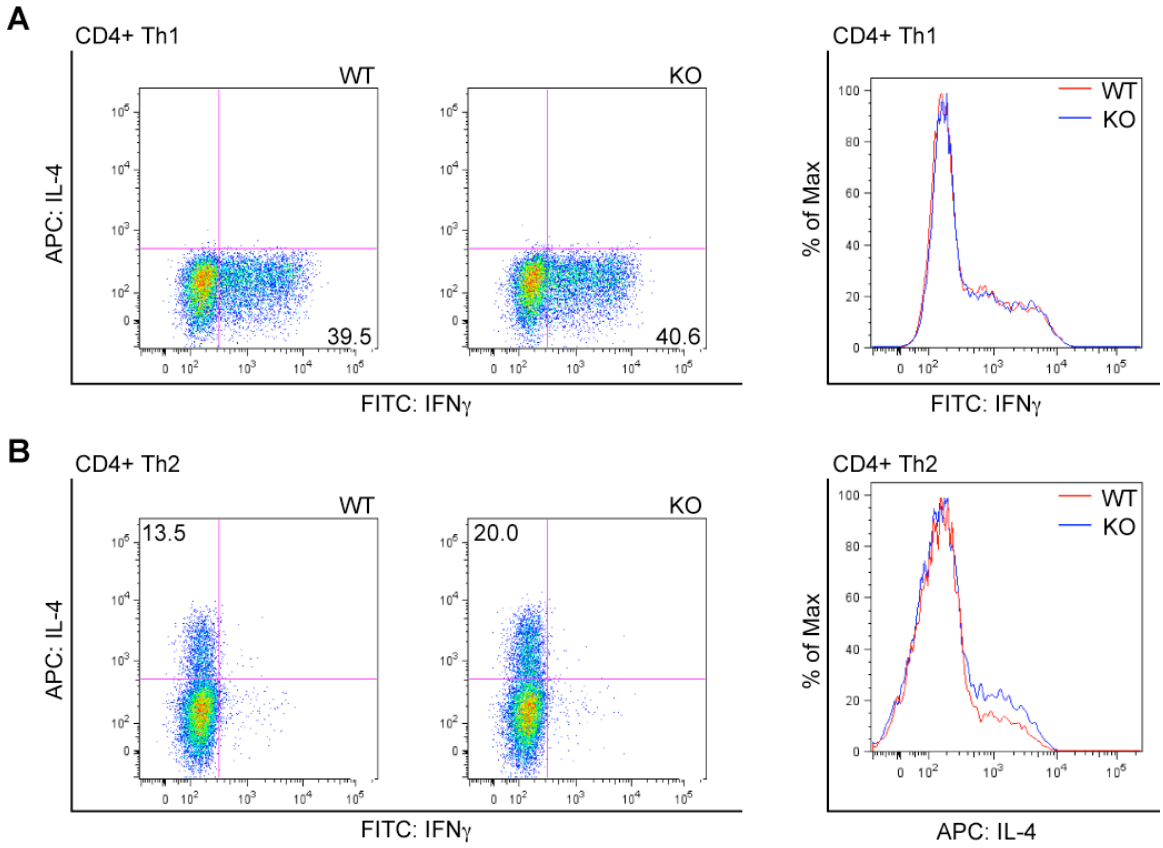

FIGURE 26: Intracellular Cytokine Staining of Th1 and Th2 Cells. *In vitro* differentiated Th1 and Th2 cells were stimulated with PMA (50ng/ml) and ionomycin (1μM) in the presence of brefeldin A (1μg/ml). Cells were fixed and stained with antibodies to detect IL-4, IFNγ, and CD4. After staining, the $CD4^+$ Th1 (A) and Th2 cells (B) were analyzed by flow cytometry. Percentages of cytokine producing cells are indicated.

NIP45-mediated IL-4 transcription is positively regulated by arginine methylation. PRMT1 methylates the N-terminus of NIP45, enhancing its interaction with NFAT, and thereby driving IL-4 transcription (Mowen et al., 2004). In addition, recruitment of PRMT1 to the IL-4 promoter also increases the levels of histone H4R3 methylation, a modification linked to active transcription (Fathman et al., 2010). Since PAD4 can deiminate histone H4R3 and can negatively regulate IL-4 expression, IL-4 promoter histone deimination was analyzed by chromatin immunoprepitation studies.

$CD4^+$ T cells were isolated from PAD4 WT and KO mice and were differentiated *in vitro* to Th2 cells. Half of the cells were stimulated for 2h with PMA/Ionomycin to mimic a strong TCR signal. Cells were crosslinked, and ChIP analysis was performed using antibodies specific for dimethylated histone H4R3, deiminated H4R3, or acetylated H4. H4 acetylation and dimethylation are both hallmarks of active transcription, but deimination is associated with repression. Abundance of these H4 posttranslational modifications was analyzed at both the IL-4 and IFNγ promoters, as well as at CNS I and HS IV, two important regulatory elements in the IL-4 locus control region (Figure 27). Unfortunately, no reproducible signal was detectable for deiminated H4R3 for any of the loci. Preferential enrichment of both dimethylated H4R3 and acetylated H4 at the IL-4 promoter and CNS I were comparable in WT and KO samples. The IFNγ promoter and HS IV region had much lower signals for the H4 methylation and acetylation (notice the different scales), which was expected, since the IFNγ promoter is silenced in Th2 cells and the HS IV region is associated with repression of IL-4 transcription (Figure 27). Overall, the local chromatin environment in the IL-4 regulatory region showed

no differences between PAD4 WT and KO Th2 cells. Deimination of histone H4 was not detected in any of the samples.

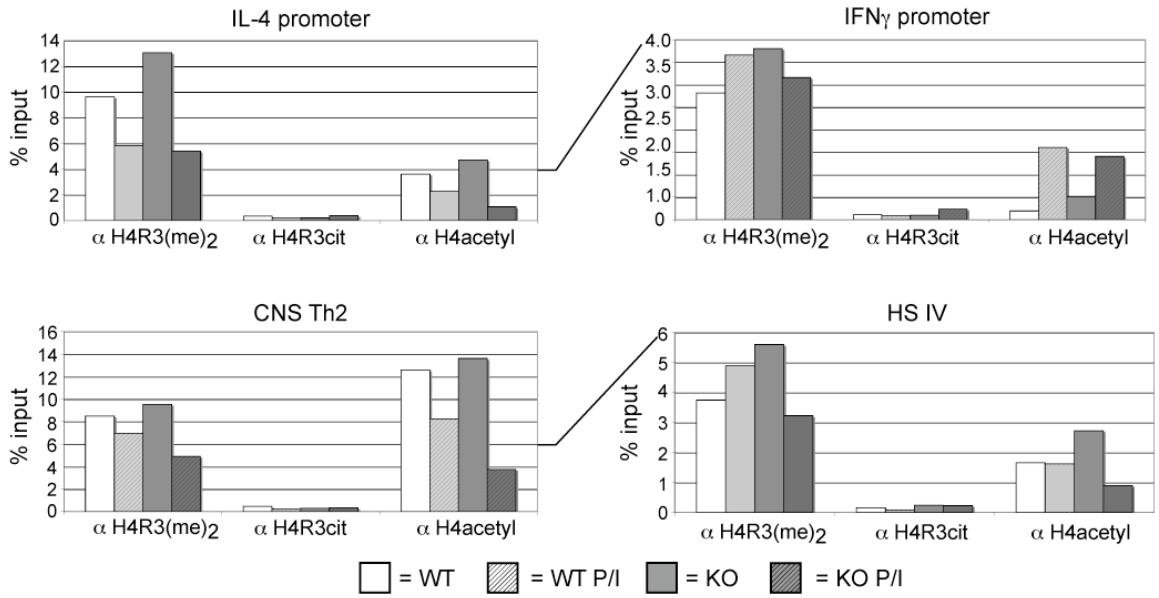

FIGURE 27: ChIP Analysis of Th2 Cells. $CD4^+$ T cells were isolated from PAD4 WT or KO mice. Cells were differentiated under Th2 conditions for 7 days. Half of the cells were stimulated with 50ng/ml PMA and 1μM ionomycin for 2h. Chromatin IPs were performed using α $H4R3(me)_2$, α H4R3cit, α H4acetyl, and α IgG control antibodies. The IL-4 promoter, the IFNγ promoter, CNS I, and HS IV regions were analyzed for the presence of those posttranslational modifications by qPCR. Abundance of the particular modification is represented as % of input. All values depicted are after subtraction of α IgG control ChIP. Lines between graphs indicate scale differences.

In conclusion, Th cells derived from PAD4 KO mice displayed several defects. Th1 cells had a slight decrease in IFNγ secretion, which was only detectable by ELISA. Th17 cells had no observable defect. Th2 cells from PAD4-deficient mice showed significantly increased IL-4 expression and secretion, substantiating a negative regulatory role for PAD4 in IL-4 expression that is not dependent on PAD4-mediated H4R3 deimination.

3.2.4 Analysis of Neutrophils Derived from PAD4 KO Mice

Neutrophils, the most abundant member of the granulocyte family, express high levels of PAD4 (Asaga et al., 2001). Human peripheral blood neutrophils have increased histone deimination when activated with inflammatory stimuli. Furthermore, those modified histones are also found in NETs released by neutrophils (Neeli et al., 2008; Wang et al., 2009). Since histones have bactericidal properties, NET release is an important defense mechanism.

To study mouse neutrophils, PAD4 WT and KO mice were injected with the neutrophil-eliciting agent casein. Neutrophils were isolated from the peritoneal cavity, purified, and stimulated with LPS. Cells were stained with various antibodies and analyzed by fluorescence microscopy (Figure 28). Staining with an antibody that was raised against human PAD4 confirmed PAD4-deficiency in the KO neutrophils (Figure 28, middle panel p62). WT neutrophils displayed an exclusively nuclear PAD4 staining pattern (Figure 28, middle panel p62). Analysis using antibodies specific for deiminated histone H4R3 or H3, revealed a complete absence of those modifications in neutrophils derived from PAD4 KO mice (Figure 28 bottom panel

p62 and top panel p63). Staining for the neutrophil-specific myeloperoxidase (MPO) was comparable between WT and KO (Figure 28, bottom panel p63).

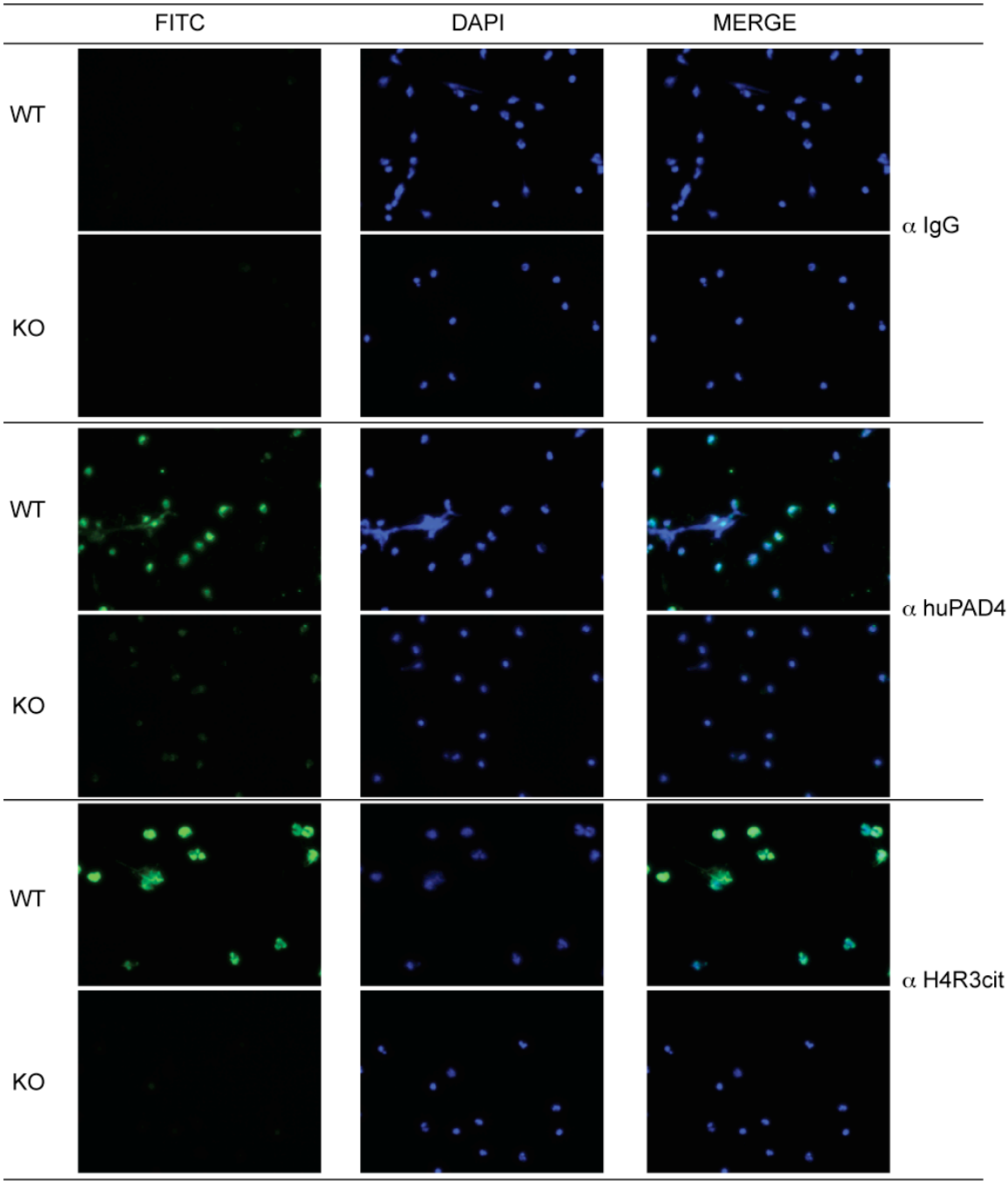

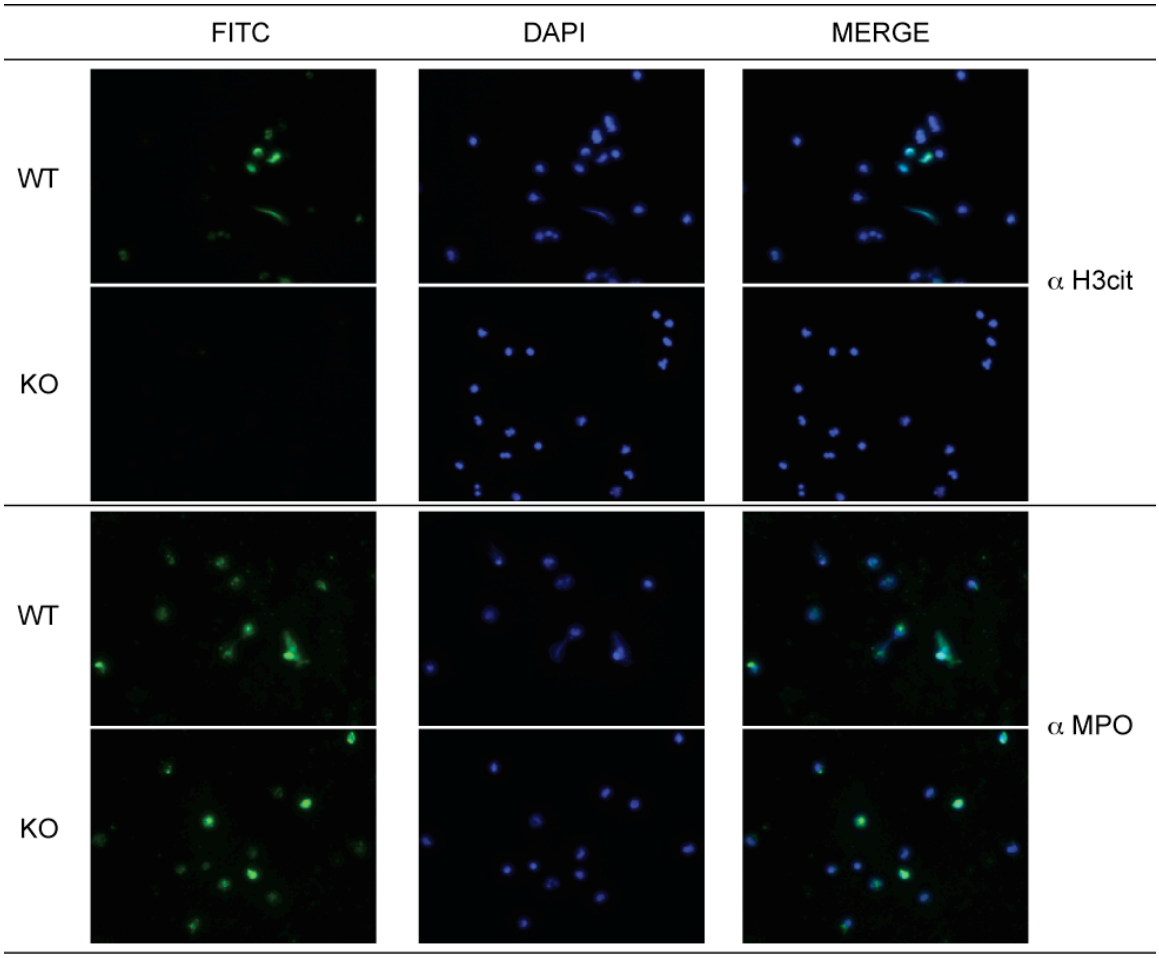

FIGURE 28: Immunofluorescence of PAD4-deficient Neutrophils. Neutrophils were isolated from WT or PAD4 KO mice and allowed to settle on poly-L-lysine coverslips. Cells were stimulated with 100ng/ml LPS for 4h in the presence of 2mM $CaCl_2$. The stimulated cells were stained with a panel of antibodies (listed on the right) and counterstained with DAPI to reveal the nuclei. Representative pictures from two independent experiments are shown. All pictures were taken with the 40x objective.

To summarize, analysis of PAD4-deficient mouse neutrophils confirmed studies of the role of PAD4 in human neutrophils (Neeli et al., 2008; Wang et al., 2009). PAD4 was expressed predominantly in the nucleus. Histone deimination was detected in LPS-treated neutrophils but was completely absent in PAD4-deficient neutrophils. Future studies are required to elucidate the role of PAD4 and deimination in neutrophil biology.

3.3 The Role of CARM1 in Bone Marrow-Derived Macrophages

The arginine methyltransferase CARM1 is a coactivator of several transcription factors, including nuclear-hormone receptors, p53, and NFκB (An et al., 2004; Chen et al., 1999; Covic et al., 2005; Miao et al., 2006). This coactivation is mediated in part by methylation of histone H3R17, a modification associated with active transcription. CARM1 has pleiotropic functions during development, which is best exemplified by the perinatal death of CARM1-deficient mice due to a lung inflation defect (Yadav et al., 2003).

Studies with CARM1-deficient MEFs identified a subset of NFκB target genes that is regulated by recruitment of CARM1 to their promoter (Covic et al., 2005; Miao et al., 2006). The requirement for CARM1 enzymatic activity in this process is under debate (Hassa et al., 2008; Jayne et al., 2009). The list of genes regulated by CARM1-mediated coactivation of NFκB includes several proinflammatory factors like IL-6, MIP-2, and IP-10 (Covic et al., 2005; Jayne et al., 2009). Since macrophages produce all of these factors upon LPS-stimulation, mice with a macrophage-specific deletion of CARM1 were generated.

3.3.1 Generation of CARM1-Deficient BMDMs

CARM1fl/fl mice (Yadav et al., 2003) were obtained, backcrossed to a pure C57BL/6 background, and intercrossed with lysM-Cre mice (Clausen et al., 1999). Several sets of CARM1fl/fl and CARM1fl/fl x lysMCre BMDMs were analyzed, but the deletion efficiency on both the protein and the mRNA level were very poor. On average 42% residual CARM1 mRNA was still detectable (Figure 29).

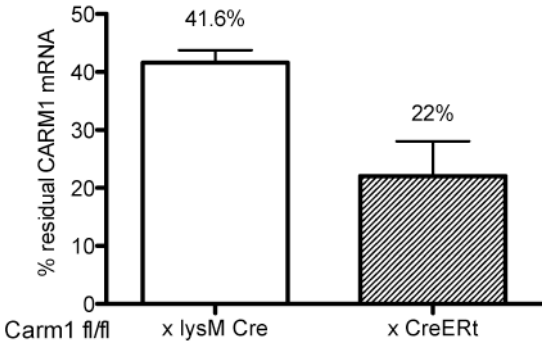

FIGURE 29: Residual CARM1 mRNA after Cre-Mediated Deletion in BMDMs. RNA was isolated from unstimulated BMDMs; the genotypes are indicated on the bottom of the figure. CARM1 mRNA content was determined by qPCR analysis. Data is plotted as % residual CARM1 mRNA, which was calculated in comparison to the matching controls, CARM1fl/fl and CARM1+/+ x CreERt, respectively.

Therefore, CARM1fl/fl mice were intercrossed with CreERt mice, a strain that allows for tamoxifen-inducible Cre-mediated gene ablation (Badea et al., 2003). BMDMs were differentiated *in vitro* in the presence of 10nM 4-hydroxy-tamoxifen (4-OHT). The CARM1-deletion efficiency was improved to 22% residual CARM1 mRNA, as compared to 42% mRNA in BMDMs from lysM-Cre deleted BMDMs (Figure 29).

All further studies were performed with CARM1 x CreERt mice. Unfortunately, BMDM differentiation in the presence of 4-OHT gave poor yields of mature BMDMs Figure 30). However, this was not due to toxic effects of 4-OHT itself but rather to the induction of Cre activity. When comparing BMDM differentiation at d6 from three different genotypes that were all generated in the presence of 4-OHT, only the bone marrow derived from CARM1fl/fl Cre- mice yielded normal amounts of BMDMs

(about $4x10^7$ cells per mouse). Bone marrow from both CARM1+/+ x CreERt and CARM1fl/fl x CreERt mice yielded less than $2.0x10^7$ cells/ mouse. Therefore, CARM1+/+ x CreERt mice were used as controls in all further studies, to account for nonspecific effects caused by the tamoxifen-mediated induction of Cre activity in those cells.

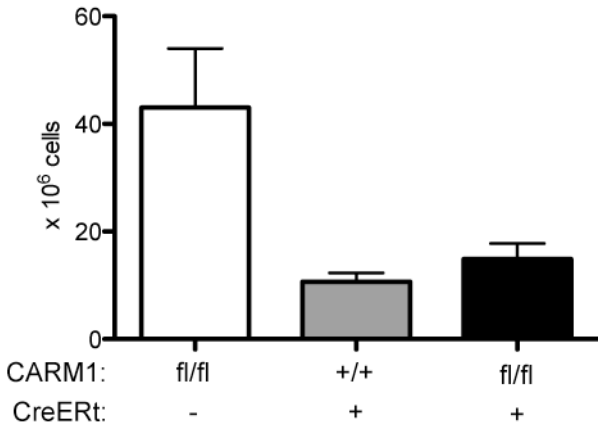

FIGURE 30: BMDM Cell Numbers After Tamoxifen Treatment. Bone marrow derived from the indicated genotypes was differentiated into BMDMs in the presence of 10nM 4-hydroxytamoxifen. After six days of culture, the mature cells were harvested, and total cell numbers were calculated.

Immunoblotting of *in vitro* generated CARM1-deficient BMDMs confirmed the absence of CARM1 on the protein level (Figure 31A). Lysates from those macrophages were also probed with an antibody against dimethylated histone H3R17. This antibody crossreacts with at least seven arginine methylated CARM1 substrates, including the splicing factors SmB and CA150 (Cheng et al., 2007; Yadav et al., 2003). Deletion of CARM1 in BMDMs also revealed reduced CARM1-dependent methylation as detected by the H3R17me antibody (Figure 31B). To ensure proper *in vitro* differentiation of the BMDMs, macrophage maturation was analyzed by flow cytometry. Mature macrophages express high levels of intergrin α M (CD11b) and the glycoprotein F4/80. CARM1-deficiency had no impact on macrophage maturation, since more than 99% of the cells expressed both CD11b and F4/80 (Figure 31C).

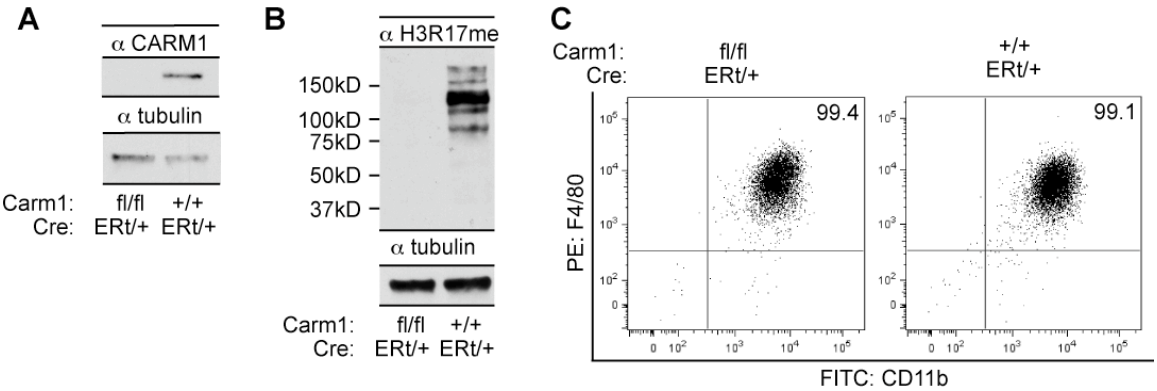

FIGURE 31: Initial Characterization of CARM1-Deficient BMDMs. Bone marrow from mice with the indicated genotypes was differentiated *in vitro* into BMDMs in the presence of 4-OHT. Cells were isolated after six days. (A) Protein lysates were prepared and analyzed for CARM1 expression levels by WB. (B) Lysates from the same cells were probed with α H3R17$(me)_2$-

specific antibody. Relevant molecular weights are indicated on the left. Equal protein loading was confirmed by probing for α tubulin (A+B). (C) The maturation status of the differentiated BMDMs was assessed by flow cytometry. Cells were stained with the pan-macrophage markers CD11b and F4/80. Cells positive for both markers are considered to be mature. Relevant percentages are indicated in the FACS plots. Data shown here are representative examples of all BMDM preps analyzed.

In conclusion, CARM1 expression was efficiently abrogated in CARM1fl/fl x CreERt BMDMs upon tamoxifen-induction of Cre activity. CARM1-deficiency did not influence the *in vitro* maturation of BMDMs. Interestingly, Cre activation by tamoxifen reduced the yields of BMDM cultures independent of CARM1.

3.3.2 Classical and Alternative Activation of CARM1-Deficient Macrophages

CARM1-suffcient and –deficient BMDMs were cultured with stimuli promoting classical or alternative activation. Alternative activation was assessed by detection of urea formation in an Arginase I activity assay (Figure 32A). Urea production was slightly increased in IL-4 treated CARM1-deficient macrophages, but this increase was not statistically significant. NO production by classically activated BMDMs was measured with the Griess assay (Figure 32B). Deletion of CARM1 had no influence on NO production by BMDMs. Therefore, CARM1 is dispensable for L-arginine metabolism in macrophages activated with stimuli for classical or alternative activation.

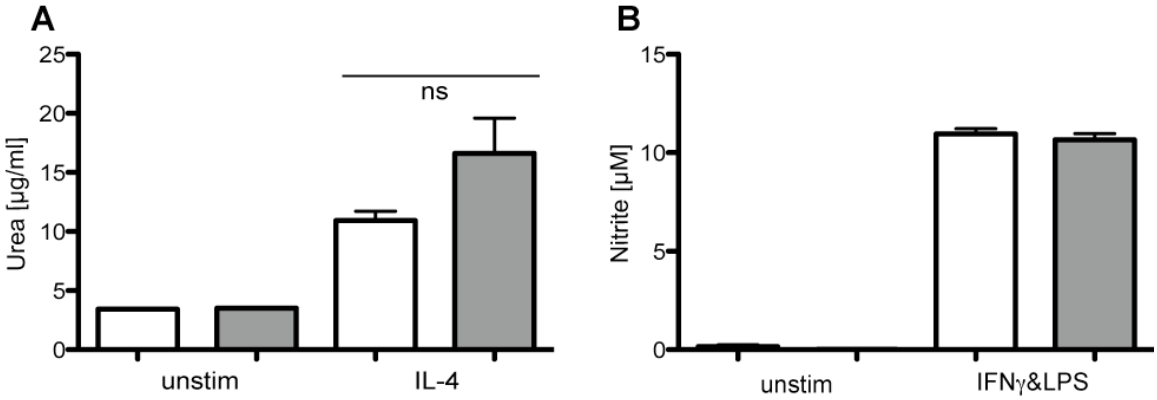

FIGURE 32: Classical vs Alternative Activation of CARM1-Deficient BMDMs. CARM1-sufficient (white bars) or –deficient BMDMs (grey bars) were stimulated in triplicates with IL-4 (10ng/ml) for 48h or IFNγ (10ng/ml) and LPS (5ng/ml) for 24h. (A) BMDM lysates were analyzed in an Arginase activity assay. Urea production was calculated by generation of a Urea standard curve. (B) Nitrite production was measured in BMDM supernatants with the Griess assay. Absolute concentrations were calculated from a standard curve.

Another hallmark of classically activated macrophages is the secretion of proinflammatory cytokines including IL-6 and TNFα. LPS-mediated induction of those cytokines is an NFκB-dependent process. NFκB-mediated expression of IL-6 is abrogated in CARM1-deficient MEFs (Jayne et al., 2009). Reconstitution of the MEFs with either active or enzymatically inactive CARM1 is sufficient to recover IL-6 production (Jayne et al., 2009). Therefore, I analyzed proinflammatory cytokine secretion in LPS-stimulated CARM1-deficient BMDMs. Surprisingly, both IL-6 and TNFα secretion was significantly elevated in CARM1-deficient BMDMs (Figure 33A and B). This effect was seen both upon LPS stimulation and upon combined IFNγ and LPS stimulation (Figure 33A and B). LPS-mediated induction of IL-10 secretion,

a MAP kinase dependent process, was not affected by the absence of CARM1 (Figure 33C).

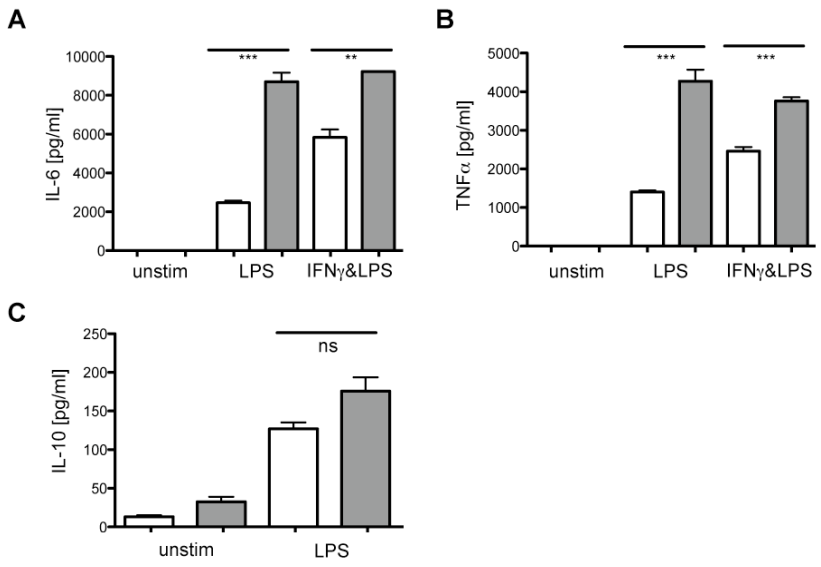

FIGURE 33: Cytokine Production by CARM1-Deficient BMDMs. CARM1-sufficient (white bars) and –deficient BMDMs were stimulated in triplicates with 5ng/ml LPS and 10ng/ml IFNγ as indicated. (A) IL-6 secretion was analyzed by ELISA 24h after stimulation. (B) TNFα secretion was measured 6h after stimulation. (C) IL-10 secretion was assessed 24h post stimulation. Data are represented as mean +/- SEM.

In conclusion, alternatively activated CARM1-deficient BMDMs had normal Arginase I activity. Upon classical activation, NO production was unaffected by CARM1 deletion. IL-6 and TNFα levels were elevated in CARM1-deficient BMDMs upon LPS or IFNγ + LPS stimulation, but IL-10 levels were unaffected. These data suggest that CARM1 may act as a negative regulator of NFκB-mediated IL-6 and TNFα production in BMDMs.

3.3.3 Glucocorticoid-Mediated Suppression of Inflammatory Cytokine Production in CARM1-Deficient BMDMs

CARM1 is a potent coactivator of nuclear hormone receptor signaling (Stallcup et al., 2003). Glucocorticoid-receptor (GR) signaling represses transcriptional responses to inflammatory signals (for review: (De Bosscher et al., 2003)). Treatment of primary macrophages with the GR-agonist dexamethasone (dex) represses a subset of LPS-induced genes, including IL-6, TNFα, and IP-10 (Ogawa et al., 2005). Interestingly, IL-6 and IP-10 expression is sensitive to CARM1-mediated coactivation of NFκB-signaling in MEFs (Covic et al., 2005; Jayne et al., 2009). Therefore, CARM1-deficient BMDMs were stimulated with LPS in the presence or absence of dexamethasone, to elucidate the role of CARM1 in GR-mediated repression of inflammatory cytokine production (Figure 34). Supernatants from BMDMs were analyzed 6h (Figure 34A) and 24h (Figure 34B) after stimulation to analyze the secretion of IL-6 and TNFα. LPS stimulation recapitulated the results from Figure 33. Dexamethasone treatment reduced cytokine production in both CARM1-sufficient and –deficient MEFs, but not to the same extent. CARM1-deficient BMDMs secreted significantly more IL-6 and TNFα than CARM1-sufficient BMDMs, both upon LPS and LPS + dex stimulation (Figure 34A and B).

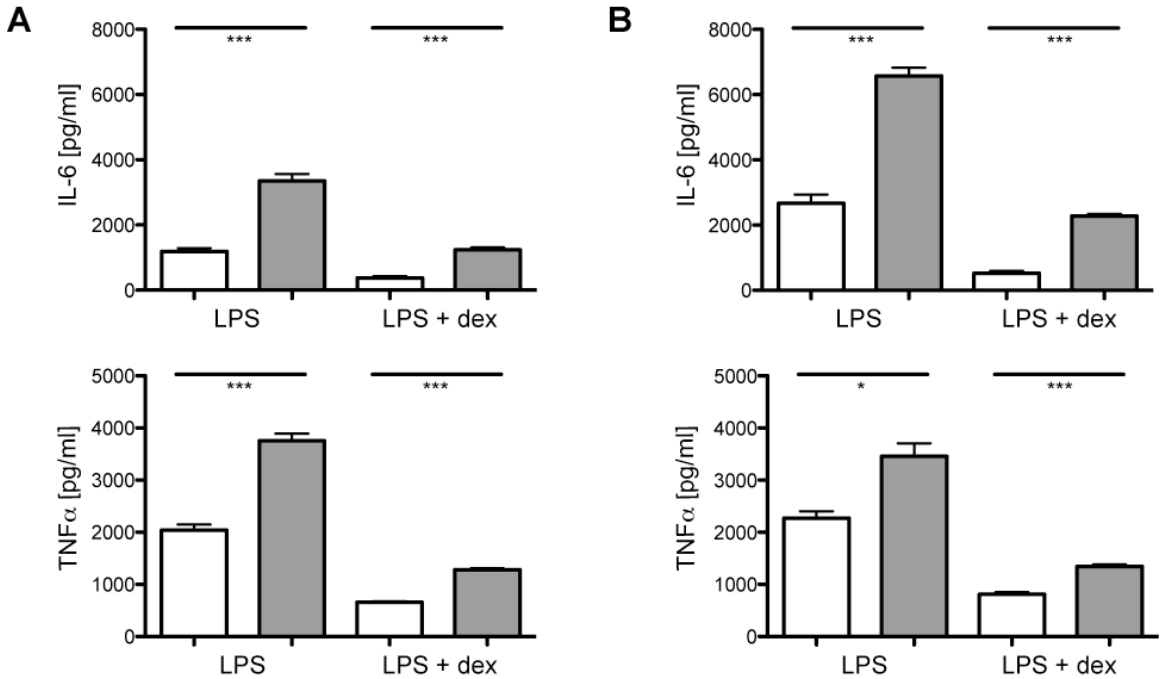

FIGURE 34: Dexamethasone-Mediated Suppression of IL-6 and TNFα Secretion by BMDMs. BMDMs from CARM1-sufficient (white bars) and –deficient (grey bars) mice were stimulated in triplicates with 100ng/ml LPS in the absence or presence of 1μM dexamethasone. IL-6 and TNFα cytokine secretion was measured by ELISA 6h (A) or 24h (B) post stimulation. Values are presented as mean +/- SEM.

To understand if the dysregulation of IL-6 and TNFα is a direct or indirect consequence of CARM1-deficiency, BMDMs were stimulated with LPS or LPS + dex for 3h in the presence or absence of the protein biosynthesis inhibitor cycloheximide (CHX). The cells were harvested, and mRNA levels were quantified by qPCR. Transcript levels of IL-6, TNFα, IP-10 and CARM1 were analyzed relative to the housekeeping gene HPRT (Figure 35). qPCR analysis of CARM1 mRNA levels confirmed the efficient deletion of CARM1 to about 20% of the WT levels (Figure 35, lower right). IL-6 mRNA levels reflected the elevated IL-6 secretion that was observed in the cytokine ELISAs (Figure 34). CARM1-deficient BMDMs exhibited increased IL-6 transcript levels upon LPS and LPS + dex stimulation compared to their wildtype counterparts. Cycloheximide-treatment abolished the increase in IL-6 transcripts in CARM1-deficient BMDMs upon LPS stimulation but not upon LPS + dex stimulation (Figure 35, upper left). TNFα transcript regulation was not affected by CARM1 deletion (Figure 35, lower left). IP-10 transcript was regulated in a similar fashion as IL-6. CARM1-deficient BMDMs had elevated IP-10 mRNA levels upon LPS and LPS + dex stimulation compared to CARM1-sufficient BMDMs. The effect of cycloheximide on IP-10 levels will require further analysis because of the large error bars in those samples (Figure 35, upper right).

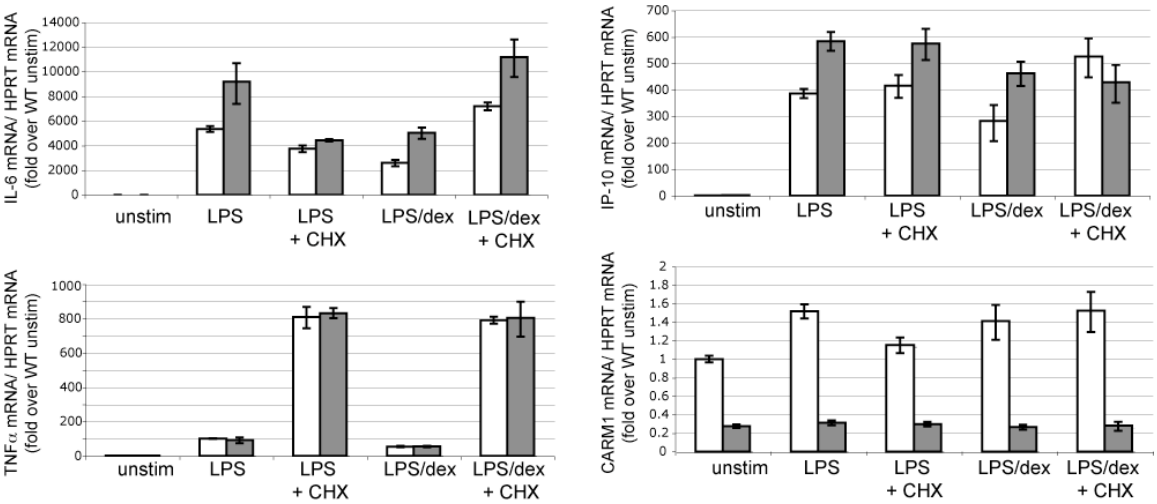

FIGURE 35: qPCR Analysis of CARM1-deficient BMDMs. RNA was isolated from cells that had been stimulated for 3h with LPS (100ng/ml), dexamethasone (1μM), and cycloheximide (10μg/ml) as indicated. White bars represent RNA derived from CARM1-sufficient BMDMs, and grey bars represent CARM1-deficient BMDMs. Transcript levels of IL-6, TNFα, IP-10, and CARM1 were analyzed relative to HPRT using the ΔΔCt method. Data is expressed relative to results obtained with cDNA from unstimulated CARM1-sufficient BMDMs.

In conclusion, LPS stimulated CARM1-deficient cells produced significantly more IL-6 and TNFα than the CARM1-sufficient counterparts, but dexamethasone treatment potently reduced cytokine expression in both sets of cells. Therefore it seems that CARM1-deficiency in BMDMs has little or no effect on GR-mediated suppression of IL-6 and TNFα secretion. qPCR analysis revealed that the effect of CARM1 on IL-6 and IP-10 was at least partially regulated at the transcript level, but the effect of CARM1-deletion on TNFα was regulated posttranscriptionally.

4 Discussion and Outlook

Arginine modifying enzymes are potent regulators of many cellular processes. In this thesis, I focused on two arginine modifying enzymes, PAD4 and CARM1, and their roles in immune regulation. The first part of my thesis focused on the role of the peptidylarginine deiminase PAD4. I discovered that PAD4 can interact with and deiminate NIP45. Furthermore, PAD4 is a negative regulator of NIP45-mediated IL-4 secretion in Th2 cells. In addition, I generated PAD4-deficient mice. The mice are viable and display normal B and T cell development. In the second part of this thesis, I analyzed the role of the arginine methyltransferase CARM1 in macrophages. CARM1-deficiency leads to dysregulation of proinflammatory cytokine production in BMDMs.

4.1 Regulation of NIP45-mediated IL-4 Transcription by PAD4

Cytokine secretion by Th cells is a highly regulated process. Th2 cells secrete IL-4 upon antigen encounter. IL-4 is a potent mediator of humoral immunity and clearance of extracellular pathogens. In addition, Th2 cells require IL-4 during differentiation and lineage maintenance, as IL-4 mediated signals are potent suppressors of Th1 lineage choice. Th2 responses need to be tightly controlled, since elevated type 2 cytokine levels are associated with allergy, asthma, and fibrosis.

The NFAT-interacting protein NIP45 is a central regulator of type 2 immunity (Fathman et al., 2010; Hodge et al., 1996; Mowen and David, 2001; Mowen et al., 2004). NIP45-deficient mice show severe defects in Th2-mediated immune responses, including a strong reduction in IL-4 secretion by Th2 cells. Furthermore, NIP45 KO mice display delayed expulsion of worms in a *Trichinella spiralis* infection model, a process driven by type 2 cytokines (Fathman et al., 2010). NIP45-mediated IL-4 expression is regulated by arginine methylation. The arginine methyltransferase PRMT1 methylates multiple arginines in the N-terminus of NIP45, thereby, facilitating the formation of a tripartite NFAT/NIP45/PRMT1 complex. This complex binds to the IL-4 promoter and drives gene expression (Mowen et al., 2004). NIP45 deficiency leads to a reduction of dimethylated histone H4R3 levels at the IL-4 promoter, underscoring a positive regulatory role for PRMT1 under physiological conditions (Fathman et al., 2010). In summary, PRMT1 activity drives the assembly of the NFAT/NIP45/PRMT1 complex that is required for full transcriptional activity of the IL-4 promoter. IL-4 transcription needs tight control, since aberrant expression has severe consequences for the host. Therefore, I set out to study the negative regulation of IL-4 expression. Since arginine methylation is a positive regulator of NIP45-mediated IL-4 transcription, I hypothesized that arginine deimination could negatively regulate this process.

Histone arginine methylation is regulated by arginine deimination. Besides catalyzing the conversion of arginine to citrulline, the peptidylarginine deiminase PAD4 also converts monomethylated arginine into citrulline, a process referred to as demethylimination (Cuthbert et al., 2004; Wang et al., 2004). Deiminated arginines cannot be methylated by PRMTs. Methylation of NIP45 might be regulated similarly. I focused on the role of PAD4 in NIP45-mediated IL-4 transcription in Th2 cells for two reasons: First, PAD2 and PAD4 are the only PAD family members expressed in T cells (Vossenaar et al., 2004). Second, PAD4 is the only nuclear PAD family member (Nakashima et al., 2002), which is relevant since NIP45 is a nuclear protein as well.

PAD4 expression in Th2 cells, albeit at low levels, was confirmed on the RNA transcript level. Furthermore, PAD4 could deiminate NIP45 both *in vitro* and *in vivo*. Interestingly, deimination of NIP45 with recombinant PAD4 could prevent subsequent methylation by PRMT1, whereas PRMT1-mediated methylation of NIP45 had no influence on subsequent deimination. This data suggests that the arginines modified by PAD4 and PRMT1 only partially overlap. Indeed, deimination analysis of NIP45 deletion mutants revealed that deimination of NIP45 was not confined to the PRMT1-targeted glycine- and arginine-rich N-terminus (Mowen et al., 2004) but was distributed throughout the protein. To identify the actual deiminination sites, *in vitro* deiminated NIP45 was analyzed by mass spectrometry. Though we obtained poor sequence coverage, I identified four deiminated arginine residues at positions R32, R37, R103, and R104. R103 and R104 are part of the NLS of NIP45, but mutation of these residues to a glutamine residue to mimic deimination had no effect on nuclear localization of NIP45. I engineered R->Q point-mutants for all four sites and tested the capacity of those mutants to potentiate IL-4 secretion from M12 cells. The R37Q mutation negatively affected NIP45-mediated IL-4 secretion; all other mutants showed little or no defect. It is of interest to address how deimination of R37 affects endogenous IL-4 transcription. It will be important to test whether the R37Q mutation destabilizes the NFAT/NIP45/PRMT1 complex. Generation of a NIP45 mutant with all four R->Q substitutions might reveal an additive effect for those deimination sites. Since neither the N-terminal sequence of NIP45 nor the C-terminus could be resolved in our mass spectrometric studies, future analyses are needed to resolve the modifications at the N-terminus and the C-terminus.

To address the effects of PAD4 on NIP45-mediated IL-4 transcription in a more direct way, I performed coexpression studies of PAD4, NIP45 and NFAT in M12 cells. PAD4 suppressed NIP45-mediated IL-4 expression and secretion. Interestingly, the same effect could be achieved by coexpression of an enzymatically inactive point mutant of PAD4. This suggests that PAD4 negatively regulates NIP45-mediated IL-4 secretion independent of its catalytic activity. In addition, Th2 cells from PAD4-deficient mice secreted significantly more IL-4 than their WT counterparts. An initial analysis of the IL-4 locus control region by ChIP revealed no differences between PAD4 WT and KO Th2 cells.

There are several mechanisms for PAD4-mediated suppression of NIP45-driven IL-4 expression conceivable: First, since PAD4 could interact with NIP45 and NFAT, PAD4 might compete with PRMT1 for NFAT/NIP45 binding. Competitive expression of PAD4 and PRMT1 with NFAT/NIP45 should address if the arginine-modifying enzymes are vying for the same binding sites. Coexpression of PAD4 with PRMT1/NFAT/NIP45 followed by immunoprecipitation of NIP45 should reveal a decreased association of PRMT1 with NIP45/NFAT, if PAD4 competes for binding of NIP45. In addition, the NIP45 deletion mutants could be used to map PRMT1-, PAD4-, and NFAT-binding sites on NIP45.

Second, deimination of NIP45 might be required under circumstances when the amount of cellular PAD4 is limited. Endogenous PAD4 levels are likely to be much lower than the levels observed in experiments using overexpression systems, and they might not be sufficient to compete for binding. Therefore, PAD4-mediated deimination of NIP45 may inhibit PRMT1 and NIP45 association. To test if PAD4 enzymatic activity would be required under physiological conditions, PAD4-deficient Th2 cells could be retrovirally transduced with active or inactive PAD4. The transduced cells could be sorted into high- and low-expressing cells and analyzed for their IL-4 expression capacities. If PAD4 catalytic activity were required, PAD4 KO Th2 cell IL-4 production would only be restored to WT levels in the presence of the catalytically active PAD4.

Third, PAD4 might inhibit IL-4 expression independent of NIP45. To identify a role for PAD4 in IL-4 expression independent of NIP45, I will try to identify novel interaction partners of PAD4. To this end, I have generated two monoclonal

antibodies against PAD4, which will be used to immunoprecipitate PAD4 from Th2 cells. The IPs will then be analyzed by mass spectrometry to identify interacting proteins. In my preliminary analysis, both antibodies could immunoprecipitate endogenous PAD4 (data not shown). In addition, these antibodies will also be useful for ChIP-Seq studies, a technique that combines chromatin immunoprecipitation with high-throughput DNA sequencing to reveal genomic binding sites of PAD4.

In conclusion, I propose that PAD4 is a negative regulator of IL-4 secretion. PAD4 can deiminate NIP45, but the requirement for deimination of NIP45 in IL-4 transcriptional regulation remains unclear. Since PAD4 can interact with NIP45 and NFAT, it might displace PRMT1 from the trimeric NFAT/NIP45/PRMT1 complex. In addition, PRMT1 can methylate PAD4 *in vitro,* which might serve to regulate PAD4 activity or binding (Figure 36).

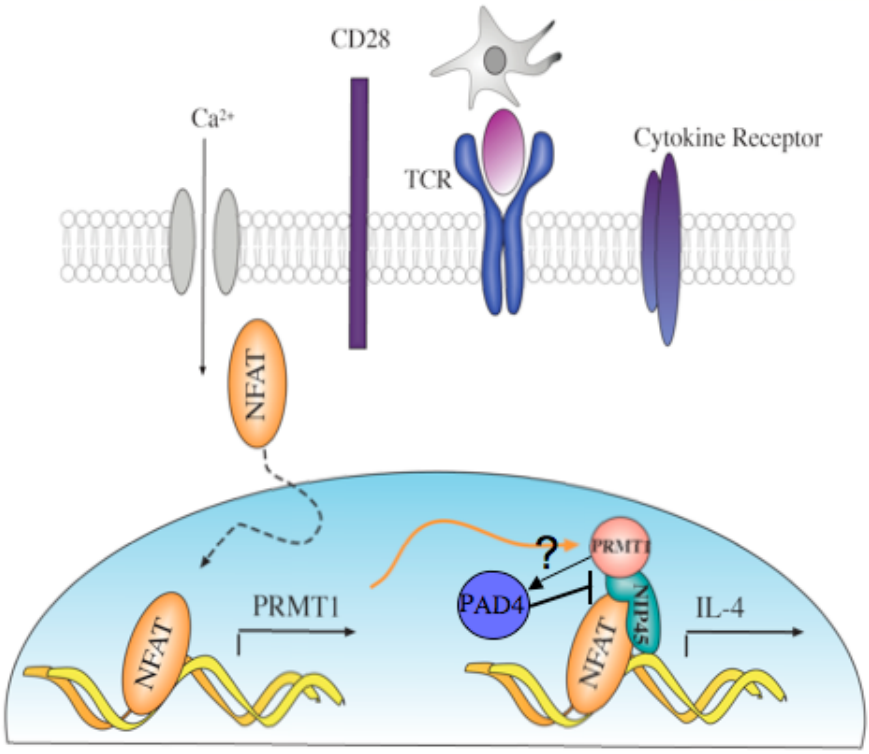

FIGURE 36: Model of PAD4-mediated Regulation of IL-4 Transcription (adapted from Kerri Mowen)

It is interesting to speculate about a role for PAD4-mediated deimination of NIP45 in a broader sense. Not much is known about the biology of NIP45. NIP45 is part of the RENi protein family comprised of Rad60, Esc2, and NIP45. The RENi family is characterized by the presence of two carboxyterminal Small Ubiquitin-like Modifier (SUMO)-like domains (Novatchkova et al., 2005). The SUMO-like domain of NIP45 can interact with the E2 SUMO ligase Ubc9, thereby, inhibiting polysumoylation of Ubc9 targets (Sekiyama et al., 2010). Since PAD4 could deiminate residues throughout NIP45, PAD4 might also modify residues in the two SUMO-like domains, potentially affecting the interaction of NIP45 with Ubc9. Interestingly, NFAT1, the interaction partner of NIP45, is a target of Ubc9-mediated sumoylation (Terui et al., 2004). The sumoylation of NFAT is important for nuclear retention and transcriptional activity of NFAT1. NIP45 might be required to limit NFAT sumoylation to mono- or di-sumoylation and prevent polysumoylation, which would target NFAT for degradation. If deimination of NIP45 would decrease the interaction of NIP45 with the E2 SUMO-ligase Ubc9, this could lead to polysumoylation of NFAT

and subsequent degradation, providing another possible mechanism for negative regulation of IL-4 expression. Therefore, I will test the effect of PAD4-mediated deimination of NIP45 on the sumoylation of NFAT by coexpression of NFAT, NIP45, PAD4 and SUMO1, and subsequent immunoprecipitation of NFAT to analyze how its sumoylation status is affected by the presence of PAD4.

NIP45 interacts with members of the TNF Receptor Associated Factor (TRAF) family (Bryce et al., 2006; Lieberson et al., 2001). TRAFs are intracellular signaling mediators of the TNF-receptor superfamily (for review: (Ha et al., 2009)). TRAF signaling mediates pleiotropic cellular activities, including survival, proliferation, inflammation, and lymphocyte activation. Interaction of NIP45 with TRAF1 (Bryce et al., 2006) or TRAF2 (Lieberson et al., 2001) negatively affected IL-4 expression in IL-4 reporter assays and overexpression studies in M12 cells. It is interesting to speculate that PAD4-mediated deimination of NIP45 might facilitate binding of TRAFs to potentiate negative regulation of IL-4. This hypothesis can be tested by overexpression of NFAT, NIP45, PAD4 and TRAF1 or TRAF2 in M12 cells. If PAD4 and TRAFs cooperate in the negative regulation of IL-4 expression, I would expect to see even stronger repression of IL-4 secretion when PAD4 and TRAF1 or TRAF2 are coexpressed.

4.2 Generation of PAD4-Deficient Mice

Although PAD4 has a restricted expression pattern (Vossenaar et al., 2004), PAD4 dysregulation has been associated with severe pathological conditions, including RA (Anzilotti et al., 2010), MS (Wood et al., 2008), and malignant tumors (Chang and Fang, 2009). The PAD4-specific conditional KO strain will be an important tool to further the understanding of PAD4 biology, especially in difficult-to-access cell types like neutrophils. The PAD4fl/fl mice are currently being bred onto the lysM-Cre strain, the Lck-Cre strain, and the Cre-ERt strain. The initial characterization was performed in mice that had been crossed with the CMV-Cre mouse line that deletes the floxed gene segments in all tissues. PAD4-/- mice are viable and display no overt developmental phenotypes. B and T cell development was analyzed more closely, but was comparable between WT and KO PAD4 mice.

Th2 cells from PAD4-deficient mice displayed elevated IL-4 secretion, substantiating a proposed role for PAD4 in negative regulation of IL-4 secretion (see 4.1). Thus it will be interesting to challenge mice with a T cell-specific deletion of PAD4 (PAD4 x Lck-Cre) with *Trichinella spiralis*, a parasitic nematode, which elicits a strong type 2 immune response. The working hypothesis would be that PAD4-deficient mice should have an overactive type 2 response with elevated serum IL-4 levels and faster expulsion kinetics of the parasites. PAD4-deficient Th1 cells displayed a small but significant decrease in IFNγ secretion upon TCR stimulation. Therefore, it would be of interest to challenge the mice with *Leishmania major*. C57BL/6 mice are resistant to infection but defects in type 1 immunity will convert the resistant strain into a susceptible strain. If the IFNγ-secretion defect in PAD4-deficient Th1 cells is robust, the PAD4-deficient mice should be more susceptible to *L. major* infection, which can be assessed by bacterial burden and serum IFNγ levels.

PAD4 is highly expressed in granulocytes, especially neutrophils (Asaga et al., 2001). PAD4-mediated histone deimination promotes chromatin decondensation, which is a prerequisite for NET release (Neeli et al., 2008; Wang et al., 2009). Indeed, I demonstrated that histone deimination in murine neutrophils was absolutely dependent on PAD4. The initial characterization of neutrophils derived from PAD4 mice will be expanded further to analyze the role of PAD4 in neutrophil biology. It will be interesting to test, whether PAD4 deficiency will affect neutrophil effector functions, especially degranulation, cytokine release, ROS production, and bacterial killing. Furthermore, NET formation in PAD4 WT and KO neutrophils will be

characterized *in vitro* both qualitatively (bacterial killing assays) and quantitatively (IF enumeration), to address whether PAD4-mediated deimination is important for NET release.

By generating PAD4fl/fl x lysM Cre mice, I will have a valuable tool to address the role of PAD4 in neutrophil and macrophage function *in vivo*. Subcutaneous or pulmonary challenge with *C. albicans* can be used to assess NET-mediated trapping of the pathogen (Urban et al., 2009). PAD4 protein is expressed in monocytes and macrophages, but PAD4 mRNA is only detected in monocytes (Vossenaar et al., 2004). Therefore, it will be of interest to study both PAD4 mRNA and protein stability in monocytes and macrophages. Furthermore, PAD4fl/fl x lysM Cre mice will be used to characterize macrophage function both *in vitro* and *in vivo*. The initial *in vitro* characterization will include the assessment of classical versus alternative activation in BMDMs. I am especially interested in the glucocorticoid-receptor mediated suppression of proinflammatory cytokines since PAD4 is a negative regulator of nuclear-hormone receptor transcription (Cuthbert et al., 2004; Wang et al., 2004). If PAD4-mediated negative regulation of GR-mediated signaling were important in macrophages, I would expect to see enhanced suppression of proinflammatory cytokine secretion in PAD4-deficient BMDMs.

Since PAD4 dysregulation has been implicated in various diseases, cell type-specific deletion of PAD4 will be a useful tool to elucidate the contribution of PAD4 to disease. PAD4 has been implicated in RA in several ways: PAD4 mRNA and protein can be found in the arthritic joint (Chang et al., 2005b; Foulquier et al., 2007). Autoantibodies against citrullinated peptides are detected in patients even prior to clinical diagnosis of RA (Nielen et al., 2004; Vencovsky et al., 2003). A polymorphism in PAD4 has been associated with enhanced susceptibility to RA (Suzuki et al., 2003). It will be of interest to test the involvement of PAD4 in RA disease development and progression. There are several mouse models for RA available.

The K/BxN serum transfer model induces RA-like disease in mice by injection of serum containing an autoantibody against GPI (glucose-6-phosphate isomerase) (Kouskoff et al., 1996; Monach et al., 2007). This model allows isolated analysis of the effector-phase of the disease downstream of autoantibody production. I will examine the susceptibility of PAD4-deficient mice (PAD4-/- and PAD4fl/fl x lysM Cre) to inflammatory arthritis using the K/BxN serum transfer model. This model has several advantages. Since C57BL/6 mice are susceptible to RA induction in this model, the PAD4 mice do not need to be backcrossed onto a different genetic background. In addition, previous studies have demonstrated that neutrophils contribute to disease development in the K/BxN model (Monach et al., 2010; Wipke and Allen, 2001). If PAD4 deficiency diminishes the proinflammatory capacities of neutrophils and macrophages, I would predict ameliorated disease in PAD4-deficient mice.

The collagen-induced arthritis (CIA) model is an antigen-induced model of RA (Rosloniec et al., 2001). The CIA model requires backcrossing of the mice onto a susceptible mouse strain, e.g. DBA/1. Collagen-induced arthritis depends on the breakdown of T cell tolerance and autoantibody production (Monach et al., 2004). Importantly, joints from arthritic mice display elevated PAD4 protein expression and citrullinated protein deposits (Vossenaar et al., 2003a). Therefore, it will be interesting to test how the absence of PAD4 will affect disease onset and severity in this model. I hypothesize that in the absence of PAD4 the mice will have ameliorated disease. Furthermore, serum and joints from arthritic PAD4 WT and KO mice will be analyzed for anti-cyclic citrullinated peptide autoantibodies, to test if PAD4 is required for development of citrullinated autoantigens and, subsequently, autoantibodies.

The role of PAD4 in apoptosis is controversial. PAD4 has been described to both promote apoptosis and cell cycle arrest (Hung et al., 2007; Liu et al., 2006) and

inhibit apoptosis (Li et al., 2008; Yao et al., 2008). Therefore, I propose to generate PAD4-deficient MEFs, which can be used to study the effects of PAD4-deficiency on apoptosis induction by chemical induction (doxorubicin, staurosporine, etc) or by radiation (UV). If PAD4 promotes apoptosis, PAD4-deficient MEFs should display less apoptotic features or a delay in apoptosis progression.

In conclusion, I generated a PAD4 conditional KO mouse strain that will serve as a valuable tool to further the understanding of PAD4 biology. The role of PAD4 in neutrophils is of special interest, since it might shed light on the disease mechanism of RA.

4.3 The Role of CARM1 in Bone Marrow-Derived Macrophages

The arginine methyltransferase CARM1 coactivates several transcription factors, including NFκB (Covic et al., 2005; Miao et al., 2006). CARM1 interacts with p65, and this association is independent of the arginine methyltransferase activity of CARM1 (Covic et al., 2005). CARM1 mediates NFκB coactivation in complex with members of the p160 coactivator family and the acetyltransferases p300/CBP (Covic et al., 2005; Miao et al., 2006). Recruitment of CARM1 to gene promoters coincides with histone H3R17 methylation, a chromatin modification associated with active transcription (Covic et al., 2005; Miao et al., 2006).

The role of CARM1 in NFκB-mediated transcriptional regulation has been studied in CARM1-deficient MEFs. Upregulation of a subset of NFκB target genes, including IP-10, MIP2 and ICAM-1, upon LPS or TNFα-mediated stimulation was decreased in CARM1-deficient cells (Covic et al., 2005). CARM1-deficiency had no effect on activation of NFκB measured by IκB degradation or nuclear translocation of p65 (Covic et al., 2005). Furthermore, coactivation by CARM1 was dependent on its catalytic activity (Covic et al., 2005). TNFα stimulation of 293T cells after knockdown of CARM1 revealed a role for CARM1 in the coactivation of the NFκB target genes IL-8, IP-10, and TNFα (Miao et al., 2006). Complementation of CARM1-deficient MEFs with active or enzymatically inactive CARM1 permitted the discovery of a group of NFκB target genes that were dependent on CARM1 but independent of its enzymatic activity, including IL-6 and MIP2 (Jayne et al., 2009). In contrast, MIP2 was also described as a CARM1-dependent NFκB target gene that required arginine methyltransferase activity (Covic et al., 2005; Hassa et al., 2008).

To establish a model system to study the role of CARM1 in proinflammatory cytokine production, I generated CARM1-deficient BMDMs to study the role of CARM1 in proinflammatory cytokine production. The generation of a macrophage-specific deletion by breeding of CARM1fl/fl mice to the lysM-Cre strain proved to be unsuccessful. The deletion efficiency was variable both on the protein and the mRNA level, which led to inconsistencies between experiments. Indeed, other investigators have reported inefficient deletion by lysM-Cre in macrophages (Greenblatt et al., 2010). Therefore, I established a novel model of *in vitro* deletion of CARM1 by crossing CARM1fl/fl mice with the tamoxifen-inducible CreERt strain. In this model system, deletion efficiency was improved and sufficient for my studies. It is interesting to note that even with tamoxifen-induced CARM1 deletion I could still detect residual mRNA. This phenomenon might reflect the existence of a few non-deleted bone marrow cells that can outcompete CARM1-deficient cells during BMDM differentiation.

According to published data, I expected to see defects in LPS-induced IL-6 and TNFα expression in CARM1-deficient BMDMs. Surprisingly, CARM1-deficiency resulted in significantly increased IL-6 and TNFα cytokine production upon LPS

stimulation. These data suggest that CARM1 is required for negative regulation of NFκB-dependent proinflammatory cytokine production. Indeed, CARM1-mediated methylation of p160 coactivators and p300/CBP has been described to destabilize the coactivator complex, thereby, initiating termination of transcription (Lee et al., 2005a; Naeem et al., 2007). Therefore, I propose to assess coactivator complex stability and the kinetics of transcriptional termination in CARM1-deficient BMDMs. I have not ruled out the possibility that the observed increase in IL-6 and TNFα secretion is due to hyperproliferation of CARM1-deficient BMDMs, but the observation that IL-10 secretion is not changed in CARM1-deficient BMDMs would argue against that possibility. Nevertheless, I will measure tritiated thymidine incorporation to assess proliferation of BMDMs upon LPS stimulation in future studies. Furthermore, it is important to study the effect of CARM1-deficieny on NFκB signaling by analyzing IκB degradation kinetics as well as p65 translocation to the nucleus. Finally, I will address p65 and coactivator binding to the IL-6 and TNFα promoters upon LPS stimulation by ChIP and EMSA studies. I would predict to see no differences in NFκB signaling between CARM1-sufficient and –deficient BMDMs, but prolonged promoter association of p65 and the p160/p300/CBP coactivator complex in CARM1-deficient BMDMs, thereby, proposing a role for CARM1 in methylation-mediated destabilization of the coactivator complex.

Since CARM1 seems to be a negative regulator of NFκB-mediated IL-6 and TNFα production, I determined whether this was due to a direct effect of CARM1. I performed analysis of IL-6 and TNFα transcription upon LPS stimulation in the absence or presence of the protein biosynthesis inhibitor cycloheximide. LPS-induced expression of the IL-6 mRNA was increased in CARM1-deficient BMDMs in parallel to elevated IL-6 secretion and was sensitive to cycloheximide treatment. Cycloheximide-sensitivity suggests that CARM1 is an indirect regulator of IL-6 expression that requires synthesis of other mediators. Microarray-analysis comparing LPS-stimulated CARM1-sufficient and –deficient BMDMs will enable identification of the cycloheximide-sensitive CARM1 targets that regulate IL-6 expression. Interestingly, analysis of LPS-induced TNFα expression revealed no difference between CARM1-sufficient and –deficient BMDMs. Since we had observed significantly more TNFα production on the protein level in CARM1-deficient BMDMs, these results suggest a role for CARM1 in the translational regulation of TNFα. Alternatively, CARM1 might regulate TNFα by affecting its mRNA stability, and the 3h post stimulation timepoint that I analyzed may have missed the window of regulation. Indeed, CARM1 methylates the mRNA stabilizer HuR upon LPS stimulation in a macrophage cell line (Li et al., 2002). HuR stabilizes TNFα mRNA by binding to the AU-rich elements in the 3'UTR of TNFα (Dean et al., 2001). Therefore I will perform a more thorough kinetic analysis of the TNFα mRNA levels comparing CARM1-sufficient and –deficient BMDMs to elucidate if HuR methylation by CARM1 could affect the stabilization of TNFα transcript.

CARM1 was originally identified as a coactivator for nuclear hormone receptor-mediated transcription (Chen et al., 1999). Glucocorticoid receptor signaling is involved in repression of the transcriptional response to inflammatory stimuli (Ogawa et al., 2005). The glucocorticoid receptor agonist dexamethasone is a potent anti-inflammatory drug that is used in treatment of inflammatory conditions like RA (Bijlsma et al., 2002). Glucocorticoid-receptor stimulation leads to Transrepression of NFκB family members (De Bosscher et al., 2003). Since CARM1 is a coactivator of glucocorticoid receptor-mediated transcription, I tested whether CARM1-deficient BMDMs were defective in dexamethasone-mediated transrepression of proinflammatory cytokines. LPS-induced IL-6 and TNFα expression was effectively repressed by dexamethasone treatment in both CARM1-sufficient and –deficient

macrophages. Although the CARM1-deficient cells produced significantly more IL-6 and TNFα than CARM1-sufficient cells upon LPS + dex treatment, the levels were still much lower compared to LPS treatment alone. The significant increase is more likely due to the overall loss of CARM1 and elevation in IL-6 and TNFα transcription. I conclude that CARM1 is not involved in glucocorticoid-receptor mediated trans-repression of NFκB-mediated proinflammatory cytokine expression.

5 Summary

Arginine modifying enzymes are important transcriptional regulators involved in many cellular processes. Cytokine expression by immune cells is a highly regulated process, since cytokine imbalance is associated with severe pathological consequences including autoimmunity, autoinflammation and asthma.

Th2 mediated IL-4 expression is a tightly regulated process. The NFAT-interacting protein NIP45 is an essential regulator of IL-4 expression by Th2 cells. Furthermore, NIP45-mediated IL-4 expression is enhanced by arginine methylation of NIP45. Here, I demonstrate that arginine deimination of NIP45 by PAD4 negatively regulates IL-4 expression. PAD4 can deiminate NIP45 both *in vitro* and *in vivo*. Overexpression of PAD4 can suppress NIP45-mediated IL-4 expression. Interestingly, the suppressive activity of PAD4 is independent of its catalytic activity. Furthermore, Th2 cells from PAD4-deficient mice that I generated for this thesis display elevated IL-4 secretion. Taken together, I have established that PAD4 is a negative regulator of IL-4 expression. Although PAD4 can deiminate NIP45, the catalytic activity of PAD4 is not required for suppression of NIP45-mediated IL-4 secretion.

CARM1 coactivates NFκB-mediated transcription of several proinflammatory genes including IL-6, TNFα, and IP-10 in MEFs. In contrast, I demonstrate that CARM1 is a negative regulator of NFκB-mediated proinflammatory cytokine secretion in macrophages. CARM1-deficient BMDMs secrete significantly more IL-6 and TNFα upon LPS stimulation than CARM1-sufficient BMDMs, without exhibiting a difference in IL-10 secretion. In addition, CARM1 is reported to coactivate glucocorticoid-receptor mediated transcription. Here, I show that glucocorticoid-mediated trans-repression of NFκB in BMDMs is not regulated by CARM1.

In conclusion, the results from this thesis reveal novel roles for arginine modifying enzymes in cytokine expression by Th2 cells and macrophages. PAD4 is a negative regulator of NIP45-mediated IL-4 secretion in Th2 cells. In addition, the generation of the PAD4 conditional knockout strain will allow a more detailed analysis of PAD4 in immune regulation. Furthermore, CARM1 is a negative regulator of NFκB-mediated proinflammatory cytokine secretion in macrophages, revealing cell-type specific differences for CARM1 function in macrophages and MEFs.

6 Zusammenfassung

Die posttranslationale Modifizierung von Argininen durch Arginin-Methyltransferasen oder Arginin-Deiminasen, spielt eine wichtige Rolle in verschiedensten zellulären Prozessen. Die Sekretion von Zytokinen durch Zellen des Immunsystems ist stark reguliert, u.a. durch posttranslationale Modifikation. Fehlregulation von Zytokinen hat pathologische Konsequenzen, wie z.B. Autoimmunität, Inflammation und Asthma.

Th2 Zellen sind die Hauptproduzenten des Zytokins IL-4, dessen Produktion ebenfalls stark reguliert ist. NIP45, ein Protein das mit NFAT interagiert, ist ein wichtiger Modulator der IL-4 Sekretion durch Th2 Zellen. Die Methylierung von Argininen im NIP45-Protein hat einen positiven Effekt auf IL-4 Expression. Im Rahmen dieser Doktorarbeit konnte gezeigt werden, dass die Deimination von Argininen im NIP45-Protein durch PAD4 einen negativen Effekt auf IL-4 Protein Expression hat. PAD4 deiminiert NIP45 sowohl *in vitro* als auch *in vivo*. Überexpression von PAD4 führt zu Repression von IL-4 Sekretion durch NIP45. Dieser Effekt ist allerdings unabhängig von der enzymatischen Aktivität von PAD4. Um den Effekt von PAD4 auf IL-4 Produktion genauer zu untersuchen, wurden PAD4 cKO Mäuse generiert. Interessanterweise weisen Th2 Zellen, die aus PAD4-defizienten Mäusen isoliert wurden, erhöhte IL-4 Sekretion auf. Daraus schliesse ich, dass PAD4 einen negativen Effekt auf NIP45-induzierte IL-4 Expression hat. Obwohl PAD4 NIP45 deiminieren kann, scheint dieser Effekt nicht verantwortlich für die Regulierung von IL-4 Sekretion durch Th2 Zellen zu spielen.

CARM1 ist ein Koaktivator von NFκB. In MEFs konnte gezeigt werden, dass CARM1 die Expression der proinflammatorischen Zytokine IL-6, TNFα und IP-10 positiv reguliert. Im Rahmen dieser Studie konnte erstmalig gezeigt werden, dass CARM1 einen negativen Einfluss auf die proinflammatorische Zytokin-Expression in Makrophagen hat. CARM1-Deletion in Makrophagen führt zu vermehrter Sekretion von IL-6 und TNFα nach Stimulierung der Zellen mit LPS. CARM1 hat keinen Einfluss auf die Sekretion von IL-10. Desweiteren wurde die Rolle von CARM1 in der Transrepression von NFκB durch Glukokortikoide untersucht. Die Repression der proinflammatorischen Zytokin-Expression in CARM1-defizienten Makrophagen ist intakt.

Zusammenfassend konnte im Rahmen dieser Arbeit eine neue Rolle sowohl für PAD4 als auch CARM1 in der Immunregulation gezeigt werden. PAD4 ist wichtig für die Deaktivierung der NIP45-induzierten IL-4 Expression in Th2 Zellen. Ausserdem werden die generierten PAD4-defizienten Mäuse hilfreich in der weiteren Analyse von PAD4 sein. Trotz der Funktion für CARM1 in der Koaktivierung von NFκB in MEFs, scheint CARM1 einen negativen Effekt auf die Expression der NFκB-abhängigen Zytokine IL-6 und TNFα zu haben.

7 References

Abramovich, C., Yakobson, B., Chebath, J., and Revel, M. (1997). A protein-arginine methyltransferase binds to the intracytoplasmic domain of the IFNAR1 chain in the type I interferon receptor. The EMBO journal *16*, 260-266.

Aderem, A., and Underhill, D.M. (1999). Mechanisms of phagocytosis in macrophages. Annual review of immunology *17*, 593-623.

Altschuler, L., Wook, J.O., Gurari, D., Chebath, J., and Revel, M. (1999). Involvement of receptor-bound protein methyltransferase PRMT1 in antiviral and antiproliferative effects of type I interferons. J Interferon Cytokine Res *19*, 189-195.

Alwine, J.C., Kemp, D.J., and Stark, G.R. (1977). Method for detection of specific RNAs in agarose gels by transfer to diazobenzyloxymethyl-paper and hybridization with DNA probes. Proceedings of the National Academy of Sciences of the United States of America *74*, 5350-5354.

An, W., Kim, J., and Roeder, R.G. (2004). Ordered cooperative functions of PRMT1, p300, and CARM1 in transcriptional activation by p53. Cell *117*, 735-748.

Andrade, F., Darrah, E., Gucek, M., Cole, R.N., Rosen, A., and Zhu, X. (2010). Autocitrullination of human peptidylarginine deiminase 4 regulates protein citrullination during cell activation. Arthritis and rheumatism.

Ansel, K.M., Djuretic, I., Tanasa, B., and Rao, A. (2006). Regulation of Th2 differentiation and Il4 locus accessibility. Annual review of immunology *24*, 607-656.

Ansel, K.M., Greenwald, R.J., Agarwal, S., Bassing, C.H., Monticelli, S., Interlandi, J., Djuretic, I.M., Lee, D.U., Sharpe, A.H., Alt, F.W., and Rao, A. (2004). Deletion of a conserved Il4 silencer impairs T helper type 1-mediated immunity. Nature immunology *5*, 1251-1259.

Anzilotti, C., Pratesi, F., Tommasi, C., and Migliorini, P. (2010). Peptidylarginine deiminase 4 and citrullination in health and disease. Autoimmunity reviews *9*, 158-160.

Arita, K., Hashimoto, H., Shimizu, T., Nakashima, K., Yamada, M., and Sato, M. (2004). Structural basis for Ca(2+)-induced activation of human PAD4. Nature structural & molecular biology *11*, 777-783.

Arita, K., Shimizu, T., Hashimoto, H., Hidaka, Y., Yamada, M., and Sato, M. (2006). Structural basis for histone N-terminal recognition by human peptidylarginine deiminase 4. Proceedings of the National Academy of Sciences of the United States of America *103*, 5291-5296.

Asaga, H., Nakashima, K., Senshu, T., Ishigami, A., and Yamada, M. (2001). Immunocytochemical localization of peptidylarginine deiminase in human eosinophils and neutrophils. Journal of leukocyte biology *70*, 46-51.

Asaga, H., Yamada, M., and Senshu, T. (1998). Selective deimination of vimentin in calcium ionophore-induced apoptosis of mouse peritoneal macrophages. Biochemical and biophysical research communications *243*, 641-646.

Bachand, F. (2007). Protein arginine methyltransferases: from unicellular eukaryotes to humans. Eukaryotic cell *6*, 889-898.

Bachand, F., and Silver, P.A. (2004). PRMT3 is a ribosomal protein methyltransferase that affects the cellular levels of ribosomal subunits. The EMBO journal *23*, 2641-2650.

Badea, T.C., Wang, Y., and Nathans, J. (2003). A noninvasive genetic/pharmacologic strategy for visualizing cell morphology and clonal relationships in the mouse. J Neurosci *23*, 2314-2322.

Barton, A., Bowes, J., Eyre, S., Spreckley, K., Hinks, A., John, S., and Worthington, J. (2004). A functional haplotype of the PADI4 gene associated with rheumatoid arthritis in a Japanese population is not associated in a United Kingdom population. Arthritis and rheumatism *50*, 1117-1121.

Bates, I.R., Libich, D.S., Wood, D.D., Moscarello, M.A., and Harauz, G. (2002). An Arg/Lys-->Gln mutant of recombinant murine myelin basic protein as a mimic of the deiminated form implicated in multiple sclerosis. Protein expression and purification *25*, 330-341.

Bauer, U.M., Daujat, S., Nielsen, S.J., Nightingale, K., and Kouzarides, T. (2002). Methylation at arginine 17 of histone H3 is linked to gene activation. EMBO reports *3*, 39-44.

Bedford, M.T., and Clarke, S.G. (2009). Protein arginine methylation in mammals: who, what, and why. Molecular cell *33*, 1-13.

Bedford, M.T., Reed, R., and Leder, P. (1998). WW domain-mediated interactions reveal a spliceosome-associated protein that binds a third class of proline-rich motif: the proline glycine and methionine-rich motif. Proceedings of the National Academy of Sciences of the United States of America *95*, 10602-10607.

Bedford, M.T., and Richard, S. (2005). Arginine methylation an emerging regulator of protein function. Molecular cell *18*, 263-272.

Beniac, D.R., Wood, D.D., Palaniyar, N., Ottensmeyer, F.P., Moscarello, M.A., and Harauz, G. (2000). Cryoelectron microscopy of protein-lipid complexes of human myelin basic protein charge isomers differing in degree of citrullination. Journal of structural biology *129*, 80-95.

Bijlsma, J.W., Van Everdingen, A.A., Huisman, M., De Nijs, R.N., and Jacobs, J.W. (2002). Glucocorticoids in rheumatoid arthritis: effects on erosions and bone. Annals of the New York Academy of Sciences *966*, 82-90.

Blanchet, F., Cardona, A., Letimier, F.A., Hershfield, M.S., and Acuto, O. (2005). CD28 costimulatory signal induces protein arginine methylation in T cells. The Journal of experimental medicine *202*, 371-377.

Blanchet, F., Schurter, B.T., and Acuto, O. (2006). Protein arginine methylation in lymphocyte signaling. Current opinion in immunology *18*, 321-328.

Boisvert, F.M., Chenard, C.A., and Richard, S. (2005a). Protein interfaces in signaling regulated by arginine methylation. Sci STKE *2005*, re2.

Boisvert, F.M., Dery, U., Masson, J.Y., and Richard, S. (2005b). Arginine methylation of MRE11 by PRMT1 is required for DNA damage checkpoint control. Genes & development *19*, 671-676.

Boisvert, F.M., Hendzel, M.J., Masson, J.Y., and Richard, S. (2005c). Methylation of MRE11 regulates its nuclear compartmentalization. Cell cycle (Georgetown, Tex *4*, 981-989.

Boisvert, F.M., Rhie, A., Richard, S., and Doherty, A.J. (2005d). The GAR motif of 53BP1 is arginine methylated by PRMT1 and is necessary for 53BP1 DNA binding activity. Cell cycle (Georgetown, Tex *4*, 1834-1841.

Brahms, H., Meheus, L., de Brabandere, V., Fischer, U., and Luhrmann, R. (2001). Symmetrical dimethylation of arginine residues in spliceosomal Sm protein B/B' and the Sm-like protein LSm4, and their interaction with the SMN protein. RNA (New York, N.Y *7*, 1531-1542.

Branscombe, T.L., Frankel, A., Lee, J.H., Cook, J.R., Yang, Z., Pestka, S., and Clarke, S. (2001). PRMT5 (Janus kinase-binding protein 1) catalyzes the formation of symmetric dimethylarginine residues in proteins. The Journal of biological chemistry *276*, 32971-32976.

Brinkmann, V., Reichard, U., Goosmann, C., Fauler, B., Uhlemann, Y., Weiss, D.S., Weinrauch, Y., and Zychlinsky, A. (2004). Neutrophil extracellular traps kill bacteria. Science (New York, N.Y *303*, 1532-1535.

Bryce, P.J., Oyoshi, M.K., Kawamoto, S., Oettgen, H.C., and Tsitsikov, E.N. (2006). TRAF1 regulates Th2 differentiation, allergic inflammation and nuclear localization of the Th2 transcription factor, NIP45. International immunology *18*, 101-111.

Burkhardt, H., Sehnert, B., Bockermann, R., Engstrom, A., Kalden, J.R., and Holmdahl, R. (2005). Humoral immune response to citrullinated collagen type II determinants in early rheumatoid arthritis. European journal of immunology *35*, 1643-1652.

Caponi, L., Petit-Teixeira, E., Sebbag, M., Bongiorni, F., Moscato, S., Pratesi, F., Pierlot, C., Osorio, J., Chapuy-Regaud, S., Guerrin, M.*, et al.* (2005). A family based study shows no association between rheumatoid arthritis and the PADI4 gene in a white French population. Annals of the rheumatic diseases *64*, 587-593.

Chang, B., Chen, Y., Zhao, Y., and Bruick, R.K. (2007). JMJD6 is a histone arginine demethylase. Science (New York, N.Y *318*, 444-447.

Chang, X., and Fang, K. (2009). PADI4 and tumourigenesis. Cancer cell international *10*, 7.

Chang, X., Han, J., Pang, L., Zhao, Y., Yang, Y., and Shen, Z. (2009). Increased PADI4 expression in blood and tissues of patients with malignant tumors. BMC cancer *9*, 40.

Chang, X., Yamada, R., Sawada, T., Suzuki, A., Kochi, Y., and Yamamoto, K. (2005a). The inhibition of antithrombin by peptidylarginine deiminase 4 may contribute to pathogenesis of rheumatoid arthritis. Rheumatology (Oxford, England) *44*, 293-298.

Chang, X., Yamada, R., Suzuki, A., Sawada, T., Yoshino, S., Tokuhiro, S., and Yamamoto, K. (2005b). Localization of peptidylarginine deiminase 4 (PADI4) and citrullinated protein in synovial tissue of rheumatoid arthritis. Rheumatology (Oxford, England) *44*, 40-50.

Chavanas, S., Mechin, M.C., Takahara, H., Kawada, A., Nachat, R., Serre, G., and Simon, M. (2004). Comparative analysis of the mouse and human peptidylarginine deiminase gene clusters reveals highly conserved non-coding segments and a new human gene, PADI6. Gene *330*, 19-27.

Chen, D., Ma, H., Hong, H., Koh, S.S., Huang, S.M., Schurter, B.T., Aswad, D.W., and Stallcup, M.R. (1999). Regulation of transcription by a protein methyltransferase. Science (New York, N.Y *284*, 2174-2177.

Chen, S.L., Loffler, K.A., Chen, D., Stallcup, M.R., and Muscat, G.E. (2002). The coactivator-associated arginine methyltransferase is necessary for muscle differentiation: CARM1 coactivates myocyte enhancer factor-2. The Journal of biological chemistry *277*, 4324-4333.

Chen, T., Cote, J., Carvajal, H.V., and Richard, S. (2001). Identification of Sam68 arginine glycine-rich sequences capable of conferring nonspecific RNA binding to the GSG domain. The Journal of biological chemistry *276*, 30803-30811.

Cheng, D., Cote, J., Shaaban, S., and Bedford, M.T. (2007). The arginine methyltransferase CARM1 regulates the coupling of transcription and mRNA processing. Molecular cell *25*, 71-83.

Chevillard-Briet, M., Trouche, D., and Vandel, L. (2002). Control of CBP co-activating activity by arginine methylation. The EMBO journal *21*, 5457-5466.

Clausen, B.E., Burkhardt, C., Reith, W., Renkawitz, R., and Forster, I. (1999). Conditional gene targeting in macrophages and granulocytes using LysMcre mice. Transgenic research *8*, 265-277.

Clipstone, N.A., and Crabtree, G.R. (1993). Calcineurin is a key signaling enzyme in T lymphocyte activation and the target of the immunosuppressive drugs cyclosporin A and FK506. Annals of the New York Academy of Sciences *696*, 20-30.

Corraliza, I.M., Campo, M.L., Soler, G., and Modolell, M. (1994). Determination of arginase activity in macrophages: a micromethod. Journal of immunological methods *174*, 231-235.

Cote, J., Boisvert, F.M., Boulanger, M.C., Bedford, M.T., and Richard, S. (2003). Sam68 RNA binding protein is an in vivo substrate for protein arginine N-methyltransferase 1. Molecular biology of the cell *14*, 274-287.

Covic, M., Hassa, P.O., Saccani, S., Buerki, C., Meier, N.I., Lombardi, C., Imhof, R., Bedford, M.T., Natoli, G., and Hottiger, M.O. (2005). Arginine methyltransferase CARM1 is a promoter-specific regulator of NF-kappaB-dependent gene expression. The EMBO journal *24*, 85-96.

Creasy, D.M., and Cottrell, J.S. (2004). Unimod: Protein modifications for mass spectrometry. Proteomics *4*, 1534-1536.

Cuthbert, G.L., Daujat, S., Snowden, A.W., Erdjument-Bromage, H., Hagiwara, T., Yamada, M., Schneider, R., Gregory, P.D., Tempst, P., Bannister, A.J., and Kouzarides, T. (2004). Histone deimination antagonizes arginine methylation. Cell *118*, 545-553.

Dalton, D.K., Pitts-Meek, S., Keshav, S., Figari, I.S., Bradley, A., and Stewart, T.A. (1993). Multiple defects of immune cell function in mice with disrupted interferon-gamma genes. Science (New York, N.Y *259*, 1739-1742.

Damsker, J.M., Hansen, A.M., and Caspi, R.R. (2010). Th1 and Th17 cells: adversaries and collaborators. Annals of the New York Academy of Sciences *1183*, 211-221.

Daujat, S., Bauer, U.M., Shah, V., Turner, B., Berger, S., and Kouzarides, T. (2002). Crosstalk between CARM1 methylation and CBP acetylation on histone H3. Curr Biol *12*, 2090-2097.

De Bosscher, K., Vanden Berghe, W., and Haegeman, G. (2003). The interplay between the glucocorticoid receptor and nuclear factor-kappaB or activator protein-1: molecular mechanisms for gene repression. Endocrine reviews *24*, 488-522.

Dean, J.L., Wait, R., Mahtani, K.R., Sully, G., Clark, A.R., and Saklatvala, J. (2001). The 3' untranslated region of tumor necrosis factor alpha mRNA is a target of the mRNA-stabilizing factor HuR. Molecular and cellular biology *21*, 721-730.

Dejaco, C., Klotz, W., Larcher, H., Duftner, C., Schirmer, M., and Herold, M. (2006). Diagnostic value of antibodies against a modified citrullinated vimentin in rheumatoid arthritis. Arthritis research & therapy *8*, R119.

Denis, H., Deplus, R., Putmans, P., Yamada, M., Metivier, R., and Fuks, F. (2009). Functional connection between deimination and deacetylation of histones. Molecular and cellular biology *29*, 4982-4993.

Dong, S., Zhang, Z., and Takahara, H. (2007). Estrogen-enhanced peptidylarginine deiminase type IV gene (PADI4) expression in MCF-7 cells is mediated by estrogen receptor-alpha-promoted transfactors activator protein-1, nuclear factor-Y, and Sp1. Molecular endocrinology (Baltimore, Md *21*, 1617-1629.

Downey, G.P. (1994). Mechanisms of leukocyte motility and chemotaxis. Current opinion in immunology *6*, 113-124.

Doyle, S., Vaidya, S., O'Connell, R., Dadgostar, H., Dempsey, P., Wu, T., Rao, G., Sun, R., Haberland, M., Modlin, R., and Cheng, G. (2002). IRF3 mediates a TLR3/TLR4-specific antiviral gene program. Immunity *17*, 251-263.

Duffield, J.S. (2003). The inflammatory macrophage: a story of Jekyll and Hyde. Clin Sci (Lond) *104*, 27-38.

Durant, S.T., Cho, E.C., and La Thangue, N.B. (2009). p53 methylation--the Arg-ument is clear. Cell cycle (Georgetown, Tex *8*, 801-802.

Ehrt, S., Schnappinger, D., Bekiranov, S., Drenkow, J., Shi, S., Gingeras, T.R., Gaasterland, T., Schoolnik, G., and Nathan, C. (2001). Reprogramming of the macrophage transcriptome in response to interferon-gamma and Mycobacterium tuberculosis: signaling roles of nitric oxide synthase-2 and phagocyte oxidase. The Journal of experimental medicine *194*, 1123-1140.

El Messaoudi, S., Fabbrizio, E., Rodriguez, C., Chuchana, P., Fauquier, L., Cheng, D., Theillet, C., Vandel, L., Bedford, M.T., and Sardet, C. (2006). Coactivator-associated arginine methyltransferase 1 (CARM1) is a positive regulator of the Cyclin E1 gene. Proceedings of the National Academy of Sciences of the United States of America *103*, 13351-13356.

El-Andaloussi, N., Valovka, T., Toueille, M., Hassa, P.O., Gehrig, P., Covic, M., Hubscher, U., and Hottiger, M.O. (2007). Methylation of DNA polymerase beta by protein arginine methyltransferase 1 regulates its binding to proliferating cell nuclear antigen. Faseb J *21*, 26-34.

El-Andaloussi, N., Valovka, T., Toueille, M., Steinacher, R., Focke, F., Gehrig, P., Covic, M., Hassa, P.O., Schar, P., Hubscher, U., and Hottiger, M.O. (2006). Arginine methylation regulates DNA polymerase beta. Molecular cell *22*, 51-62.

Ermert, D., Urban, C.F., Laube, B., Goosmann, C., Zychlinsky, A., and Brinkmann, V. (2009). Mouse neutrophil extracellular traps in microbial infections. Journal of innate immunity *1*, 181-193.

Farley, A.R., and Link, A.J. (2009). Identification and quantification of protein posttranslational modifications. Methods in enzymology *463*, 725-763.

Fathman, J.W., Gurish, M.F., Hemmers, S., Bonham, K., Friend, D.S., Grusby, M.J., Glimcher, L.H., and Mowen, K.A. (2010). NIP45 controls the magnitude of the type 2 T helper cell response. Proceedings of the National Academy of Sciences of the United States of America *107*, 3663-3668.

Fauquier, L., Duboe, C., Jore, C., Trouche, D., and Vandel, L. (2008). Dual role of the arginine methyltransferase CARM1 in the regulation of c-Fos target genes. Faseb J *22*, 3337-3347.

Fearon, W.R. (1939). The carbamido diacetyl reaction: a test for citrulline. The Biochemical journal *33*, 902-907.

Feng, Q., He, B., Jung, S.Y., Song, Y., Qin, J., Tsai, S.Y., Tsai, M.J., and O'Malley, B.W. (2009). Biochemical control of CARM1 enzymatic activity by phosphorylation. The Journal of biological chemistry *284*, 36167-36174.

Foulquier, C., Sebbag, M., Clavel, C., Chapuy-Regaud, S., Al Badine, R., Mechin, M.C., Vincent, C., Nachat, R., Yamada, M., Takahara, H.*, et al.* (2007). Peptidyl arginine deiminase type 2 (PAD-2) and PAD-4 but not PAD-1, PAD-3, and PAD-6 are expressed in rheumatoid arthritis synovium in close association with tissue inflammation. Arthritis and rheumatism *56*, 3541-3553.

Frankel, A., Yadav, N., Lee, J., Branscombe, T.L., Clarke, S., and Bedford, M.T. (2002). The novel human protein arginine N-methyltransferase PRMT6 is a nuclear enzyme displaying unique substrate specificity. The Journal of biological chemistry *277*, 3537-3543.

Friesen, W.J., Massenet, S., Paushkin, S., Wyce, A., and Dreyfuss, G. (2001). SMN, the product of the spinal muscular atrophy gene, binds preferentially to dimethylarginine-containing protein targets. Molecular cell *7*, 1111-1117.

Fuchs, T.A., Abed, U., Goosmann, C., Hurwitz, R., Schulze, I., Wahn, V., Weinrauch, Y., Brinkmann, V., and Zychlinsky, A. (2007). Novel cell death program leads to neutrophil extracellular traps. The Journal of cell biology *176*, 231-241.

Fujiwara, T., Mori, Y., Chu, D.L., Koyama, Y., Miyata, S., Tanaka, H., Yachi, K., Kubo, T., Yoshikawa, H., and Tohyama, M. (2006). CARM1 regulates proliferation of PC12 cells by methylating HuD. Molecular and cellular biology *26*, 2273-2285.

Gary, J.D., and Clarke, S. (1998). RNA and protein interactions modulated by protein arginine methylation. Progress in nucleic acid research and molecular biology *61*, 65-131.

Girbal-Neuhauser, E., Durieux, J.J., Arnaud, M., Dalbon, P., Sebbag, M., Vincent, C., Simon, M., Senshu, T., Masson-Bessiere, C., Jolivet-Reynaud, C.*, et al.* (1999). The epitopes targeted by the rheumatoid arthritis-associated antifilaggrin autoantibodies are posttranslationally generated on various sites of (pro)filaggrin by deimination of arginine residues. J Immunol *162*, 585-594.

Gordon, S. (2002). Pattern recognition receptors: doubling up for the innate immune response. Cell *111*, 927-930.

Gordon, S. (2003). Alternative activation of macrophages. Nat Rev Immunol *3*, 23-35.

Greenblatt, M.B., Aliprantis, A., Hu, B., and Glimcher, L.H. (2010). Calcineurin regulates innate antifungal immunity in neutrophils. The Journal of experimental medicine.

Gyorgy, B., Toth, E., Tarcsa, E., Falus, A., and Buzas, E.I. (2006). Citrullination: a posttranslational modification in health and disease. The international journal of biochemistry & cell biology *38*, 1662-1677.

Ha, H., Han, D., and Choi, Y. (2009). TRAF-mediated TNFR-family signaling. Current protocols in immunology / edited by John E. Coligan ... [et al *Chapter 11*, Unit11 19D.

Hagiwara, T., Hidaka, Y., and Yamada, M. (2005). Deimination of histone H2A and H4 at arginine 3 in HL-60 granulocytes. Biochemistry *44*, 5827-5834.

Hagiwara, T., Nakashima, K., Hirano, H., Senshu, T., and Yamada, M. (2002). Deimination of arginine residues in nucleophosmin/B23 and histones in HL-60 granulocytes. Biochemical and biophysical research communications *290*, 979-983.

Harrington, L.E., Hatton, R.D., Mangan, P.R., Turner, H., Murphy, T.L., Murphy, K.M., and Weaver, C.T. (2005). Interleukin 17-producing CD4+ effector T cells develop via a lineage distinct from the T helper type 1 and 2 lineages. Nature immunology *6*, 1123-1132.

Hassa, P.O., Covic, M., Bedford, M.T., and Hottiger, M.O. (2008). Protein arginine methyltransferase 1 coactivates NF-kappaB-dependent gene expression synergistically with CARM1 and PARP1. Journal of molecular biology *377*, 668-678.

Hayashida, T., Oda, M., Ohsawa, K., Yamaguchi, A., Hosozawa, T., Locksley, R.M., Giacca, M., Masai, H., and Miyatake, S. (2006). Replication initiation from a novel origin identified in the Th2 cytokine cluster locus requires a distant conserved noncoding sequence. J Immunol *176*, 5446-5454.

Hermann-Kleiter, N., and Baier, G. (2010). NFAT pulls the strings during CD4+ T helper cell effector functions. Blood *115*, 2989-2997.

Herrmann, F., Bossert, M., Schwander, A., Akgun, E., and Fackelmayer, F.O. (2004). Arginine methylation of scaffold attachment factor A by heterogeneous nuclear ribonucleoprotein particle-associated PRMT1. The Journal of biological chemistry *279*, 48774-48779.

Higashimoto, K., Kuhn, P., Desai, D., Cheng, X., and Xu, W. (2007). Phosphorylation-mediated inactivation of coactivator-associated arginine methyltransferase 1. Proceedings of the National Academy of Sciences of the United States of America *104*, 12318-12323.

Hodge, M.R., Chun, H.J., Rengarajan, J., Alt, A., Lieberson, R., and Glimcher, L.H. (1996). NF-AT-Driven interleukin-4 transcription potentiated by NIP45. Science (New York, N.Y *274*, 1903-1905.

Hoet, R.M., Boerbooms, A.M., Arends, M., Ruiter, D.J., and van Venrooij, W.J. (1991). Antiperinuclear factor, a marker autoantibody for rheumatoid arthritis: colocalisation of the perinuclear factor and profilaggrin. Annals of the rheumatic diseases *50*, 611-618.

Hung, H.C., Lin, C.Y., Liao, Y.F., Hsu, P.C., Tsay, G.J., and Liu, G.Y. (2007). The functional haplotype of peptidylarginine deiminase IV (S55G, A82V and A112G) associated with susceptibility to rheumatoid arthritis dominates apoptosis of acute T leukemia Jurkat cells. Apoptosis *12*, 475-487.

Hunter, T. (1998). The Croonian Lecture 1997. The phosphorylation of proteins on tyrosine: its role in cell growth and disease. Philosophical transactions of the Royal Society of London *353*, 583-605.

Iberg, A.N., Espejo, A., Cheng, D., Kim, D., Michaud-Levesque, J., Richard, S., and Bedford, M.T. (2008). Arginine methylation of the histone H3 tail impedes effector binding. The Journal of biological chemistry *283*, 3006-3010.

Ikari, K., Kuwahara, M., Nakamura, T., Momohara, S., Hara, M., Yamanaka, H., Tomatsu, T., and Kamatani, N. (2005). Association between PADI4 and rheumatoid arthritis: a replication study. Arthritis and rheumatism *52*, 3054-3057.

Inagaki, M., Takahara, H., Nishi, Y., Sugawara, K., and Sato, C. (1989). Ca2+-dependent deimination-induced disassembly of intermediate filaments involves specific modification of the amino-terminal head domain. The Journal of biological chemistry *264*, 18119-18127.

Ishida-Yamamoto, A., Senshu, T., Eady, R.A., Takahashi, H., Shimizu, H., Akiyama, M., and Iizuka, H. (2002). Sequential reorganization of cornified cell keratin filaments involving filaggrin-mediated compaction and keratin 1 deimination. The Journal of investigative dermatology *118*, 282-287.

Ito, T., Yadav, N., Lee, J., Furumatsu, T., Yamashita, S., Yoshida, K., Taniguchi, N., Hashimoto, M., Tsuchiya, M., Ozaki, T.*, et al.* (2009). Arginine methyltransferase CARM1/PRMT4 regulates endochondral ossification. BMC developmental biology *9*, 47.

Jansson, M., Durant, S.T., Cho, E.C., Sheahan, S., Edelmann, M., Kessler, B., and La Thangue, N.B. (2008). Arginine methylation regulates the p53 response. Nature cell biology *10*, 1431-1439.

Jayne, S., Rothgiesser, K.M., and Hottiger, M.O. (2009). CARM1 but not its enzymatic activity is required for transcriptional coactivation of NF-kappaB-dependent gene expression. Journal of molecular biology *394*, 485-495.

Jenuwein, T., and Allis, C.D. (2001). Translating the histone code. Science (New York, N.Y *293*, 1074-1080.

Kang, C.P., Lee, H.S., Ju, H., Cho, H., Kang, C., and Bae, S.C. (2006). A functional haplotype of the PADI4 gene associated with increased rheumatoid arthritis susceptibility in Koreans. Arthritis and rheumatism *54*, 90-96.

Katsanis, N., Yaspo, M.L., and Fisher, E.M. (1997). Identification and mapping of a novel human gene, HRMT1L1, homologous to the rat protein arginine N-methyltransferase 1 (PRMT1) gene. Mamm Genome *8*, 526-529.

Kearney, P.L., Bhatia, M., Jones, N.G., Yuan, L., Glascock, M.C., Catchings, K.L., Yamada, M., and Thompson, P.R. (2005). Kinetic characterization of protein arginine deiminase 4: a transcriptional corepressor implicated in the onset and progression of rheumatoid arthritis. Biochemistry *44*, 10570-10582.

Kim, J., Lee, J., Yadav, N., Wu, Q., Carter, C., Richard, S., Richie, E., and Bedford, M.T. (2004). Loss of CARM1 results in hypomethylation of thymocyte cyclic AMP-regulated phosphoprotein and deregulated early T cell development. The Journal of biological chemistry *279*, 25339-25344.

Kim, T.W., Staschke, K., Bulek, K., Yao, J., Peters, K., Oh, K.H., Vandenburg, Y., Xiao, H., Qian, W., Hamilton, T.*, et al.* (2007). A critical role for IRAK4 kinase activity in Toll-like receptor-mediated innate immunity. The Journal of experimental medicine *204*, 1025-1036.

King, C., Tangye, S.G., and Mackay, C.R. (2008). T follicular helper (TFH) cells in normal and dysregulated immune responses. Annual review of immunology *26*, 741-766.

Kinloch, A., Lundberg, K., Wait, R., Wegner, N., Lim, N.H., Zendman, A.J., Saxne, T., Malmstr, V., and Venables, P.J. (2008). Synovial fluid is a site of citrullination of autoantigens in inflammatory arthritis. Arthritis and rheumatism *58*, 2287-2295.

Kinloch, A., Tatzer, V., Wait, R., Peston, D., Lundberg, K., Donatien, P., Moyes, D., Taylor, P.C., and Venables, P.J. (2005). Identification of citrullinated alpha-enolase as a candidate autoantigen in rheumatoid arthritis. Arthritis research & therapy *7*, R1421-1429.

Klareskog, L., Padyukov, L., Ronnelid, J., and Alfredsson, L. (2006). Genes, environment and immunity in the development of rheumatoid arthritis. Current opinion in immunology *18*, 650-655.

Klareskog, L., Widhe, M., Hermansson, M., and Ronnelid, J. (2008). Antibodies to citrullinated proteins in arthritis: pathology and promise. Current opinion in rheumatology *20*, 300-305.

Kleinschmidt, M.A., Streubel, G., Samans, B., Krause, M., and Bauer, U.M. (2008). The protein arginine methyltransferases CARM1 and PRMT1 cooperate in gene regulation. Nucleic acids research *36*, 3202-3213.

Koh, S.S., Li, H., Lee, Y.H., Widelitz, R.B., Chuong, C.M., and Stallcup, M.R. (2002). Synergistic coactivator function by coactivator-associated arginine methyltransferase (CARM) 1 and beta-catenin with two different classes of DNA-binding transcriptional activators. The Journal of biological chemistry *277*, 26031-26035.

Kouskoff, V., Korganow, A.S., Duchatelle, V., Degott, C., Benoist, C., and Mathis, D. (1996). Organ-specific disease provoked by systemic autoimmunity. Cell *87*, 811-822.

Kowenz-Leutz, E., Pless, O., Dittmar, G., Knoblich, M., and Leutz, A. (2010). Crosstalk between C/EBPbeta phosphorylation, arginine methylation, and SWI/SNF/Mediator implies an indexing transcription factor code. The EMBO journal *29*, 1105-1115.

Krause, C.D., Yang, Z.H., Kim, Y.S., Lee, J.H., Cook, J.R., and Pestka, S. (2007). Protein arginine methyltransferases: evolution and assessment of their pharmacological and therapeutic potential. Pharmacology & therapeutics *113*, 50-87.

Krones-Herzig, A., Mesaros, A., Metzger, D., Ziegler, A., Lemke, U., Bruning, J.C., and Herzig, S. (2006). Signal-dependent control of gluconeogenic key enzyme genes through coactivator-associated arginine methyltransferase 1. The Journal of biological chemistry *281*, 3025-3029.

Kubilus, J., Waitkus, R.F., and Baden, H.P. (1980). Partial purification and specificity of an arginine-converting enzyme from bovine epidermis. Biochimica et biophysica acta *615*, 246-251.

Kwak, Y.T., Guo, J., Prajapati, S., Park, K.J., Surabhi, R.M., Miller, B., Gehrig, P., and Gaynor, R.B. (2003). Methylation of SPT5 regulates its interaction with RNA polymerase II and transcriptional elongation properties. Molecular cell *11*, 1055-1066.

Kzhyshkowska, J., Schutt, H., Liss, M., Kremmer, E., Stauber, R., Wolf, H., and Dobner, T. (2001). Heterogeneous nuclear ribonucleoprotein E1B-AP5 is methylated in its Arg-Gly-Gly (RGG) box and interacts with human arginine methyltransferase HRMT1L1. The Biochemical journal *358*, 305-314.

Lakowski, T.M., and Frankel, A. (2009). Kinetic analysis of human protein arginine N-methyltransferase 2: formation of monomethyl- and asymmetric dimethyl-arginine residues on histone H4. The Biochemical journal *421*, 253-261.

Lawson, B.R., Manenkova, Y., Ahamed, J., Chen, X., Zou, J.P., Baccala, R., Theofilopoulos, A.N., and Yuan, C. (2007). Inhibition of transmethylation down-regulates CD4 T cell activation and curtails development of autoimmunity in a model system. J Immunol *178*, 5366-5374.

Lee, D.Y., Teyssier, C., Strahl, B.D., and Stallcup, M.R. (2005a). Role of protein methylation in regulation of transcription. Endocrine reviews *26*, 147-170.

Lee, J., and Bedford, M.T. (2002). PABP1 identified as an arginine methyltransferase substrate using high-density protein arrays. EMBO reports *3*, 268-273.

Lee, J., Sayegh, J., Daniel, J., Clarke, S., and Bedford, M.T. (2005b). PRMT8, a new membrane-bound tissue-specific member of the protein arginine methyltransferase family. The Journal of biological chemistry *280*, 32890-32896.

Lee, Y.H., Coonrod, S.A., Kraus, W.L., Jelinek, M.A., and Stallcup, M.R. (2005c). Regulation of coactivator complex assembly and function by protein arginine methylation and demethylimination. Proceedings of the National Academy of Sciences of the United States of America *102*, 3611-3616.

Lee, Y.H., Koh, S.S., Zhang, X., Cheng, X., and Stallcup, M.R. (2002). Synergy among nuclear receptor coactivators: selective requirement for protein methyltransferase and acetyltransferase activities. Molecular and cellular biology *22*, 3621-3632.

Lee, Y.H., and Stallcup, M.R. (2009). Minireview: protein arginine methylation of nonhistone proteins in transcriptional regulation. Molecular endocrinology (Baltimore, Md *23*, 425-433.

Li, H., Park, S., Kilburn, B., Jelinek, M.A., Henschen-Edman, A., Aswad, D.W., Stallcup, M.R., and Laird-Offringa, I.A. (2002). Lipopolysaccharide-induced methylation of HuR, an mRNA-stabilizing protein, by CARM1. Coactivator-associated arginine methyltransferase. The Journal of biological chemistry *277*, 44623-44630.

Li, P., Wang, D., Yao, H., Doret, P., Hao, G., Shen, Q., Qiu, H., Zhang, X., Wang, Y., Chen, G., and Wang, Y. (2010). Coordination of PAD4 and HDAC2 in the regulation of p53-target gene expression. Oncogene.

Li, P., Yao, H., Zhang, Z., Li, M., Luo, Y., Thompson, P.R., Gilmour, D.S., and Wang, Y. (2008). Regulation of p53 target gene expression by peptidylarginine deiminase 4. Molecular and cellular biology *28*, 4745-4758.

Lieberson, R., Mowen, K.A., McBride, K.D., Leautaud, V., Zhang, X., Suh, W.K., Wu, L., and Glimcher, L.H. (2001). Tumor necrosis factor receptor-associated factor (TRAF)2 represses the T helper cell type 2 response through interaction with NFAT-interacting protein (NIP45). The Journal of experimental medicine *194*, 89-98.

Lin, W.J., Gary, J.D., Yang, M.C., Clarke, S., and Herschman, H.R. (1996). The mammalian immediate-early TIS21 protein and the leukemia-associated BTG1 protein interact with a protein-arginine N-methyltransferase. The Journal of biological chemistry *271*, 15034-15044.

Liu, G.Y., Liao, Y.F., Chang, W.H., Liu, C.C., Hsieh, M.C., Hsu, P.C., Tsay, G.J., and Hung, H.C. (2006). Overexpression of peptidylarginine deiminase IV features in apoptosis of haematopoietic cells. Apoptosis *11*, 183-196.

Loos, T., Mortier, A., Gouwy, M., Ronsse, I., Put, W., Lenaerts, J.P., Van Damme, J., and Proost, P. (2008). Citrullination of CXCL10 and CXCL11 by peptidylarginine deiminase: a naturally occurring posttranslational modification of chemokines and new dimension of immunoregulation. Blood.

Loos, T., Opdenakker, G., Van Damme, J., and Proost, P. (2009). Citrullination of CXCL8 increases this chemokine's ability to mobilize neutrophils into the blood circulation. Haematologica *94*, 1346-1353.

Lukong, K.E., and Richard, S. (2004). Arginine methylation signals mRNA export. Nature structural & molecular biology *11*, 914-915.

Luo, Y., and Dorf, M.E. (2001). Isolation of mouse neutrophils. Current protocols in immunology / edited by John E. Coligan ... [et al *Chapter 3*, Unit 3 20.

Ma, H., Baumann, C.T., Li, H., Strahl, B.D., Rice, R., Jelinek, M.A., Aswad, D.W., Allis, C.D., Hager, G.L., and Stallcup, M.R. (2001). Hormone-dependent, CARM1-directed, arginine-specific methylation of histone H3 on a steroid-regulated promoter. Curr Biol *11*, 1981-1985.

Ma, J., Chen, T., Mandelin, J., Ceponis, A., Miller, N.E., Hukkanen, M., Ma, G.F., and Konttinen, Y.T. (2003). Regulation of macrophage activation. Cell Mol Life Sci *60*, 2334-2346.

Macian, F. (2005). NFAT proteins: key regulators of T-cell development and function. Nat Rev Immunol *5*, 472-484.

Mackaness, G.B. (1964). The Immunological Basis of Acquired Cellular Resistance. The Journal of experimental medicine *120*, 105-120.

Malech, H.L., and Nauseef, W.M. (1997). Primary inherited defects in neutrophil function: etiology and treatment. Seminars in hematology *34*, 279-290.

Maragoudakis, M.E., Tsopanoglou, N.E., and Andriopoulou, P. (2002). Mechanism of thrombin-induced angiogenesis. Biochemical Society transactions *30*, 173-177.

Martinez, A., Valdivia, A., Pascual-Salcedo, D., Lamas, J.R., Fernandez-Arquero, M., Balsa, A., Fernandez-Gutierrez, B., de la Concha, E.G., and Urcelay, E. (2005). PADI4 polymorphisms are not associated with rheumatoid arthritis in the Spanish population. Rheumatology (Oxford, England) *44*, 1263-1266.

Masson-Bessiere, C., Sebbag, M., Girbal-Neuhauser, E., Nogueira, L., Vincent, C., Senshu, T., and Serre, G. (2001). The major synovial targets of the rheumatoid arthritis-specific antifilaggrin autoantibodies are deiminated forms of the alpha- and beta-chains of fibrin. J Immunol *166*, 4177-4184.

McBride, A.E., and Silver, P.A. (2001). State of the arg: protein methylation at arginine comes of age. Cell *106*, 5-8.

Mechin, M.C., Coudane, F., Adoue, V., Arnaud, J., Duplan, H., Charveron, M., Schmitt, A.M., Takahara, H., Serre, G., and Simon, M. (2010). Deimination is regulated at multiple levels including auto-deimination of peptidylarginine deiminases. Cell Mol Life Sci.

Meister, G., Eggert, C., Buhler, D., Brahms, H., Kambach, C., and Fischer, U. (2001). Methylation of Sm proteins by a complex containing PRMT5 and the putative U snRNP assembly factor pICln. Curr Biol *11*, 1990-1994.

Miao, F., Li, S., Chavez, V., Lanting, L., and Natarajan, R. (2006). Coactivator-associated arginine methyltransferase-1 enhances nuclear factor-kappaB-mediated gene transcription through methylation of histone H3 at arginine 17. Molecular endocrinology (Baltimore, Md *20*, 1562-1573.

Monach, P., Hattori, K., Huang, H., Hyatt, E., Morse, J., Nguyen, L., Ortiz-Lopez, A., Wu, H.J., Mathis, D., and Benoist, C. (2007). The K/BxN mouse model of inflammatory arthritis: theory and practice. Methods in molecular medicine *136*, 269-282.

Monach, P.A., Benoist, C., and Mathis, D. (2004). The role of antibodies in mouse models of rheumatoid arthritis, and relevance to human disease. Advances in immunology *82*, 217-248.

Monach, P.A., Nigrovic, P.A., Chen, M., Hock, H., Lee, D.M., Benoist, C., and Mathis, D. (2010). Neutrophils in a mouse model of autoantibody-mediated arthritis: critical producers of Fc receptor gamma, the receptor for C5a, and lymphocyte function-associated antigen 1. Arthritis and rheumatism *62*, 753-764.

Moscarello, M.A., Mastronardi, F.G., and Wood, D.D. (2007). The role of citrullinated proteins suggests a novel mechanism in the pathogenesis of multiple sclerosis. Neurochemical research *32*, 251-256.

Moscarello, M.A., Wood, D.D., Ackerley, C., and Boulias, C. (1994). Myelin in multiple sclerosis is developmentally immature. The Journal of clinical investigation *94*, 146-154.

Mosser, D.M., and Edwards, J.P. (2008). Exploring the full spectrum of macrophage activation. Nat Rev Immunol *8*, 958-969.

Mowen, K.A., and David, M. (2001). Analysis of protein arginine methylation and protein arginine-methyltransferase activity. Sci STKE *2001*, PL1.

Mowen, K.A., Schurter, B.T., Fathman, J.W., David, M., and Glimcher, L.H. (2004). Arginine methylation of NIP45 modulates cytokine gene expression in effector T lymphocytes. Molecular cell *15*, 559-571.

Mowen, K.A., Tang, J., Zhu, W., Schurter, B.T., Shuai, K., Herschman, H.R., and David, M. (2001). Arginine methylation of STAT1 modulates IFNalpha/beta-induced transcription. Cell *104*, 731-741.

Munder, M., Eichmann, K., and Modolell, M. (1998). Alternative metabolic states in murine macrophages reflected by the nitric oxide synthase/arginase balance: competitive regulation by CD4+ T cells correlates with Th1/Th2 phenotype. J Immunol *160*, 5347-5354.

Munder, M., Eichmann, K., Moran, J.M., Centeno, F., Soler, G., and Modolell, M. (1999). Th1/Th2-regulated expression of arginase isoforms in murine macrophages and dendritic cells. J Immunol *163*, 3771-3777.

Naeem, H., Cheng, D., Zhao, Q., Underhill, C., Tini, M., Bedford, M.T., and Torchia, J. (2007). The activity and stability of the transcriptional coactivator p/CIP/SRC-3 are regulated by CARM1-dependent methylation. Molecular and cellular biology *27*, 120-134.

Nakashima, K., Hagiwara, T., Ishigami, A., Nagata, S., Asaga, H., Kuramoto, M., Senshu, T., and Yamada, M. (1999). Molecular characterization of peptidylarginine deiminase in HL-60

cells induced by retinoic acid and 1alpha,25-dihydroxyvitamin D(3). The Journal of biological chemistry *274*, 27786-27792.

Nakashima, K., Hagiwara, T., and Yamada, M. (2002). Nuclear localization of peptidylarginine deiminase V and histone deimination in granulocytes. The Journal of biological chemistry *277*, 49562-49568.

Nathan, C. (2006). Neutrophils and immunity: challenges and opportunities. Nat Rev Immunol *6*, 173-182.

Nathan, C., and Shiloh, M.U. (2000). Reactive oxygen and nitrogen intermediates in the relationship between mammalian hosts and microbial pathogens. Proceedings of the National Academy of Sciences of the United States of America *97*, 8841-8848.

Nauseef, W.M. (2007). How human neutrophils kill and degrade microbes: an integrated view. Immunological reviews *219*, 88-102.

Neeli, I., Khan, S.N., and Radic, M. (2008). Histone deimination as a response to inflammatory stimuli in neutrophils. J Immunol *180*, 1895-1902.

Nielen, M.M., van Schaardenburg, D., Reesink, H.W., van de Stadt, R.J., van der Horst-Bruinsma, I.E., de Koning, M.H., Habibuw, M.R., Vandenbroucke, J.P., and Dijkmans, B.A. (2004). Specific autoantibodies precede the symptoms of rheumatoid arthritis: a study of serial measurements in blood donors. Arthritis and rheumatism *50*, 380-386.

Nomiyama, T., Perez-Tilve, D., Ogawa, D., Gizard, F., Zhao, Y., Heywood, E.B., Jones, K.L., Kawamori, R., Cassis, L.A., Tschop, M.H., and Bruemmer, D. (2007). Osteopontin mediates obesity-induced adipose tissue macrophage infiltration and insulin resistance in mice. The Journal of clinical investigation *117*, 2877-2888.

Novatchkova, M., Bachmair, A., Eisenhaber, B., and Eisenhaber, F. (2005). Proteins with two SUMO-like domains in chromatin-associated complexes: the RENi (Rad60-Esc2-NIP45) family. BMC bioinformatics *6*, 22.

O'Garra, A. (1998). Cytokines induce the development of functionally heterogeneous T helper cell subsets. Immunity *8*, 275-283.

O'Shea, J.J., and Paul, W.E. (2010). Mechanisms underlying lineage commitment and plasticity of helper CD4+ T cells. Science (New York, N.Y *327*, 1098-1102.

Ogawa, S., Lozach, J., Benner, C., Pascual, G., Tangirala, R.K., Westin, S., Hoffmann, A., Subramaniam, S., David, M., Rosenfeld, M.G., and Glass, C.K. (2005). Molecular determinants of crosstalk between nuclear receptors and toll-like receptors. Cell *122*, 707-721.

Ohkura, N., Takahashi, M., Yaguchi, H., Nagamura, Y., and Tsukada, T. (2005). Coactivator-associated arginine methyltransferase 1, CARM1, affects pre-mRNA splicing in an isoform-specific manner. The Journal of biological chemistry *280*, 28927-28935.

Ordonez, A., Martinez-Martinez, I., Corrales, F.J., Miqueo, C., Minano, A., Vicente, V., and Corral, J. (2009). Effect of citrullination on the function and conformation of antithrombin. The FEBS journal *276*, 6763-6772.

Pahlich, S., Zakaryan, R.P., and Gehring, H. (2006). Protein arginine methylation: Cellular functions and methods of analysis. Biochimica et biophysica acta *1764*, 1890-1903.

Paik, W.K., and Kim, S. (1967). Enzymatic methylation of protein fractions from calf thymus nuclei. Biochemical and biophysical research communications *29*, 14-20.

Park, H., Li, Z., Yang, X.O., Chang, S.H., Nurieva, R., Wang, Y.H., Wang, Y., Hood, L., Zhu, Z., Tian, Q., and Dong, C. (2005). A distinct lineage of CD4 T cells regulates tissue inflammation by producing interleukin 17. Nature immunology *6*, 1133-1141.

Passalacqua, G., and Ciprandi, G. (2008). Allergy and the lung. Clinical and experimental immunology *153 Suppl 1*, 12-16.

Pawlak, M.R., Scherer, C.A., Chen, J., Roshon, M.J., and Ruley, H.E. (2000). Arginine N-methyltransferase 1 is required for early postimplantation mouse development, but cells deficient in the enzyme are viable. Molecular and cellular biology *20*, 4859-4869.

Pike, R.N., Potempa, J., Skinner, R., Fitton, H.L., McGraw, W.T., Travis, J., Owen, M., Jin, L., and Carrell, R.W. (1997). Heparin-dependent modification of the reactive center arginine of antithrombin and consequent increase in heparin binding affinity. The Journal of biological chemistry *272*, 19652-19655.

Pritzker, L.B., Joshi, S., Gowan, J.J., Harauz, G., and Moscarello, M.A. (2000). Deimination of myelin basic protein. 1. Effect of deimination of arginyl residues of myelin basic protein on its structure and susceptibility to digestion by cathepsin D. Biochemistry *39*, 5374-5381.

Proost, P., Loos, T., Mortier, A., Schutyser, E., Gouwy, M., Noppen, S., Dillen, C., Ronsse, I., Conings, R., Struyf, S.*, et al.* (2008). Citrullination of CXCL8 by peptidylarginine deiminase alters receptor usage, prevents proteolysis, and dampens tissue inflammation. The Journal of experimental medicine *205*, 2085-2097.

Raijmakers, R., Zendman, A.J., Egberts, W.V., Vossenaar, E.R., Raats, J., Soede-Huijbregts, C., Rutjes, F.P., van Veelen, P.A., Drijfhout, J.W., and Pruijn, G.J. (2007). Methylation of arginine residues interferes with citrullination by peptidylarginine deiminases in vitro. Journal of molecular biology *367*, 1118-1129.

Rao, A., Luo, C., and Hogan, P.G. (1997). Transcription factors of the NFAT family: regulation and function. Annual review of immunology *15*, 707-747.

Rogers, G., Winter, B., McLaughlan, C., Powell, B., and Nesci, A. (1999). Hair follicle peptidylarginine deiminase. Experimental dermatology *8*, 362-363.

Rogers, G., Winter, B., McLaughlan, C., Powell, B., and Nesci, T. (1997). Peptidylarginine deiminase of the hair follicle: characterization, localization, and function in keratinizing tissues. The Journal of investigative dermatology *108*, 700-707.

Rogers, G.E. (1962). Occurrence of citrulline in proteins. Nature *194*, 1149-1151.

Rogers, G.E., Harding, H.W., and Llewellyn-Smith, I.J. (1977). The origin of citrulline-containing proteins in the hair follicle and the chemical nature of trichohyalin, an intracellular precursor. Biochimica et biophysica acta *495*, 159-175.

Rogers, G.E., and Simmonds, D.H. (1958). Content of citrulline and other amino-acids in a protein of hair follicles. Nature *182*, 186-187.

Rosloniec, E.F., Cremer, M., Kang, A., and Myers, L.K. (2001). Collagen-induced arthritis. Current protocols in immunology / edited by John E. Coligan ... [et al *Chapter 15*, Unit 15 15.

Sandler, N.G., Mentink-Kane, M.M., Cheever, A.W., and Wynn, T.A. (2003). Global gene expression profiles during acute pathogen-induced pulmonary inflammation reveal divergent roles for Th1 and Th2 responses in tissue repair. J Immunol *171*, 3655-3667.

Sayegh, J., Webb, K., Cheng, D., Bedford, M.T., and Clarke, S.G. (2007). Regulation of protein arginine methyltransferase 8 (PRMT8) activity by its N-terminal domain. The Journal of biological chemistry *282*, 36444-36453.

Schellekens, G.A., de Jong, B.A., van den Hoogen, F.H., van de Putte, L.B., and van Venrooij, W.J. (1998). Citrulline is an essential constituent of antigenic determinants recognized by rheumatoid arthritis-specific autoantibodies. The Journal of clinical investigation *101*, 273-281.

Schurter, B.T., Koh, S.S., Chen, D., Bunick, G.J., Harp, J.M., Hanson, B.L., Henschen-Edman, A., Mackay, D.R., Stallcup, M.R., and Aswad, D.W. (2001). Methylation of histone H3 by coactivator-associated arginine methyltransferase 1. Biochemistry *40*, 5747-5756.

Sebbag, M., Simon, M., Vincent, C., Masson-Bessiere, C., Girbal, E., Durieux, J.J., and Serre, G. (1995). The antiperinuclear factor and the so-called antikeratin antibodies are the same rheumatoid arthritis-specific autoantibodies. The Journal of clinical investigation *95*, 2672-2679.

Sekiyama, N., Arita, K., Ikeda, Y., Hashiguchi, K., Ariyoshi, M., Tochio, H., Saitoh, H., and Shirakawa, M. (2010). Structural basis for regulation of poly-SUMO chain by a SUMO-like domain of Nip45. Proteins *78*, 1491-1502.

Senshu, T., Akiyama, K., Ishigami, A., and Nomura, K. (1999). Studies on specificity of peptidylarginine deiminase reactions using an immunochemical probe that recognizes an enzymatically deiminated partial sequence of mouse keratin K1. Journal of dermatological science *21*, 113-126.

Senshu, T., Akiyama, K., Kan, S., Asaga, H., Ishigami, A., and Manabe, M. (1995). Detection of deiminated proteins in rat skin: probing with a monospecific antibody after modification of citrulline residues. The Journal of investigative dermatology *105*, 163-169.

Senshu, T., Kan, S., Ogawa, H., Manabe, M., and Asaga, H. (1996). Preferential deimination of keratin K1 and filaggrin during the terminal differentiation of human epidermis. Biochemical and biophysical research communications *225*, 712-719.

Shevach, E.M. (2009). Mechanisms of foxp3+ T regulatory cell-mediated suppression. Immunity *30*, 636-645.

Shuai, K., and Liu, B. (2003). Regulation of JAK-STAT signalling in the immune system. Nat Rev Immunol *3*, 900-911.

Silveira, I.G., Burlingame, R.W., von Muhlen, C.A., Bender, A.L., and Staub, H.L. (2007). Anti-CCP antibodies have more diagnostic impact than rheumatoid factor (RF) in a population tested for RF. Clinical rheumatology *26*, 1883-1889.

Simon, M., Vincent, C., Haftek, M., Girbal, E., Sebbag, M., Gomes-Daudrix, V., and Serre, G. (1995). The rheumatoid arthritis-associated autoantibodies to filaggrin label the fibrous matrix of the cornified cells but not the profilaggrin-containing keratohyalin granules in human epidermis. Clinical and experimental immunology *100*, 90-98.

Smith, J.J., Rucknagel, K.P., Schierhorn, A., Tang, J., Nemeth, A., Linder, M., Herschman, H.R., and Wahle, E. (1999). Unusual sites of arginine methylation in Poly(A)-binding protein II and in vitro methylation by protein arginine methyltransferases PRMT1 and PRMT3. The Journal of biological chemistry *274*, 13229-13234.

Southern, E.M. (1975). Detection of specific sequences among DNA fragments separated by gel electrophoresis. 1975. Biotechnology (Reading, Mass *24*, 122-139.

Stallcup, M.R. (2001). Role of protein methylation in chromatin remodeling and transcriptional regulation. Oncogene *20*, 3014-3020.

Stallcup, M.R., Kim, J.H., Teyssier, C., Lee, Y.H., Ma, H., and Chen, D. (2003). The roles of protein-protein interactions and protein methylation in transcriptional activation by nuclear

receptors and their coactivators. The Journal of steroid biochemistry and molecular biology *85*, 139-145.

Stein, M., Keshav, S., Harris, N., and Gordon, S. (1992). Interleukin 4 potently enhances murine macrophage mannose receptor activity: a marker of alternative immunologic macrophage activation. The Journal of experimental medicine *176*, 287-292.

Stensland, M.E., Pollmann, S., Molberg, O., Sollid, L.M., and Fleckenstein, B. (2009). Primary sequence, together with other factors, influence peptide deimination by peptidylarginine deiminase-4. Biological chemistry *390*, 99-107.

Strahl, B.D., and Allis, C.D. (2000). The language of covalent histone modifications. Nature *403*, 41-45.

Struyf, S., Noppen, S., Loos, T., Mortier, A., Gouwy, M., Verbeke, H., Huskens, D., Luangsay, S., Parmentier, M., Geboes, K.*, et al.* (2009). Citrullination of CXCL12 differentially reduces CXCR4 and CXCR7 binding with loss of inflammatory and anti-HIV-1 activity via CXCR4. J Immunol *182*, 666-674.

Suzuki, A., Yamada, R., Chang, X., Tokuhiro, S., Sawada, T., Suzuki, M., Nagasaki, M., Nakayama-Hamada, M., Kawaida, R., Ono, M.*, et al.* (2003). Functional haplotypes of PADI4, encoding citrullinating enzyme peptidylarginine deiminase 4, are associated with rheumatoid arthritis. Nature genetics *34*, 395-402.

Swiercz, R., Person, M.D., and Bedford, M.T. (2005). Ribosomal protein S2 is a substrate for mammalian PRMT3 (protein arginine methyltransferase 3). The Biochemical journal *386*, 85-91.

Szabo, S.J., Sullivan, B.M., Peng, S.L., and Glimcher, L.H. (2003). Molecular mechanisms regulating Th1 immune responses. Annual review of immunology *21*, 713-758.

Takahara, H., Okamoto, H., and Sugawara, K. (1986). Affinity chromatography of peptidylarginine deiminase from rabbit skeletal muscle on a column of soybean trypsin inhibitor (Kunitz)-Sepharose. Journal of biochemistry *99*, 1417-1424.

Tang, J., Frankel, A., Cook, R.J., Kim, S., Paik, W.K., Williams, K.R., Clarke, S., and Herschman, H.R. (2000a). PRMT1 is the predominant type I protein arginine methyltransferase in mammalian cells. The Journal of biological chemistry *275*, 7723-7730.

Tang, J., Gary, J.D., Clarke, S., and Herschman, H.R. (1998). PRMT 3, a type I protein arginine N-methyltransferase that differs from PRMT1 in its oligomerization, subcellular localization, substrate specificity, and regulation. The Journal of biological chemistry *273*, 16935-16945.

Tang, J., Kao, P.N., and Herschman, H.R. (2000b). Protein-arginine methyltransferase I, the predominant protein-arginine methyltransferase in cells, interacts with and is regulated by interleukin enhancer-binding factor 3. The Journal of biological chemistry *275*, 19866-19876.

Tanikawa, C., Ueda, K., Nakagawa, H., Yoshida, N., Nakamura, Y., and Matsuda, K. (2009). Regulation of protein Citrullination through p53/PADI4 network in DNA damage response. Cancer research *69*, 8761-8769.

Tarcsa, E., Marekov, L.N., Mei, G., Melino, G., Lee, S.C., and Steinert, P.M. (1996). Protein unfolding by peptidylarginine deiminase. Substrate specificity and structural relationships of the natural substrates trichohyalin and filaggrin. The Journal of biological chemistry *271*, 30709-30716.

Terui, Y., Saad, N., Jia, S., McKeon, F., and Yuan, J. (2004). Dual role of sumoylation in the nuclear localization and transcriptional activation of NFAT1. The Journal of biological chemistry *279*, 28257-28265.

Teyssier, C., Ma, H., Emter, R., Kralli, A., and Stallcup, M.R. (2005). Activation of nuclear receptor coactivator PGC-1alpha by arginine methylation. Genes & development *19*, 1466-1473.

Urban, C.F., Ermert, D., Schmid, M., Abu-Abed, U., Goosmann, C., Nacken, W., Brinkmann, V., Jungblut, P.R., and Zychlinsky, A. (2009). Neutrophil extracellular traps contain calprotectin, a cytosolic protein complex involved in host defense against Candida albicans. PLoS pathogens *5*, e1000639.

van der Helm-van Mil, A.H., Verpoort, K.N., le Cessie, S., Huizinga, T.W., de Vries, R.R., and Toes, R.E. (2007). The HLA-DRB1 shared epitope alleles differ in the interaction with smoking and predisposition to antibodies to cyclic citrullinated peptide. Arthritis and rheumatism *56*, 425-432.

van Venrooij, G.E., van Melick, H.H., Eckhardt, M.D., and Boon, T.A. (2008). Diagnostic and predictive value of voiding diary data versus prostate volume, maximal free urinary flow rate, and Abrams-Griffiths number in men with lower urinary tract symptoms suggestive of benign prostatic hyperplasia. Urology *71*, 469-474.

van Venrooij, W.J., and Pruijn, G.J. (2000). Citrullination: a small change for a protein with great consequences for rheumatoid arthritis. Arthritis research *2*, 249-251.

Vander Cruyssen, B., Cantaert, T., Nogueira, L., Clavel, C., De Rycke, L., Dendoven, A., Sebag, M., Deforce, D., Vincent, C., Elewaut, D.*, et al.* (2006). Diagnostic value of anti-human citrullinated fibrinogen ELISA and comparison with four other anti-citrullinated protein assays. Arthritis research & therapy *8*, R122.

Vencovsky, J., Machacek, S., Sedova, L., Kafkova, J., Gatterova, J., Pesakova, V., and Ruzickova, S. (2003). Autoantibodies can be prognostic markers of an erosive disease in early rheumatoid arthritis. Annals of the rheumatic diseases *62*, 427-430.

Vignali, D.A., Collison, L.W., and Workman, C.J. (2008). How regulatory T cells work. Nat Rev Immunol *8*, 523-532.

Vossenaar, E.R., Nijenhuis, S., Helsen, M.M., van der Heijden, A., Senshu, T., van den Berg, W.B., van Venrooij, W.J., and Joosten, L.A. (2003a). Citrullination of synovial proteins in murine models of rheumatoid arthritis. Arthritis and rheumatism *48*, 2489-2500.

Vossenaar, E.R., Radstake, T.R., van der Heijden, A., van Mansum, M.A., Dieteren, C., de Rooij, D.J., Barrera, P., Zendman, A.J., and van Venrooij, W.J. (2004). Expression and activity of citrullinating peptidylarginine deiminase enzymes in monocytes and macrophages. Annals of the rheumatic diseases *63*, 373-381.

Vossenaar, E.R., Zendman, A.J., van Venrooij, W.J., and Pruijn, G.J. (2003b). PAD, a growing family of citrullinating enzymes: genes, features and involvement in disease. Bioessays *25*, 1106-1118.

Wang, H., Huang, Z.Q., Xia, L., Feng, Q., Erdjument-Bromage, H., Strahl, B.D., Briggs, S.D., Allis, C.D., Wong, J., Tempst, P., and Zhang, Y. (2001). Methylation of histone H4 at arginine 3 facilitating transcriptional activation by nuclear hormone receptor. Science (New York, N.Y *293*, 853-857.

Wang, Y., Li, M., Stadler, S., Correll, S., Li, P., Wang, D., Hayama, R., Leonelli, L., Han, H., Grigoryev, S.A.*, et al.* (2009). Histone hypercitrullination mediates chromatin decondensation and neutrophil extracellular trap formation. The Journal of cell biology *184*, 205-213.

Wang, Y., Wysocka, J., Sayegh, J., Lee, Y.H., Perlin, J.R., Leonelli, L., Sonbuchner, L.S., McDonald, C.H., Cook, R.G., Dou, Y.*, et al.* (2004). Human PAD4 regulates histone arginine methylation levels via demethylimination. Science (New York, N.Y *306*, 279-283.

Wegner, N., Lundberg, K., Kinloch, A., Fisher, B., Malmstrom, V., Feldmann, M., and Venables, P.J. (2010). Autoimmunity to specific citrullinated proteins gives the first clues to the etiology of rheumatoid arthritis. Immunological reviews *233*, 34-54.

Wipke, B.T., and Allen, P.M. (2001). Essential role of neutrophils in the initiation and progression of a murine model of rheumatoid arthritis. J Immunol *167*, 1601-1608.

Wolf, S.S. (2009). The protein arginine methyltransferase family: an update about function, new perspectives and the physiological role in humans. Cell Mol Life Sci *66*, 2109-2121.

Wood, D.D., Ackerley, C.A., Brand, B., Zhang, L., Raijmakers, R., Mastronardi, F.G., and Moscarello, M.A. (2008). Myelin localization of peptidylarginine deiminases 2 and 4: comparison of PAD2 and PAD4 activities. Laboratory investigation; a journal of technical methods and pathology *88*, 354-364.

Wood, D.D., Bilbao, J.M., O'Connors, P., and Moscarello, M.A. (1996). Acute multiple sclerosis (Marburg type) is associated with developmentally immature myelin basic protein. Annals of neurology *40*, 18-24.

Xu, W., Chen, H., Du, K., Asahara, H., Tini, M., Emerson, B.M., Montminy, M., and Evans, R.M. (2001). A transcriptional switch mediated by cofactor methylation. Science (New York, N.Y *294*, 2507-2511.

Yadav, N., Cheng, D., Richard, S., Morel, M., Iyer, V.R., Aldaz, C.M., and Bedford, M.T. (2008). CARM1 promotes adipocyte differentiation by coactivating PPARgamma. EMBO reports *9*, 193-198.

Yadav, N., Lee, J., Kim, J., Shen, J., Hu, M.C., Aldaz, C.M., and Bedford, M.T. (2003). Specific protein methylation defects and gene expression perturbations in coactivator-associated arginine methyltransferase 1-deficient mice. Proceedings of the National Academy of Sciences of the United States of America *100*, 6464-6468.

Yamagata, K., Daitoku, H., Takahashi, Y., Namiki, K., Hisatake, K., Kako, K., Mukai, H., Kasuya, Y., and Fukamizu, A. (2008). Arginine methylation of FOXO transcription factors inhibits their phosphorylation by Akt. Molecular cell *32*, 221-231.

Yao, H., Li, P., Venters, B.J., Zheng, S., Thompson, P.R., Pugh, B.F., and Wang, Y. (2008). Histone Arg modifications and p53 regulate the expression of OKL38, a mediator of apoptosis. The Journal of biological chemistry *283*, 20060-20068.

Yokoyama, W.M., Christensen, M., Santos, G.D., and Miller, D. (2006). Production of monoclonal antibodies. Current protocols in immunology / edited by John E. Coligan ... [et al *Chapter 2*, Unit 2 5.

Yoshimoto, T., Boehm, M., Olive, M., Crook, M.F., San, H., Langenickel, T., and Nabel, E.G. (2006). The arginine methyltransferase PRMT2 binds RB and regulates E2F function. Experimental cell research *312*, 2040-2053.

Yue, W.W., Hassler, M., Roe, S.M., Thompson-Vale, V., and Pearl, L.H. (2007). Insights into histone code syntax from structural and biochemical studies of CARM1 methyltransferase. The EMBO journal *26*, 4402-4412.

Zhao, X., Jankovic, V., Gural, A., Huang, G., Pardanani, A., Menendez, S., Zhang, J., Dunne, R., Xiao, A., Erdjument-Bromage, H.*, et al.* (2008). Methylation of RUNX1 by PRMT1 abrogates SIN3A binding and potentiates its transcriptional activity. Genes & development *22*, 640-653.

Zhou, L., Chong, M.M., and Littman, D.R. (2009). Plasticity of CD4+ T cell lineage differentiation. Immunity *30*, 646-655.

Zhu, J., and Paul, W.E. (2010). Heterogeneity and plasticity of T helper cells. Cell research *20*, 4-12.

Zika, E., Fauquier, L., Vandel, L., and Ting, J.P. (2005). Interplay among coactivator-associated arginine methyltransferase 1, CBP, and CIITA in IFN-gamma-inducible MHC-II gene expression. Proceedings of the National Academy of Sciences of the United States of America *102*, 16321-16326.

8 Acknowledgements

My sincerest gratitude goes to Prof. Kerri Mowen of the Scripps Research Institute. I would like to thank Kerri for inviting me into her lab and providing me with all the fascinating projects I have been working on in the past years. I learned many valuable lessons, most importantly how to do thorough research. I would also like to thank Prof. Jens Brüning for agreeing to supervise my thesis in Cologne, making my stay in San Diego possible.

In addition, I would like to especially thank Prof. Jonathan Howard and Prof. Einhard Schierenberg for their last minute efforts to make my July 5th defense possible as well as Dr. Thomas Wunderlich for agreeing to be part of my thesis committee.

Furthermore, I would like to thank Sanja Arandjelovic, Sony Leming, Myles Dillon, Colin Thom, Anthony Fernadez, Bonnie Towle, and all the past members of the Mowen lab for their friendship and support. I am especially grateful for Sanja's help in proofreading my thesis. The Immunology community at Scripps has been a great support through the past years, and I would like to thank all G11 members. Extended thanks to all my friends in San Diego and back home for being who they are.

Mein größter Dank gilt meiner Familie für all die Unterstützung in jeglicher Form.

9 Erklärung

Ich versichere, daß ich die von mir vorgelegte Dissertation selbständig angefertigt, die benutzten Quellen und Hilfsmittel vollständig angegeben und die Stellen der Arbeit – einschließlich Tabellen, Karten und Abbildungen -, die anderen Werken im Wortlaut oder dem Sinn nach entnommen sind, in jedem Einzelfall als Entlehnung kenntlich gemacht habe; daß diese Dissertation noch keiner anderen Fakultät oder Universität zur Prüfung vorgelegen hat; daß sie noch nicht veröffentlicht worden ist sowie, daß ich eine solche Veröffentlichung vor Abschluß des Promotionsverfahrens nicht vornehmen werde.
Die Bestimmungen dieser Promotionsordnung sind mir bekannt. Die von mir vorgelegte Dissertation ist von Herrn Prof. Jens Brüning (Universitat zu Köln) und Frau Prof. Kerri Mowen (The Scripps Research Institute) betreut worden.

Ich versichere, daß ich alle Angaben wahrheitsgemäß nach bestem Wissen und Gewissen gemacht habe und verpflichte mich, jedmögliche, die obigen Angaben betreffenden Veränderungen, dem Dekanat unverzüglich mitzuteilen.

San Diego, im Mai 2010

Saskia Hemmers

10 Curriculum Vitae

Persönliche Daten

Name	Saskia Hemmers
Geburtsdatum	23. Mai 1980
Geburtsort	Bonn
Adresse	Bertha-von-Suttnerstr. 4B 53840 Troisdorf
Nationalität	deutsch

Bildungsweg

Seit 10/2005	auswärtige Promotion am Scripps Research Institute (La Jolla, CA, USA) im Department of Immunology and Microbial Science in der Arbeitsgruppe von Prof. Kerri Mowen; betreut durch Prof. Jens Brüning
03/2005	Diplom in Biologie, Universität zu Köln
2004 - 2005	Diplomarbeit im Institute fur Genetik an der Universität zu Köln im Labor von Prof. Ari Waisman betreut durch Prof. Jens Brüning zum Thema: “Approaching T Cell Selection: Generation of the HYflip Strain as a New TCRa Switch-on Mouse Model to Investigate Positive and Negative Selection”
02/2004	Diplomprüfungen im Hauptfach Genetik und in den Nebenfächern Biochemie und Organische Chemie
09/2001	Vordiplom in Biologie, Universität zu Köln
1999 – 2005	Studium der Biologie an der Mathematisch-Naturwissenschaftlichen Fakultät der Universität zu Köln
1999	Abitur
1990 – 1999	Gymnasium zum Altenforst, Troisdorf

Praktika/ Auslandaufenthalte

03 – 10/2003	Hoffman & La Roche, Basel, Schweiz